

H.D.R.



T2K

Neutrinos and applications : an oscillating trip

J-E.MARTEAU

Institut de Physique Nucléaire de Lyon
Université de Lyon UCBL – CNRS/IN2P3

marteau@ipnl.in2p3.fr

Jury : G.Chanfray, P.U., UCBL, président
Y.Déclais, D.R., IPNL
O.Drapier, D.R., LLR, rapporteur
H.Pessard, D.R., LAPP, rapporteur
D.Gibert, P.CNAP, GR, rapporteur



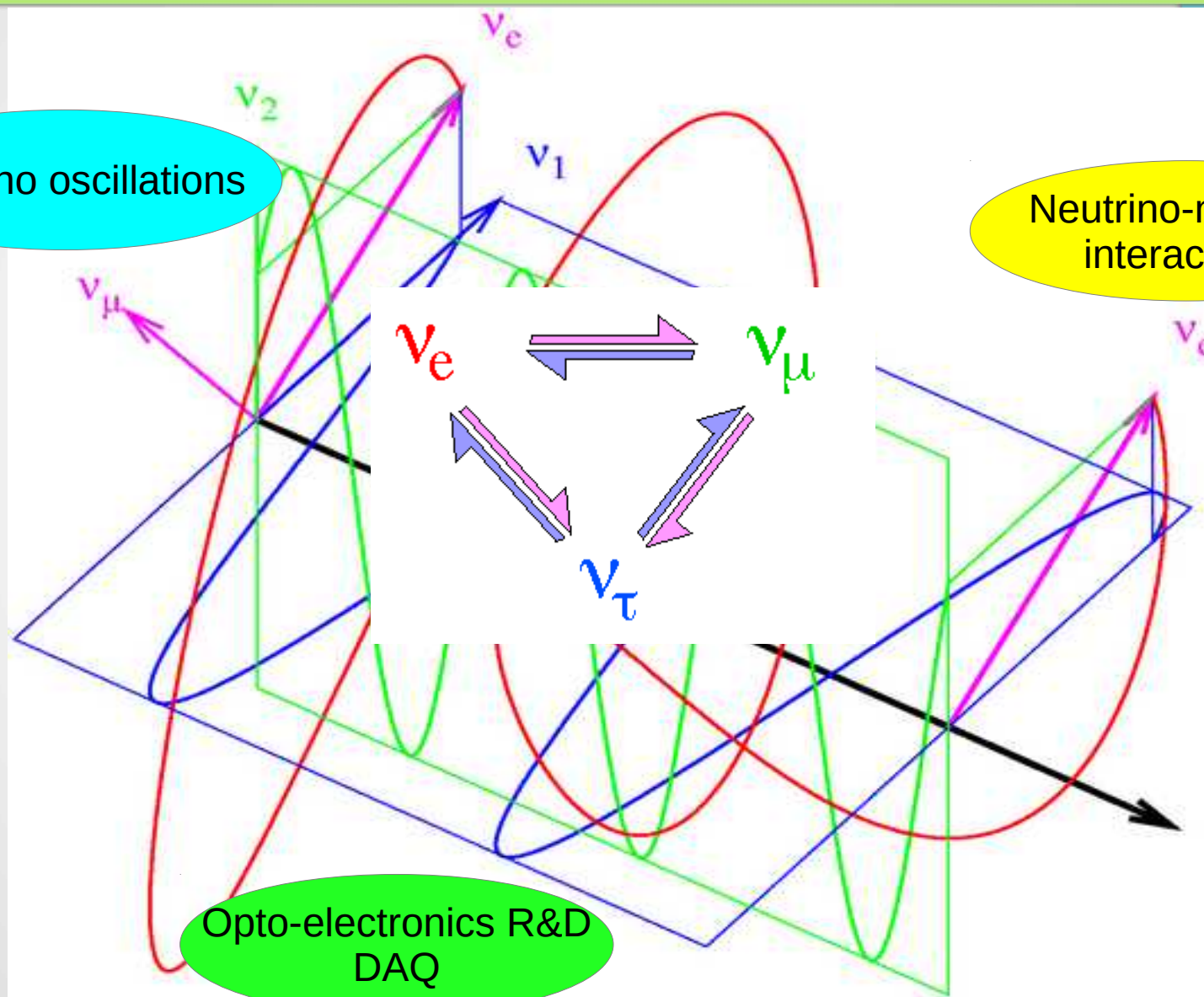
WA105



Oscillating trip : outline

Neutrino oscillations

Neutrino-nucleus interactions



Opto-electronics R&D
DAQ

Short history, large discoveries...

1930 → **PAULI** letter on β -decay : "Liebe Radioaktive Damen und Herren..."

1933 → Weak interaction theory, neutrino terminology, by **FERMI**

1956 → First electronic neutrino observation by **Reines & Cowan** ; **Wu** (1957) experiment : P-violation

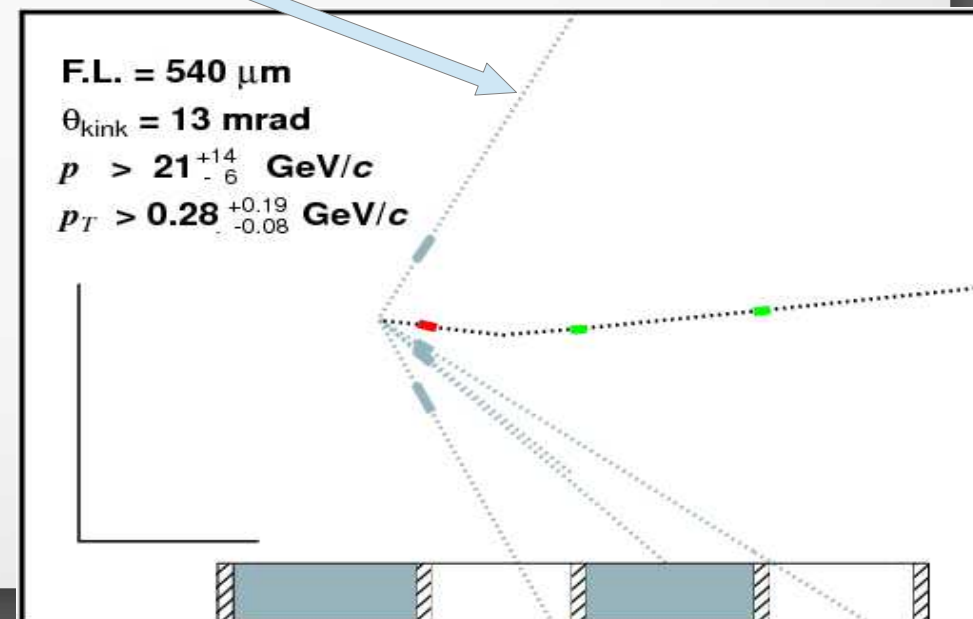
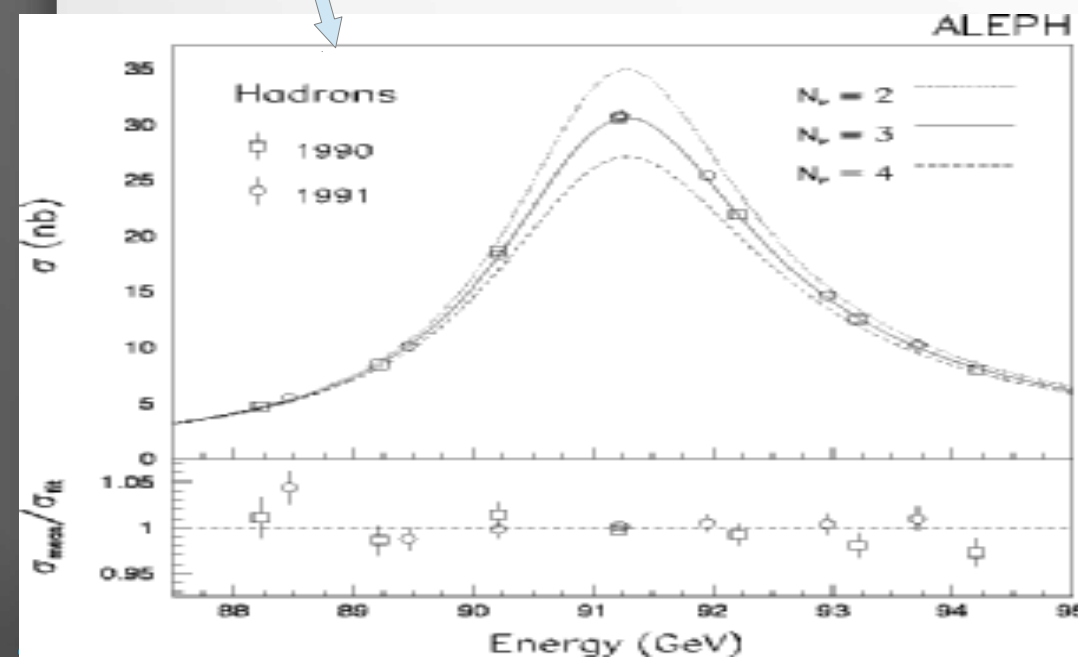
1962 → First muonic neutrino observation

1989 → **LEP** : 3 light neutrinos

1998 → **SK** : neutrino **oscillate** and **have a mass**

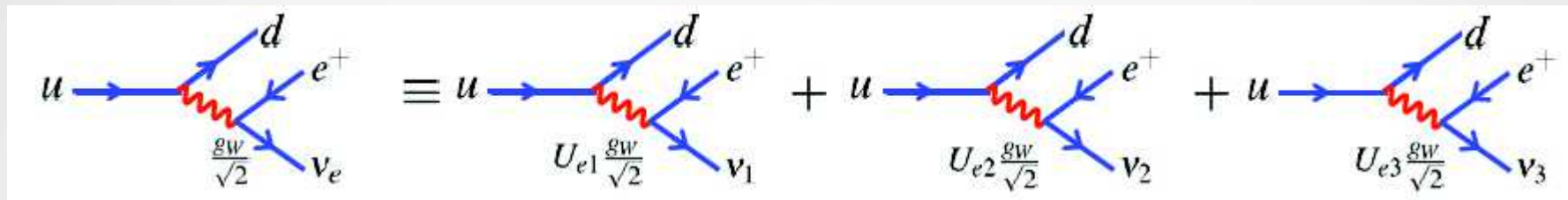
2000 → **DONUT** : first direct observation of τ neutrino

Long-standing solar + atmospheric neutrinos anomalies



ν oscillations basics

- Neutrinos are produced in flavor eigenstates of the weak interaction : ν_e, ν_μ, ν_τ
- Neutrinos propagate as mass eigenstates : ν_1, ν_2, ν_3

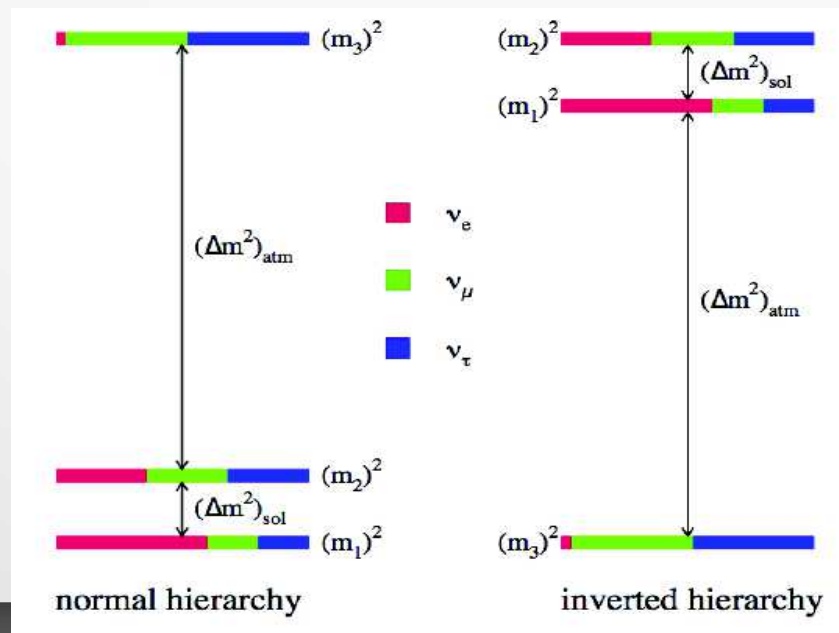


Flavor eigenstates

$\nu_{e,\mu,\tau}$

$$\nu_\alpha = \sum_i U_{\alpha i} \nu_i$$

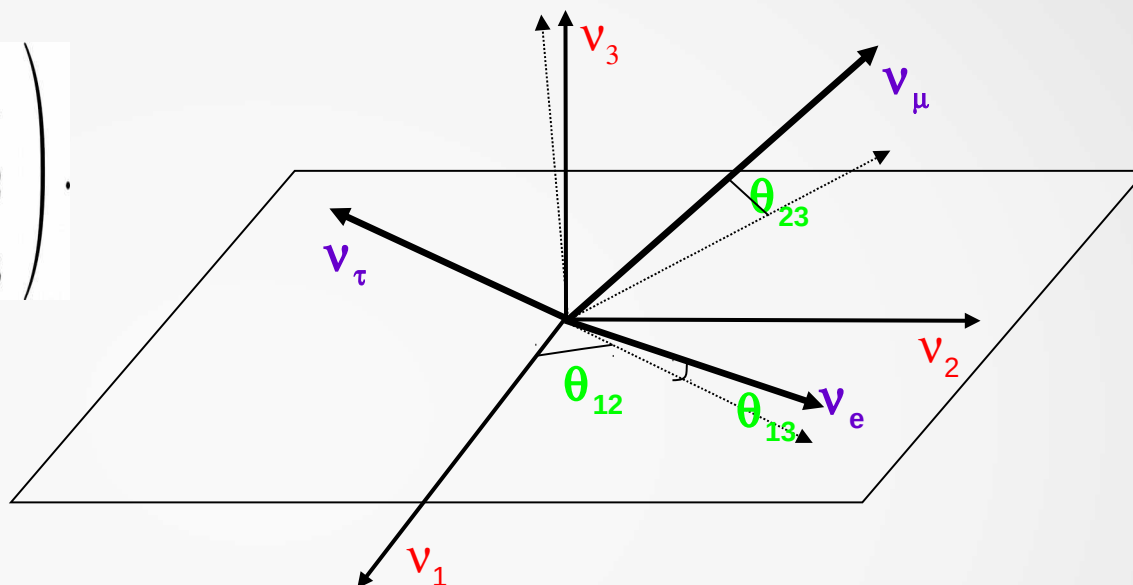
← ν_α (Flavor eigenstates) → ν_i (Mass eigenstates)



ν oscillations basics

■ Mixing matrix : Pontecorvo – Maki – Nakagawa – Sakata

$$\begin{pmatrix} \nu_e \\ \nu_\mu \\ \nu_\tau \end{pmatrix} = \begin{pmatrix} U_{e1} & U_{e2} & U_{e3} \\ U_{\mu1} & U_{\mu2} & U_{\mu3} \\ U_{\tau1} & U_{\tau2} & U_{\tau3} \end{pmatrix} \begin{pmatrix} \nu_1 \\ \nu_2 \\ \nu_3 \end{pmatrix}.$$



The unitary PMNS matrix is described as the product of three rotation matrices and a Dirac complex phase*:

$$U = \begin{pmatrix} 1 & 0 & 0 \\ 0 & c_{23} & s_{23} \\ 0 & -s_{23} & c_{23} \end{pmatrix} \begin{pmatrix} c_{13} & 0 & s_{13}e^{-i\delta} \\ 0 & 1 & 0 \\ -s_{13}e^{i\delta} & 0 & c_{13} \end{pmatrix} \begin{pmatrix} c_{12} & s_{12} & 0 \\ -s_{12} & c_{12} & 0 \\ 0 & 0 & 1 \end{pmatrix}$$

Atmospheric ν + OPERA

Reactors (L~km) + T2K

Reactors (L~100km) +
Solar ν

*Majorana neutrinos :
 $\times \text{diag} \left(e^{i\alpha_1/2}, e^{i\alpha_2/2}, 1 \right)$

ν oscillations basics

- Transition probability from one flavor (α) to another flavor (β) (PDG):

$$P(\nu_\alpha \rightarrow \nu_\beta) = \delta_{\alpha\beta} - 4 \sum_{i>j} \Re(U_{\alpha i}^* U_{\beta i} U_{\alpha j} U_{\beta j}^*) \sin^2[\Delta m_{ij}^2 (L/4E)] \\ + 2 \sum_{i>j} \Im(U_{\alpha i}^* U_{\beta i} U_{\alpha j} U_{\beta j}^*) \sin[\Delta m_{ij}^2 (L/2E)]$$

L is the distance travelled, E is the neutrino energy, and Δm_{ij}^2 is the difference in the square of the neutrino masses.

- Oscillations are function of $\Delta m^2 L/E$; for long-baseline beams, the oscillation effects are dominated by mixing between $\nu_1 - \nu_3$ and $\nu_2 - \nu_3$.
- $\Delta m_{21}^2 \ll (\Delta m_{32}^2 \simeq \Delta m_{31}^2 > 0)$ \Rightarrow mixing between $\nu_1 - \nu_3$ only becomes significant
 $\Delta m_{21}^2 \ll -(\Delta m_{31}^2 \simeq \Delta m_{32}^2 < 0)$ at very long distances or very low energies.
- Sign of Δm_{31}^2 currently unknown : mass hierarchy problem :
 ν_3 heaviest neutrino : "normal" hierarchy, ν_3 heaviest neutrino : "inverted" hierarchy

ν oscillations basics

- For a beam of muon neutrinos, the survival probability for ν_μ is given approximately by :

$$P(\nu_\mu \rightarrow \nu_\mu) \simeq 1 - \sin^2 2\theta_{23} \cdot \sin^2 (\Delta m_{32}^2 L / 4E)$$

while appearance of ν_e in vacuum is :

$$P(\nu_\mu \rightarrow \nu_e) \simeq \sin^2 2\theta_{13} \cdot \sin^2 \theta_{23} \cdot \sin^2 (\Delta m_{31}^2 L / 4E)$$

- As neutrinos travel through matter, the transition probability is modified to :

$$P(\nu_\mu \rightarrow \nu_e) \simeq \sin^2 2\theta_{13} \cdot \frac{\sin^2 \theta_{23}}{(A - 1)^2} \cdot \sin^2 ((A - 1)\Delta m_{31}^2 L / 4E)$$

where : $A = \sqrt{2}G_F N_e \frac{2E}{\Delta m_{31}^2}$

↓
Fermi coupling constant

↘ Electron density

NB A changes sign for anti-neutrinos

ν oscillations basics

- Including the effects of non-zero δ_{CP} adds additional terms to $P(\nu_\mu \rightarrow \nu_e)$ including :

$$- \frac{|\Delta m_{21}^2|}{|\Delta m_{31}^2|} \frac{\sin \delta_{\text{CP}} \sin 2\theta_{12} \sin 2\theta_{13} \sin 2\theta_{23} \cos \theta_{13}}{A(1-A)} \times$$
$$\sin(\Delta m_{31}^2 L/4E) \sin(A\Delta m_{31}^2 L/4E) \sin((1-A)\Delta m_{31}^2 L/4E)$$

- This term changes sign for antineutrinos with a different L and E dependence as for "matter" terms
- Differences between $\nu_\mu \rightarrow \nu_e$ and $\bar{\nu}_\mu \rightarrow \bar{\nu}_e$ can help to resolve the hierarchy question and provide a measurement of CP-violation in the lepton sector if δ_{CP} is found to be non-zero.

Knowns and unknowns...

From a global χ^2 analysis one can derive the 3σ ranges on the magnitude of the elements of the leptonic mixing matrix to be:

$$|U| = \begin{pmatrix} 0.801 \rightarrow 0.845 & 0.514 \rightarrow 0.580 & 0.137 \rightarrow 0.158 \\ 0.225 \rightarrow 0.517 & 0.441 \rightarrow 0.699 & 0.614 \rightarrow 0.793 \\ 0.246 \rightarrow 0.529 & 0.464 \rightarrow 0.713 & 0.590 \rightarrow 0.776 \end{pmatrix}.$$

Data sets :

- Super-Kamiokande atmospheric neutrino data SK1-4,
- (LBL) : energy distribution from MINOS and from T2K (disappearance)
- (LBL) : MINOS ν and $\bar{\nu}$ and T2K $\bar{\nu}_e$ appearance
- Solar experiments : Chlorine, Gallex/GNO and SAGE (rates), electron scattering SK1-4 (day-night spectrum, energy), SNO, Borexino (spectrum)
- Reactor experiments : CHOOZ, Palo Verde, Double Chooz (spectrum), Daya Bay & RENO (rates, spectrum), KamLAND (energy spectrum)
- Reactor (non-oscillation : flux constraints) : Bugey4, ROVNO4, Bugey3, Krasnoyarsk, ILL, Gösigen, SRP and ROVNO88

	bfp $\pm 1\sigma$
$\sin^2 \theta_{12}$	$0.304^{+0.013}_{-0.012}$
$\theta_{12}/^\circ$	$33.48^{+0.78}_{-0.75}$
$\sin^2 \theta_{23}$	$0.452^{+0.052}_{-0.028}$
$\theta_{23}/^\circ$	$42.3^{+3.0}_{-1.6}$
$\sin^2 \theta_{13}$	$0.0218^{+0.0010}_{-0.0010}$
$\theta_{13}/^\circ$	$8.50^{+0.20}_{-0.21}$
$\delta_{CP}/^\circ$	306^{+39}_{-70}
$\frac{\Delta m_{21}^2}{10^{-5} \text{ eV}^2}$	$7.50^{+0.19}_{-0.17}$
$\frac{\Delta m_{3\ell}^2}{10^{-3} \text{ eV}^2}$	$+2.457^{+0.047}_{-0.047}$

ν oscillations basics

- Next order for next generation long-baseline experiments physics case :

$$P(\nu_\mu \rightarrow \nu_e; L) \simeq 4c_{13}^2 s_{13}^2 s_{23}^2 \left\{ 1 + \frac{a}{\delta m_{31}^2} \cdot 2(1 - 2s_{13}^2) \right\} \sin^2 \frac{\delta m_{31}^2 L}{4E} + c_{13}^2 s_{13} s_{23} \left\{ -\frac{aL}{E} s_{13} s_{23} (1 - 2s_{13}^2) + \frac{\delta m_{21}^2 L}{E} s_{12} (-s_{13} s_{23} s_{12} + c_\delta c_{23} c_{12}) \right\} \sin \frac{\delta m_{31}^2 L}{2E} - 4 \frac{\delta m_{21}^2 L}{2E} s_\delta c_{13}^2 s_{13} c_{23} s_{23} c_{12} s_{12} \sin^2 \frac{\delta m_{31}^2 L}{4E}$$

Matter terms $\sim a$

CP-even

CP-odd $\sim \sin \delta$

L/E dependence

$$a \equiv 2\sqrt{2}G_F n_e E = 7.56 \times 10^{-5} \text{eV}^2 \frac{\rho}{\text{g cm}^{-3}} \frac{E}{\text{GeV}}$$

- Neutrinos-antineutrinos difference :

- CP asymmetries are largest at the 2nd, 3rd, ... maxima.
- Matter asymmetry dominates around the 1st maximum.
- Long(er) baselines, wide-band beams to cover several maxima are needed to resolve degeneracies.

$$\mathcal{A} \equiv P(\nu_\mu \rightarrow \nu_e) - P(\bar{\nu}_\mu \rightarrow \bar{\nu}_e) =$$

$$16 \frac{a}{\delta m_{31}^2} \sin^2 \frac{\delta m_{31}^2 L}{4E} c_{13}^2 s_{13}^2 s_{23}^2 (1 - 2s_{13}^2) - 4 \frac{aL}{2E} \sin \frac{\delta m_{31}^2 L}{2E} c_{13}^2 s_{13}^2 s_{23}^2 (1 - 2s_{13}^2) - 8 \frac{\delta m_{21}^2 L}{2E} \sin^2 \frac{\delta m_{31}^2 L}{4E} s_\delta c_{13}^2 s_{13} c_{23} s_{23} c_{12} s_{12}$$

Matter terms

Pure CP-term

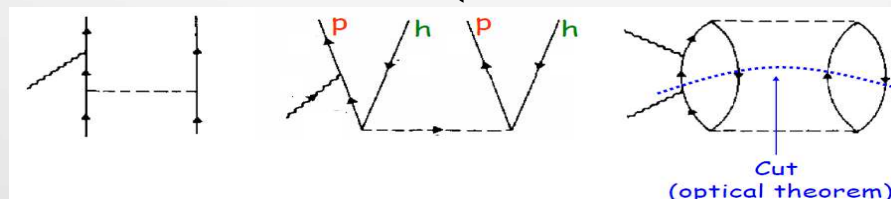
Part – I

ν -nucleus interactions

ν -nucleus interactions : motivations

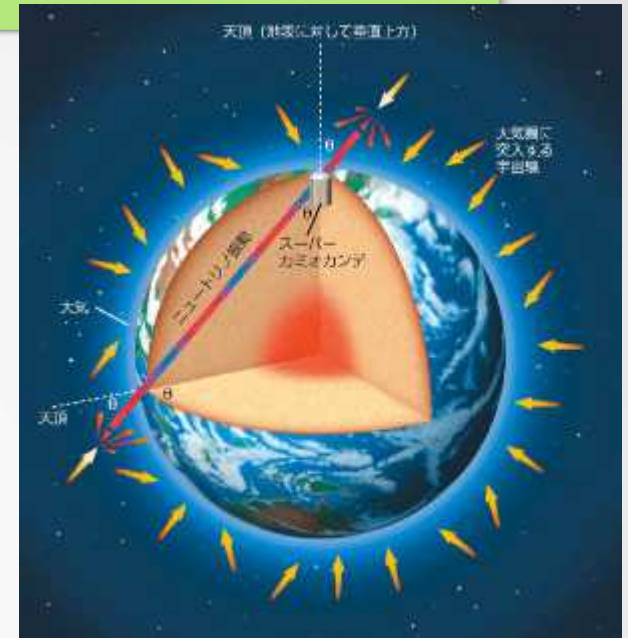
- Before '98 : exploring the effect(s) of collective nuclear states in the ν -nucleus cross-sections : $\Delta\omega \sim m_\pi \sim m_\mu - m_e$
 ➡ potential role in the atmospheric neutrinos anomaly ?

- ➡ **np-nh** states are known to be important in electron scattering : do they play a role for neutrinos (mis-identified multi-prong events) ?



ν -nucleus interactions : motivations

- After '98 : atmospheric anomaly explained by neutrino oscillations :



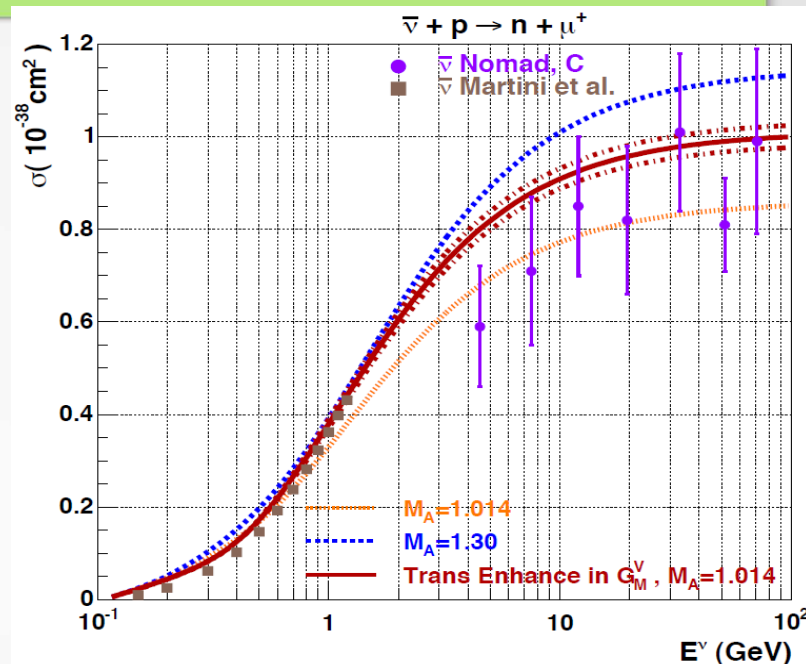
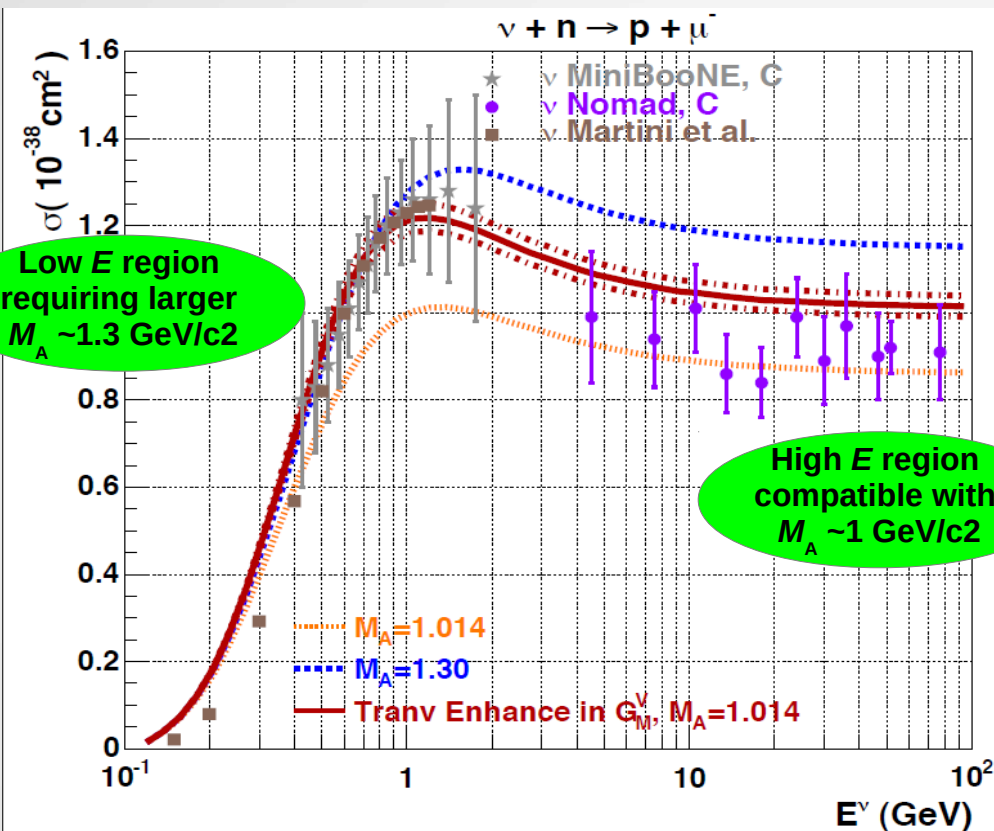
- ↳ entering an era of process confirmation and precise measurements (requires knowledge on cross-sections and a precise kinematics reconstruction)
- ↳ dedicated experiments or projects within collaboration (MINOS, T2K, MiniBOONE, Minerva, SciBOONE etc)
- ↳ more data to constrain the models (MEC, TEM, SuSA, GIBUU etc), the MC simulations (NEUT, GENIE, NUANCE, NEUGEN, NuWro, NGEN, OpNGEN etc) and... more things to be understood...

4.2.4 Open Concerns

There are four major concerns for the Phase I LBNE detector program:

1. The surface location of the LAr detector;
2. The lack of a near detector;
3. The small mass (10 kt) of the far detector;
4. Uncertainties in nuclear effects.

ν -nucleus CCQE : axial mass anomaly



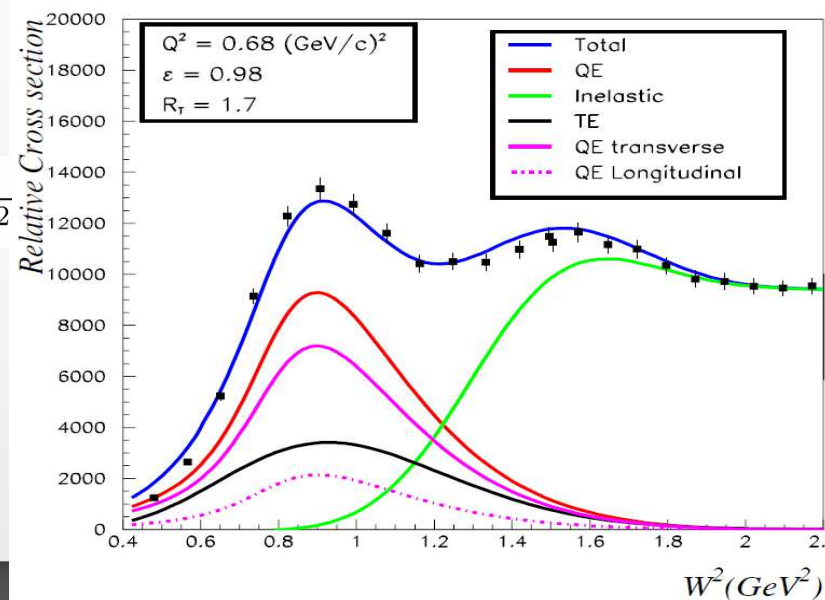
Preliminary E04-001, $E = 4.629$, $\theta = 10.661$

Keeping standard axial dipole FF : $F_A^{nuclear}(Q^2) = \frac{1}{(1 + Q^2/M_A^2)^2}$

Modify transverse response, as suggested by electron scattering : $G_M^{nuclear}(Q^2) = G_M(Q^2) \times \sqrt{1 + AQ^2 e^{-Q^2/B}}$

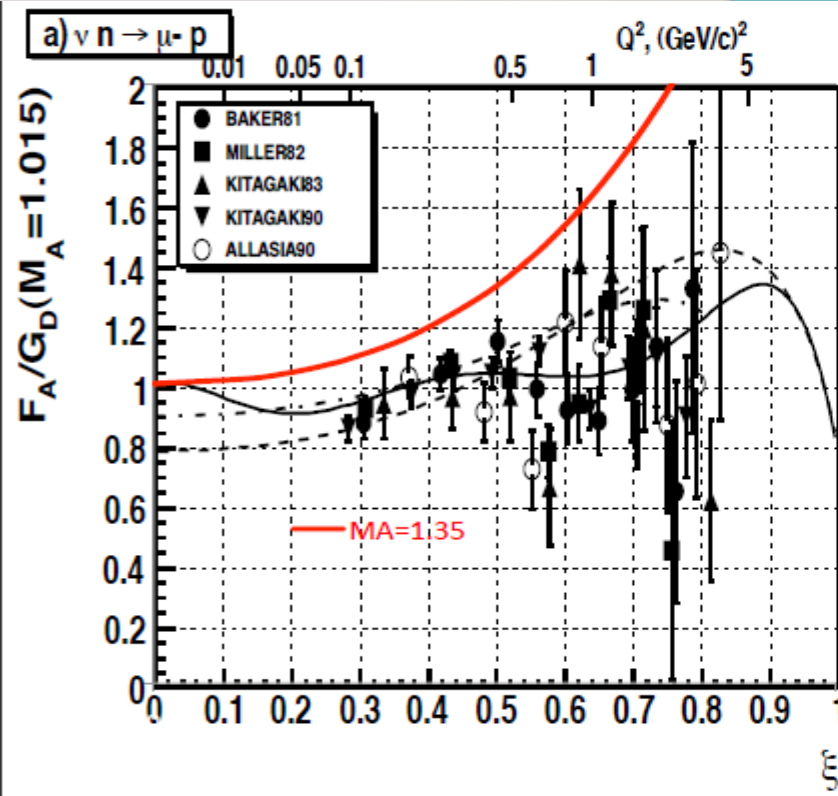
BBBA2007₂₅

Or follow alternative models...



ν -nucleus interactions : motivations

- "Axial mass anomaly" :
 - Meson Exchange Currents ?
 - Transverse Enhancement Model ?
 - Super-scaling approach ?
 - Adjusting M_A parameters exp. ?
- QE assumption for E reconstruction ?
- Neutrinos-antineutrinos comparison (CP in the lepton sector)
- $\nu_\mu - \nu_e$ comparison (appearance mode) (MINERvA first measurement not easy)
- π production (test of the FSI for hadrons)
- Coherent π production (stringent constraints on models & experimental bkg for ν_e appearance π^0 or ν_μ detection π^\pm)
- First measurements done at high E , on low A targets : scaling between the various regimes (QE, resonance, DIS, collective states etc) ?



Neutrino Quasielastic Scattering on Nuclear Targets
 Parametrizing Transverse Enhancement
 (Meson Exchange Currents),
 A. Bodek, arXiv:1106.0340

ν -nucleus CCQE : E_ν estimator

In standard RFG models the neutrino kinematics is reconstructed under the usual QE assumption :

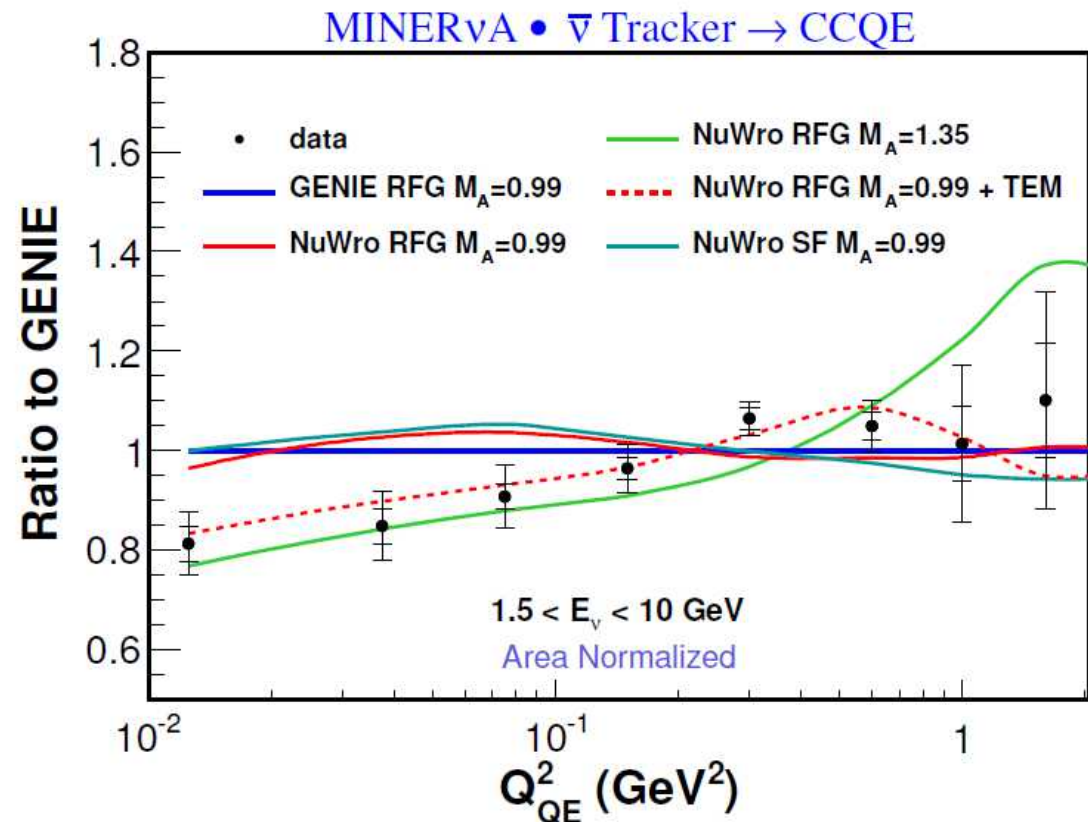
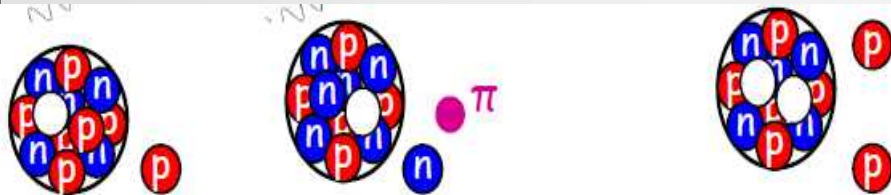
$$E_\nu^{QE} = \frac{m_n^2 - (m_p - E_b)^2 - m_\mu^2 + 2(m_p - E_b E_\mu)}{2(m_p - E_b - E_\mu + p_\mu \cos \theta_\mu)}$$

$$Q_{QE}^2 = 2E_\nu^{QE} (E_\mu - p_\mu \cos \theta_\mu) - m_\mu^2$$

Hyp. : stationary nucleon with E_b a semi-empirical binding energy accounting for the nuclear potential)

« Instead, the data best favor an RFG that is modified using empirical corrections to the cross-section derived from measurements of electron-nucleus scattering (which are thought to be necessitated by inter-nucleon correlations within the nucleus) »

Implications of recent MiNERvA results for neutrino energy reconstruction, J.Wolcott, arXiv:1501.05210



ν -nucleus interactions : formalism

- ν -nucleus interactions Feynman diagrams :



ν -nucleus interactions : formalism

- Hadronic currents reduction :

$$\langle p', s' | V_\alpha^\mu | p, s \rangle = \bar{u}(p', s') \left[F_1^v \gamma^\mu + F_2^v \sigma^{\mu\nu} \frac{i q_\nu}{2M_N} \right] \tau_\alpha u(p, s)$$

$$\langle p', s' | S^\mu | p, s \rangle = \bar{u}(p', s') \left[F_1^s \gamma^\mu + F_2^s \sigma^{\mu\nu} \frac{i q_\nu}{2M_N} \right] \mathbb{I}_\tau u(p, s)$$

$$\langle p', s' | A_\alpha^\mu | p, s \rangle = \bar{u}(p', s') \left[G_A \gamma^\mu \gamma_5 + G_P \gamma_5 \frac{q^\mu}{2M_N} \right] \tau_\alpha u(p, s)$$

- 2 x 2 operators : spin – isospin longitudinal : $(\boldsymbol{\sigma} \cdot \mathbf{q}) \tau_\alpha$
 spin – isospin transverse : $((\boldsymbol{\sigma} \times \mathbf{q}) \times \mathbf{q}) \tau_\alpha$
 charge : $\mathbb{I}_\sigma \tau_\alpha$

**Ring-RPA
approximation**

- Polarization propagators :

$$\Pi_{\alpha\beta}^{PP'}(\omega, q, q') = \sum_n \left(n \sum_{i=1}^A O_\alpha^P(i) e^{iq \cdot x(i)} 0 \frac{1}{\omega - E_n + E_0 + i\varepsilon} 0 \sum_{i=1}^A (O_\beta^{P'}(i))^\dagger e^{-iq' \cdot x(i)} n \right) -$$

$$\left(n \sum_{i=1}^A O_\beta^{P'}(i) e^{-iq' \cdot x(i)} 0 \frac{1}{\omega + E_n - E_0 - i\varepsilon} 0 \sum_{i=1}^A (O_\alpha^P(i))^\dagger e^{iq \cdot x(i)} n \right)$$

$$\Pi = \Pi^0 + \Pi^0 V \Pi$$

↪ nuclear responses

$$R_\alpha^P(\omega, q) = -\frac{1}{\pi} \text{Im} \left(\Pi_{\alpha\alpha}^{PP}(\omega, q, q) \right)$$

ν -nucleus cross-section

- CC neutrino-nucleus cross-section :

$$\frac{\partial^2 \sigma}{\partial \Omega_{lep} \partial p_{lep}} = \frac{G_F^2 \cos^2 \theta_C p_{lep}^2}{2\pi^2} \cos^2 \frac{\theta}{2} \left[G_E^2 \left(\frac{q^2}{q^2} \right)^2 R_c^{NN} \right. \text{isovector "charge" response} \\ + G_A^2 \frac{(M_\Delta - M_N)^2}{42 q^2} R_{\sigma\tau(L)} \text{spin-isospin longitudinal response} \\ + (G_M^2 \frac{q^2}{4 M_N^2} + G_A^2) \left(-\frac{q^2}{q^2} + 2 \tan^2 \frac{\theta}{2} \right) R_{\sigma\tau(T)} \text{spin-isospin transverse response} \\ \left. \pm 2 G_A G_M \frac{k + p_{lep}}{M_N} \tan^2 \frac{\theta}{2} R_{\sigma\tau(T)} \right] \begin{cases} + & (\nu) \\ - & (\bar{\nu}) \end{cases} \text{interference V-A}$$

- Transverse channel dominant
- QE longitudinal response suppressed
- Axial charge renormalized
- Relativistic corrections applied : $\omega \rightarrow \omega(1 + \frac{\omega}{2M_N})$

Including nuclear effects

- Interests of the model : analytic solution including

- RPA correlations ($V_\pi + V_\rho + g'$)

- Local density effect (local $k_F(\mathbf{R}) = [\frac{3\pi^2}{2}\rho(\mathbf{R})]^{1/3}$)

$$\Pi_{N-h}^0(\omega, \mathbf{q}) = 4 \int \frac{d^3k}{(2\pi)^3} \left[\frac{\vartheta(|\mathbf{q} + \mathbf{k}| - k_F) \vartheta(k_F - |\mathbf{k}|)}{\omega + \omega_{\mathbf{k}} - \omega_{\mathbf{q}+\mathbf{k}} + i\epsilon} - \frac{\vartheta(k_F - |\mathbf{q} + \mathbf{k}|) \vartheta(|\mathbf{k}| - k_F)}{\omega + \omega_{\mathbf{k}} - \omega_{\mathbf{q}+\mathbf{k}} - i\epsilon} \right].$$

- Full Delta-resonance width

$$\Pi_{\Delta-h}^0(q) = \frac{16}{9} \int \frac{d^3k}{(2\pi)^3} \vartheta(k_F - |\mathbf{k}|) \left[\frac{1}{\omega - \omega_{\mathbf{q}+\mathbf{k}}^\Delta + \omega_{\mathbf{k}} + i\frac{\Gamma_\Delta}{2}} - \frac{1}{\omega + \omega_{\mathbf{q}+\mathbf{k}}^\Delta - \omega_{\mathbf{k}}} \right].$$

$$\hookrightarrow \Gamma_\Delta = \Gamma_{QE} F_P - 2\text{Im}(\Sigma_{QE} + \Sigma_{2p2h} + \Sigma_{3p3h})$$

- Exclusive channels
- **np-nh** correlation states

Exclusive channels

$$R^0 = \sum_{k=1}^{N_k} R_{(k)}^0 = \sum_{k=1}^{N_k} -\frac{1}{\pi} \operatorname{Im} \left(\Pi_{(k)}^0 \right)$$

$$\Pi = \Pi^0 + \Pi^0 V \Pi$$

$$\Rightarrow \operatorname{Im} (\Pi) = |\Pi|^2 \operatorname{Im} (V) + |1 + V \Pi|^2 \operatorname{Im} (\Pi^0)$$

$$\Rightarrow R = R_{\text{coh.}} + \sum_{k=1}^{N_k} R_{(k)}$$

Coherent channel

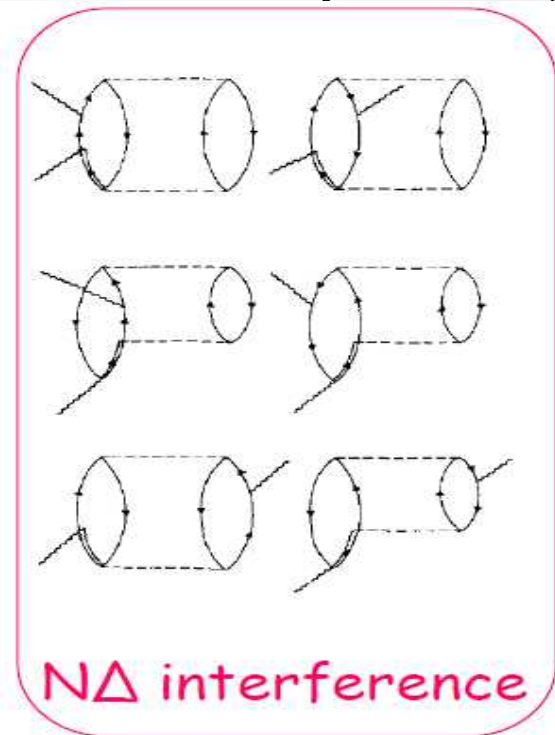
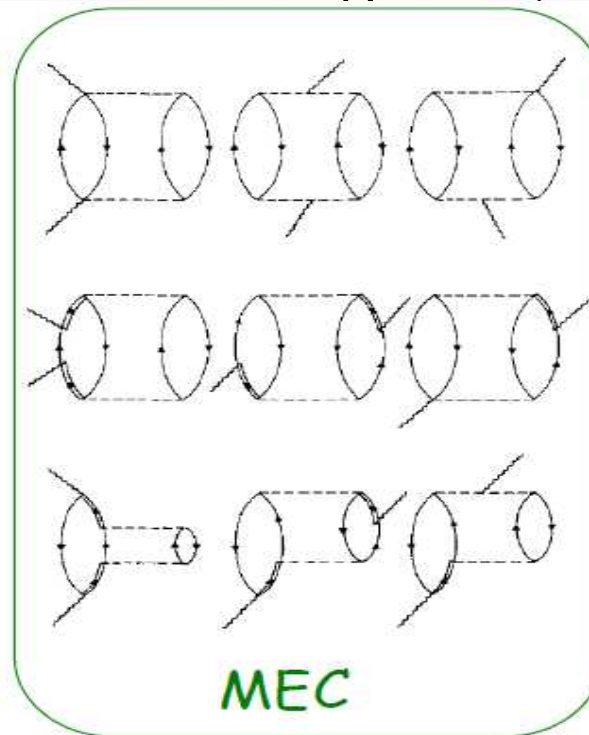
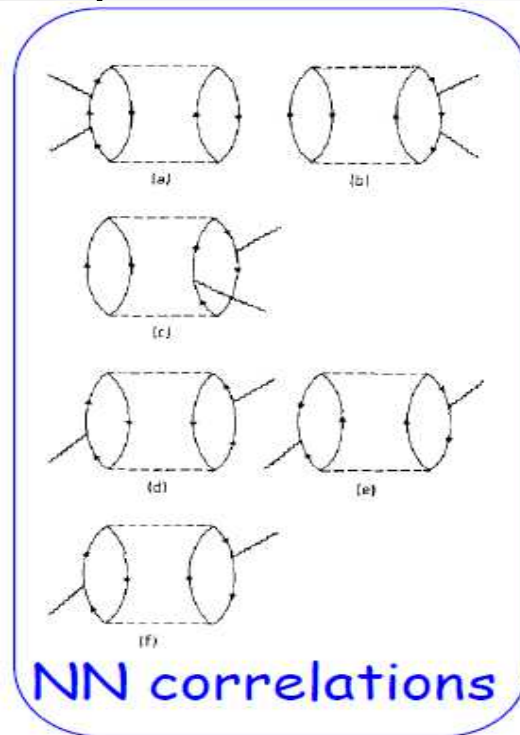
Sum rule respected

np-nh states

- Simple way to account for *np-nh* from an extrapolation of pion absorption experiments (no q dependance):

$$\begin{aligned}
 \text{Im}(\Pi_{NN}^0) &= 4\pi\rho^2 \frac{(2M_N + m_\pi)^2}{(2M_N + \omega)^2} C_1 \Phi_1(\omega) \left[\frac{1}{\omega^2} \right] \\
 \text{Im}(\Pi_{N\Delta}^0) &= -4\pi\rho^2 \frac{(2M_N + m_\pi)^2}{(2M_N + \omega)^2} C_2 \Phi_2(\omega) \text{Re} \left[\frac{1}{\omega(\omega - M_\Delta + M_N + i\frac{\Gamma_\Delta}{2})} \right. \\
 &\quad \left. + \frac{1}{\omega(\omega + M_\Delta - M_N)} \right] \\
 \text{Im}(\Pi_{\Delta\Delta}^0) &= -4\pi\rho^2 \frac{(2M_N + m_\pi)^2}{(2M_N + \omega)^2} C_3 \Phi_3(\omega) \left[\frac{1}{(\omega + M_\Delta - M_N)^2} \right],
 \end{aligned}$$

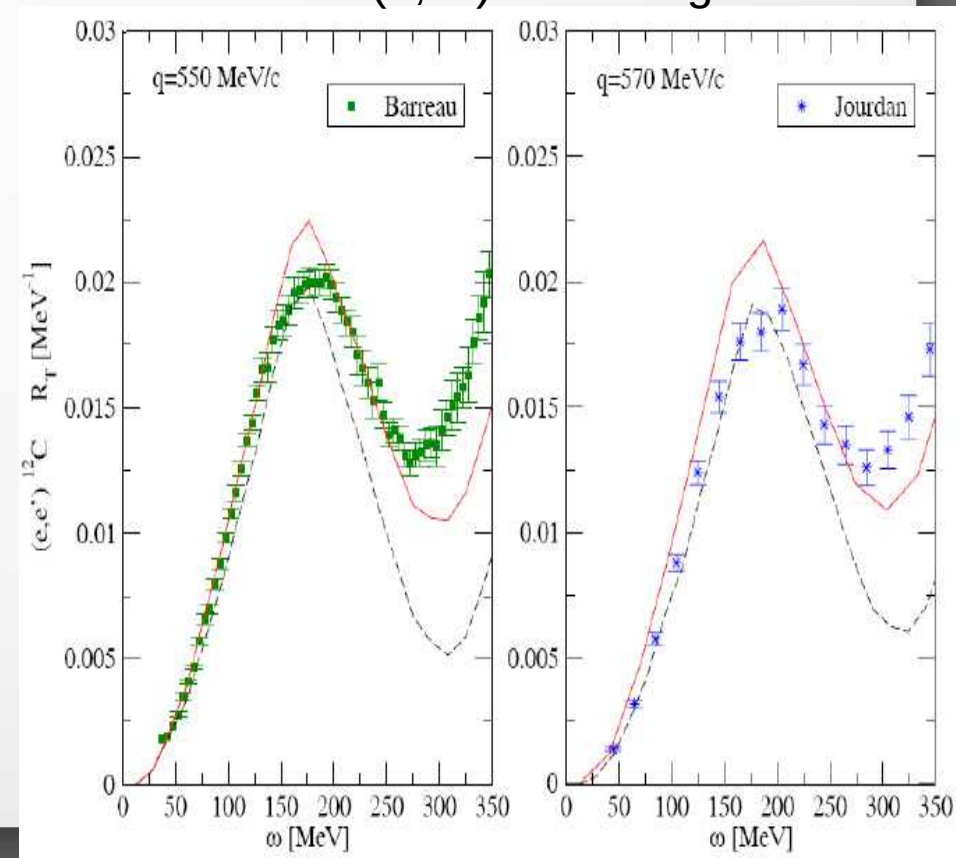
- Or explicit evaluation of >100 diagrams (Alberico et al, Ann. Phys. 154, 356 (1984))



Results

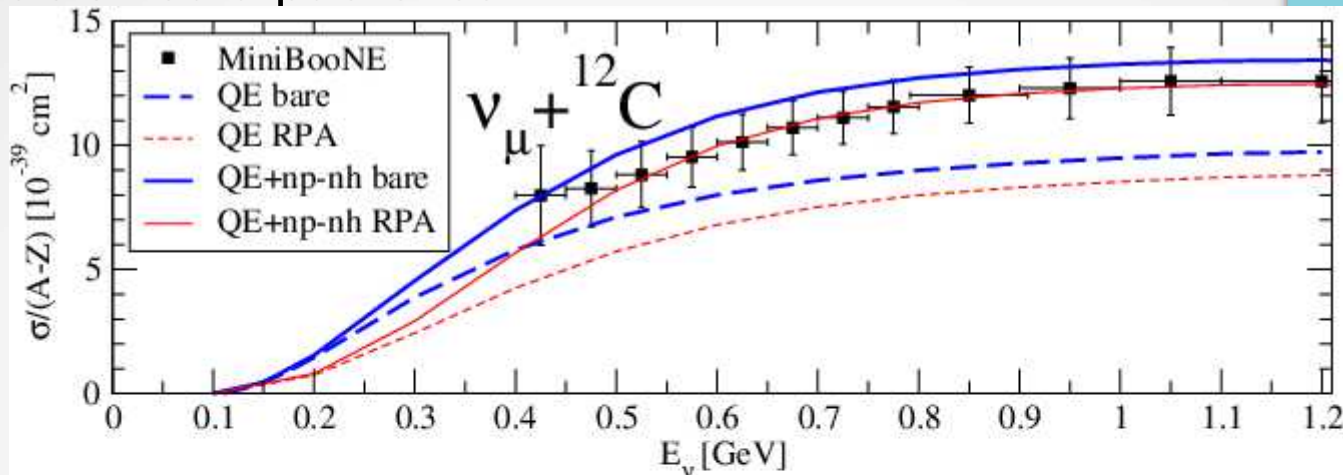
- Quenching of the responses by RPA
- *np-nh* important contributions in the "dip" region between QE peak and resonance region

(e, e') scattering



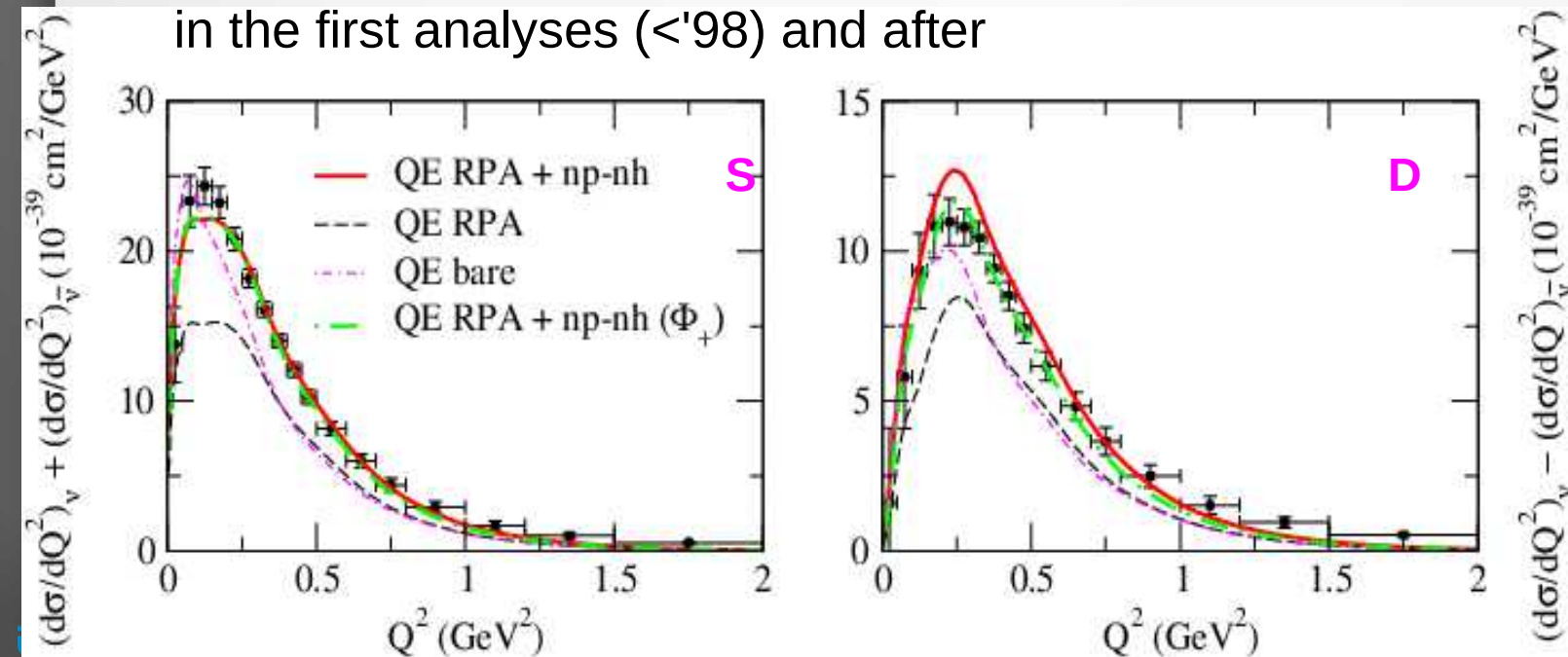
Comparison to MiniBOONE

- First precision data published



Neutrino and antineutrino quasi elastic interactions with nuclei,
M.Martini et al, arXiv : 1002.4538

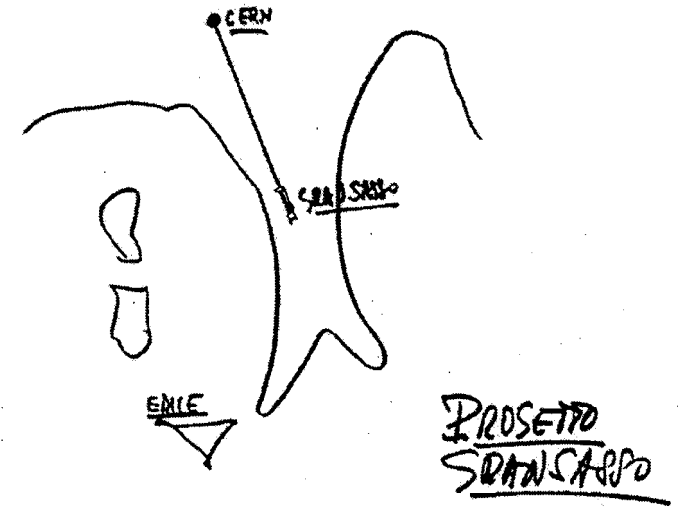
- Comparison with effective model proved the role of np - nh correlations both in the first analyses (<'98) and after



Neutrino versus antineutrino cross sections and CP violation,
M.Martini, M.Ericson, arXiv : 1501.02442

Part – II

CONDIZIONE LAVORO PUBBLICI E SENATO

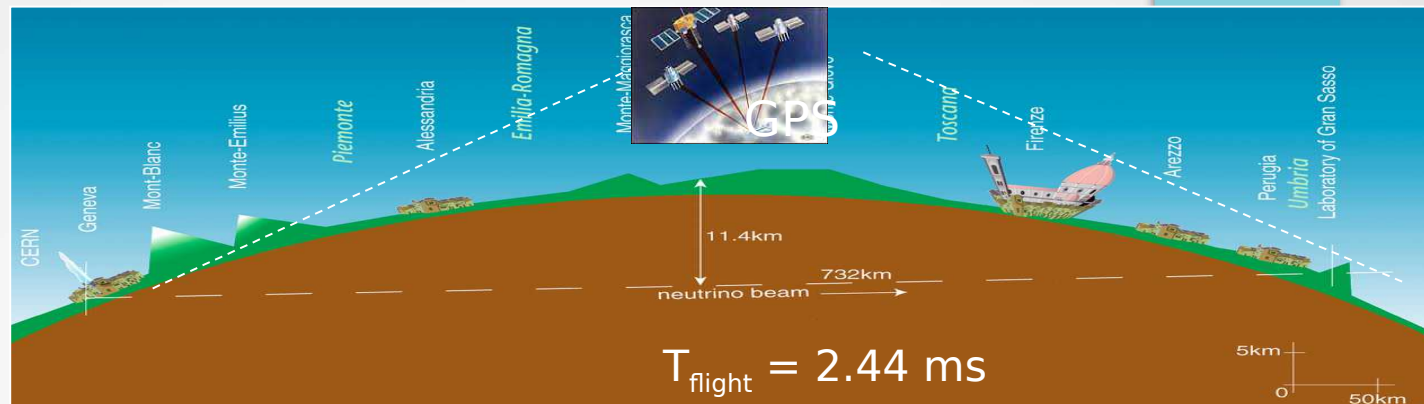


Sketch by A. Zichichi, 1979

ν oscillations

OPERA & the CNGS

Long-baseline experiments

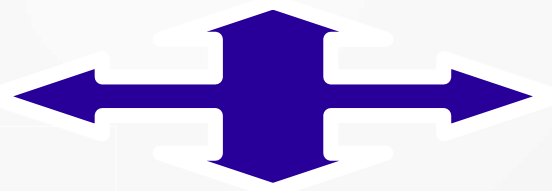


OPERA

$$-1.8 \times 10^{-6} < \frac{v_\nu - c}{c} < 2.3 \times 10^{-6}$$

Controlled beam
Fixed L, adjustable E
→ optimized L/E

Massive far detector
Events timestamps + GPS synchronization
t.o.f. measurements : constraints on v masses



T2K



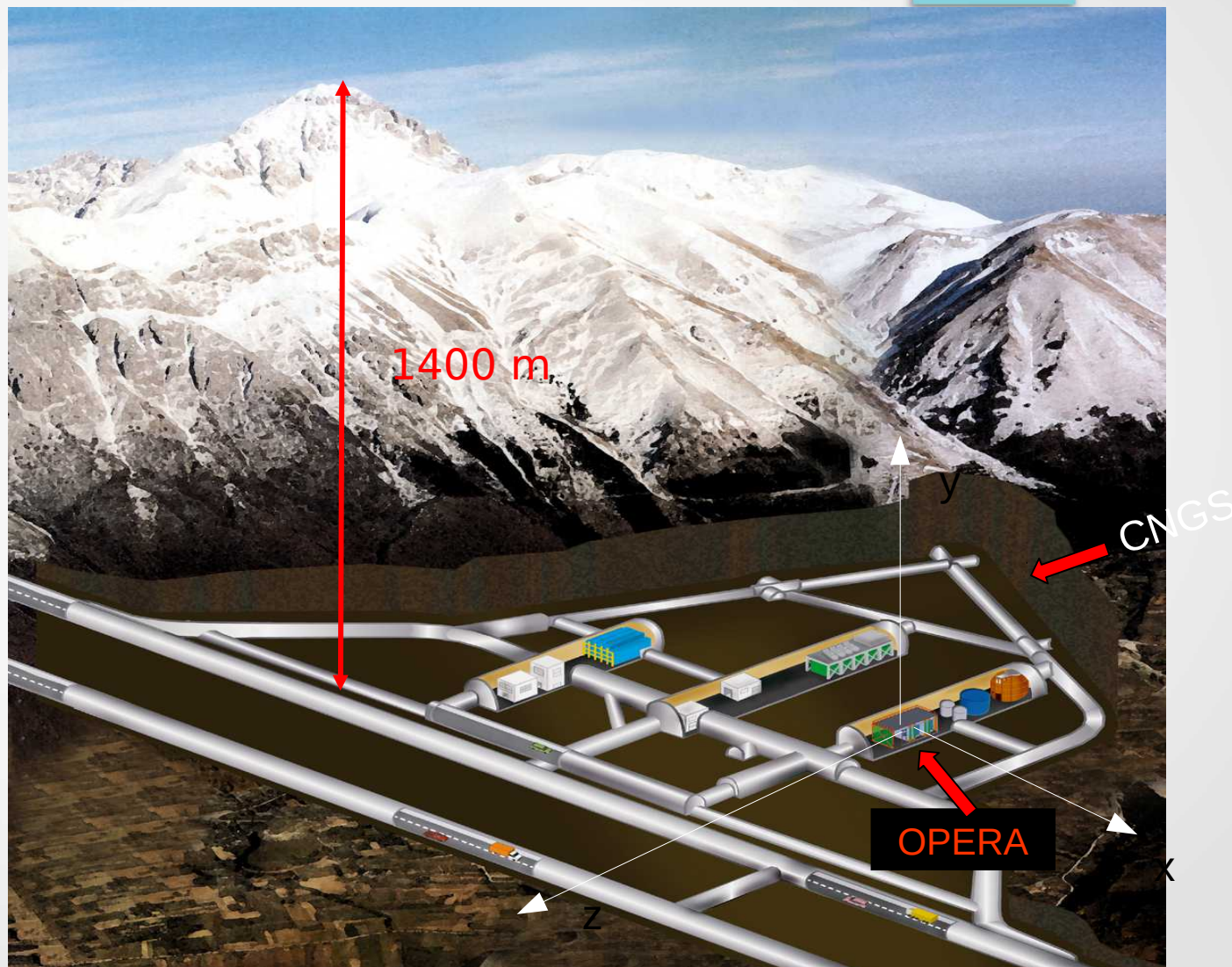
Measurement of the neutrino velocity with the OPERA detector in the CNGS beam using the 2012 dedicated data, OPERA collaboration, arXiv : 1212.1276

$$m_\nu^2 < 5.6 \text{ MeV}^2 / c^4$$

Upper bound on neutrino mass based on T2K neutrino timing measurements, T2K collaboration, arXiv : 1502.06605

Laboratori Nazionali del Gran Sasso

CNGS ?
CERN Neutrino to
Gran Sasso



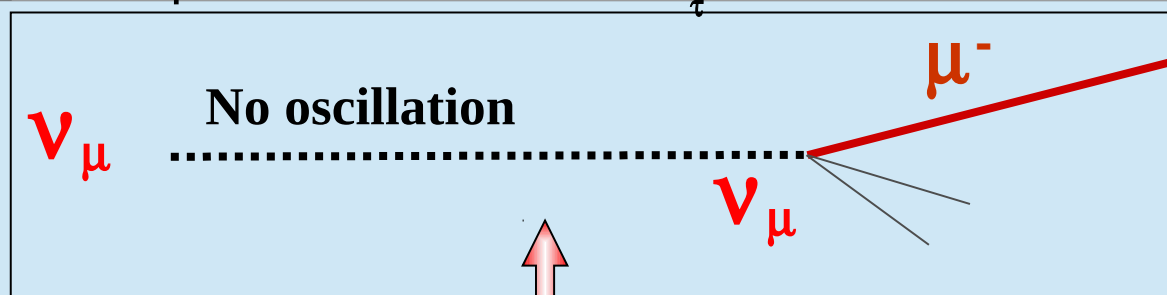
OPERA & CNGS (2000-2012)



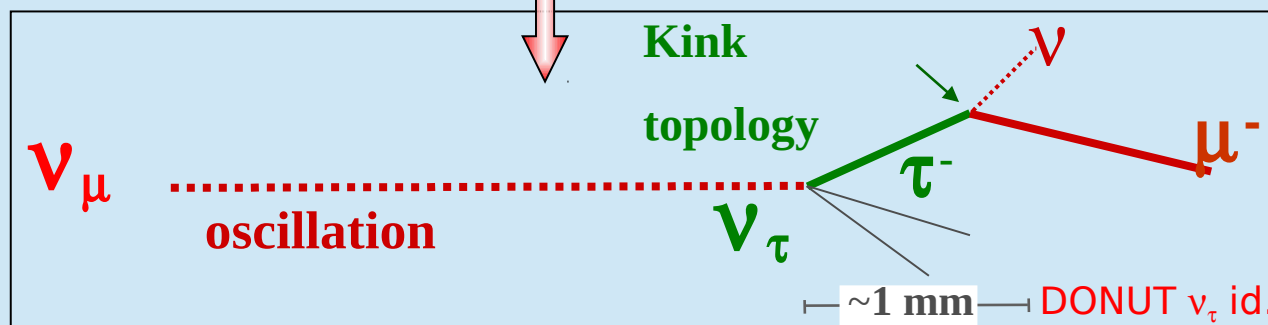
- Optimized experiment for the observation of $\nu_\mu \rightarrow \nu_\tau$
- Sensitive to atmospheric sector : $\Delta m_{23}^2, \theta_{23}$

$$U = \begin{pmatrix} 1 & 0 & 0 \\ 0 & c_{23} & s_{23} \\ 0 & -s_{23} & c_{23} \end{pmatrix} \begin{pmatrix} c_{13} & 0 & s_{13}e^{-i\delta} \\ 0 & 1 & 0 \\ -s_{13}e^{i\delta} & 0 & c_{13} \end{pmatrix} \begin{pmatrix} c_{12} & s_{12} & 0 \\ -s_{12} & c_{12} & 0 \\ 0 & 0 & 1 \end{pmatrix}$$

- Unique measurement of ν_τ CC interactions with nuclear emulsions



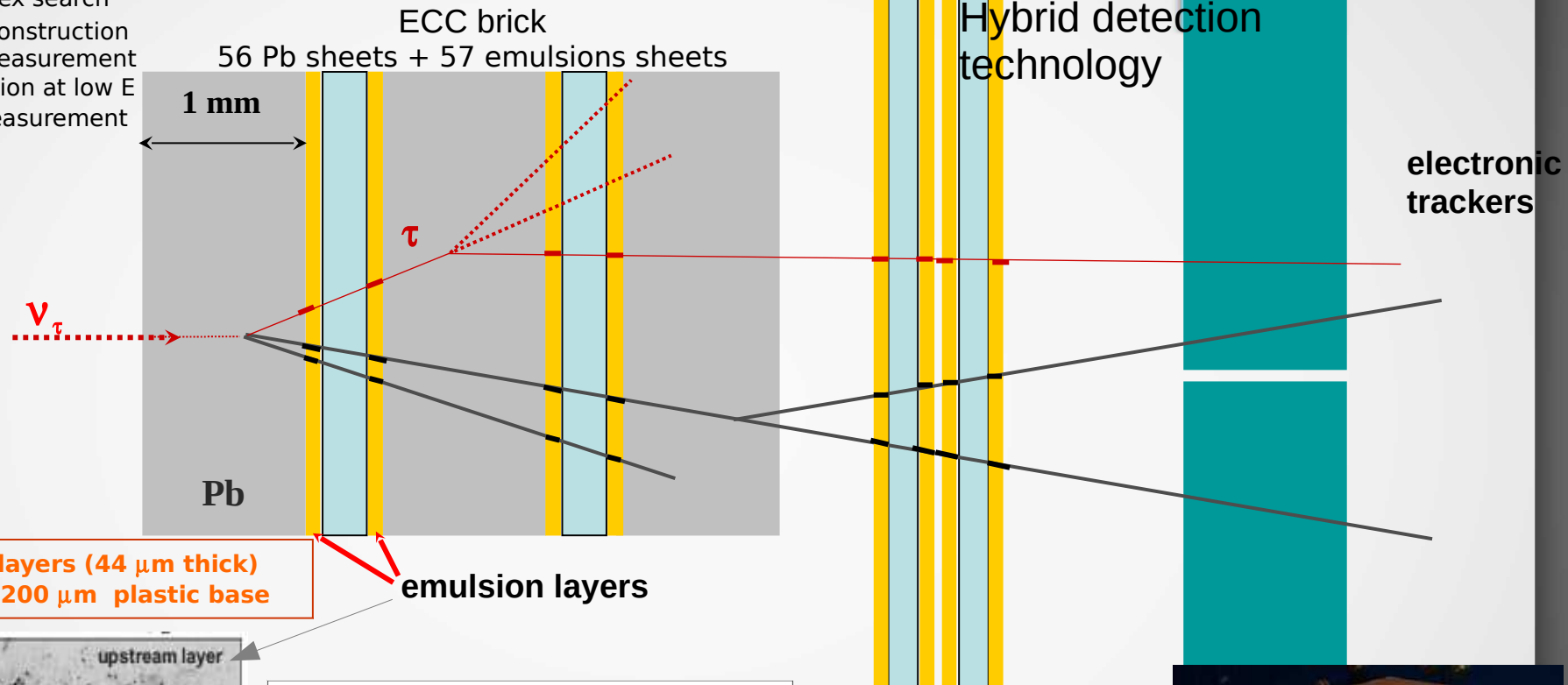
→ Would be the signal in a disappearance experiment



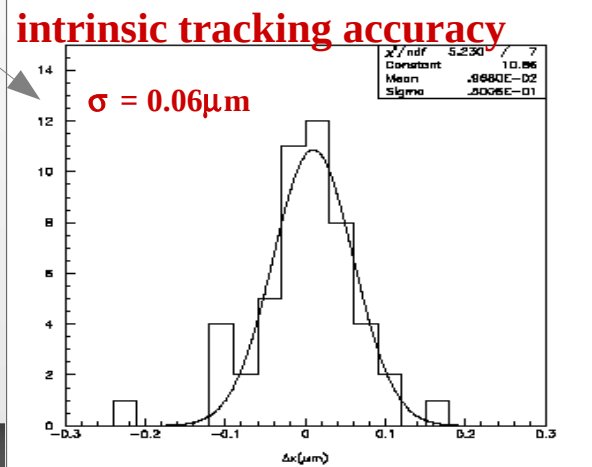
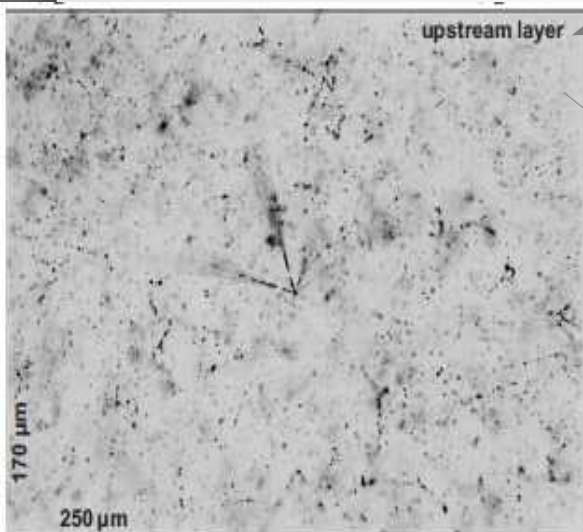
$$\left\{ \begin{array}{ll} \mu^- \nu_\tau \bar{\nu}_\mu & \text{BR} \sim 17\% \\ h^- \nu_\tau n(\pi^0) & \text{BR} \sim 49\% \\ e^- \nu_\tau \bar{\nu}_e & \text{BR} \sim 18\% \\ \pi^+ \pi^- \pi^- \nu_\tau n(\pi^0) & \text{BR} \sim 15\% \end{array} \right.$$

Oscillation Project with Emulsion tRacking Apparatus

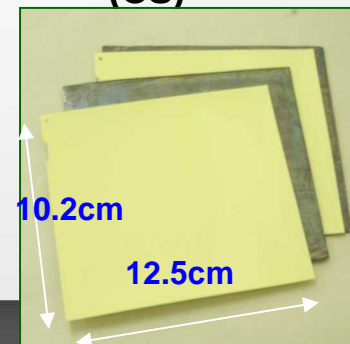
- > ν interaction vertex search
- > kink topology reconstruction
- > MCS momenta measurement
- > dE/dx e/π separation at low E
- > e id. and e/γ E measurement



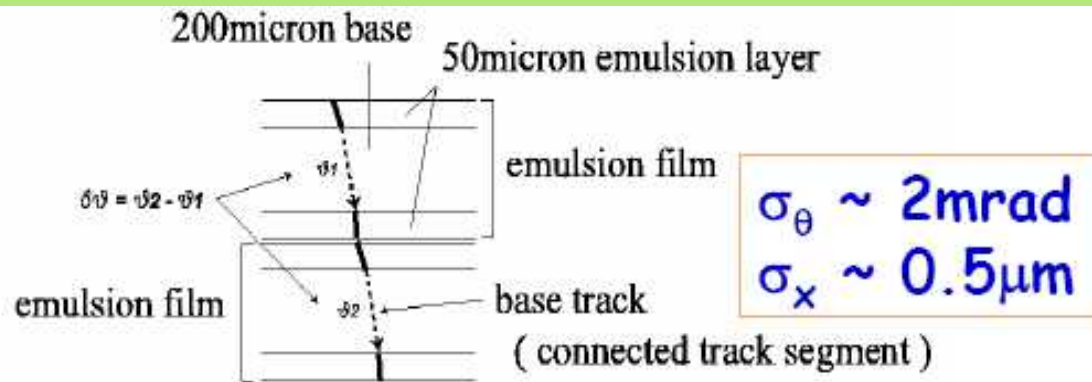
2 emulsion layers (44 μm thick)
poured on a 200 μm plastic base



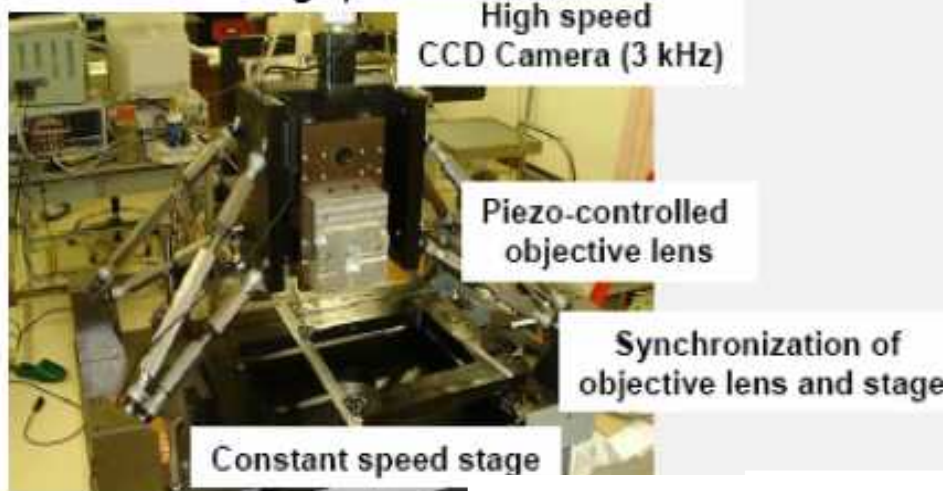
interface films
(CS)



Offline emulsion scanning



S-UTS at Nagoya



Dedicated hardware
Hard coded algorithms

European station



Customized commercial products
Software algorithms

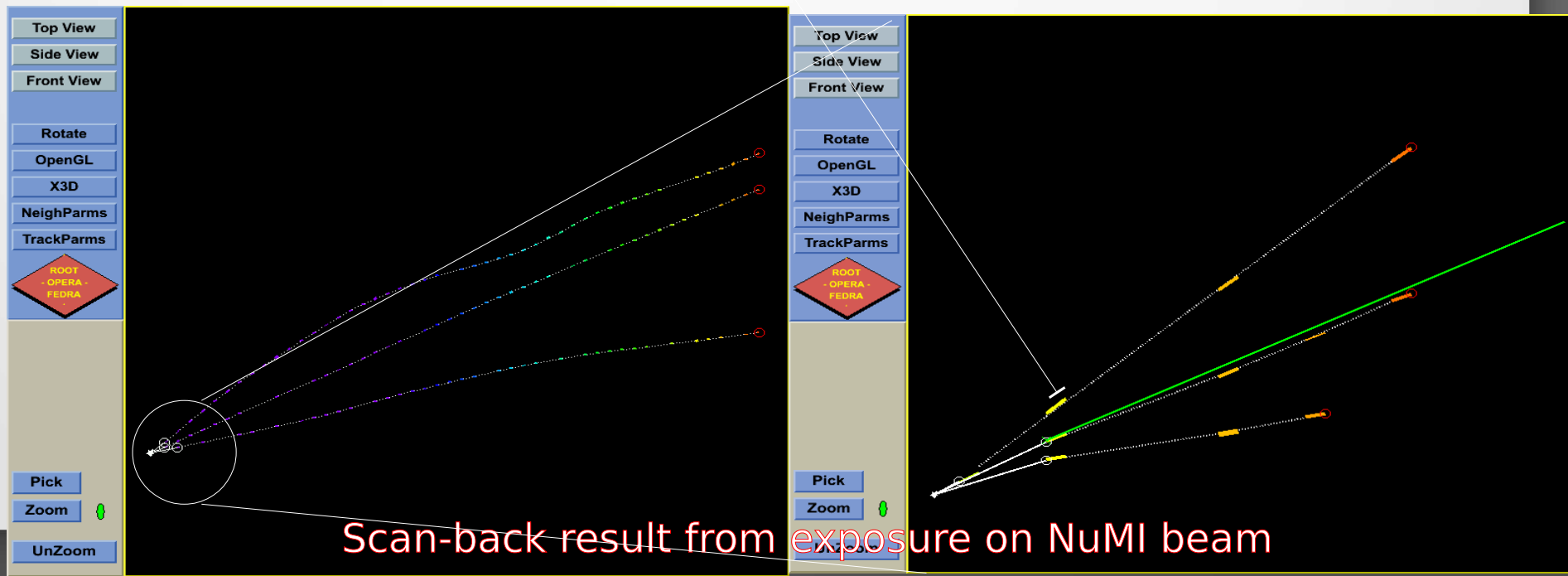
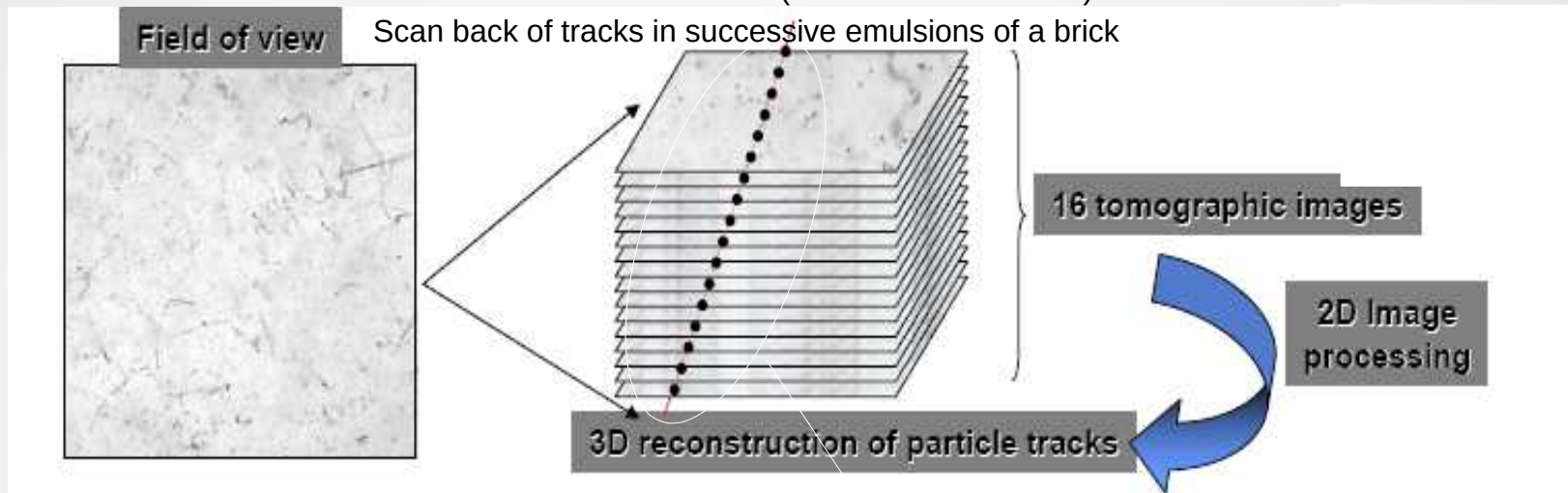
Two different systems (both operational) are running for scanning systems :
“hard”-coded oriented (Japan) or “soft”-coded oriented (Europe).
Both systems are ready and working at more than 20cm²/hour (10 required).

Offline emulsion scanning

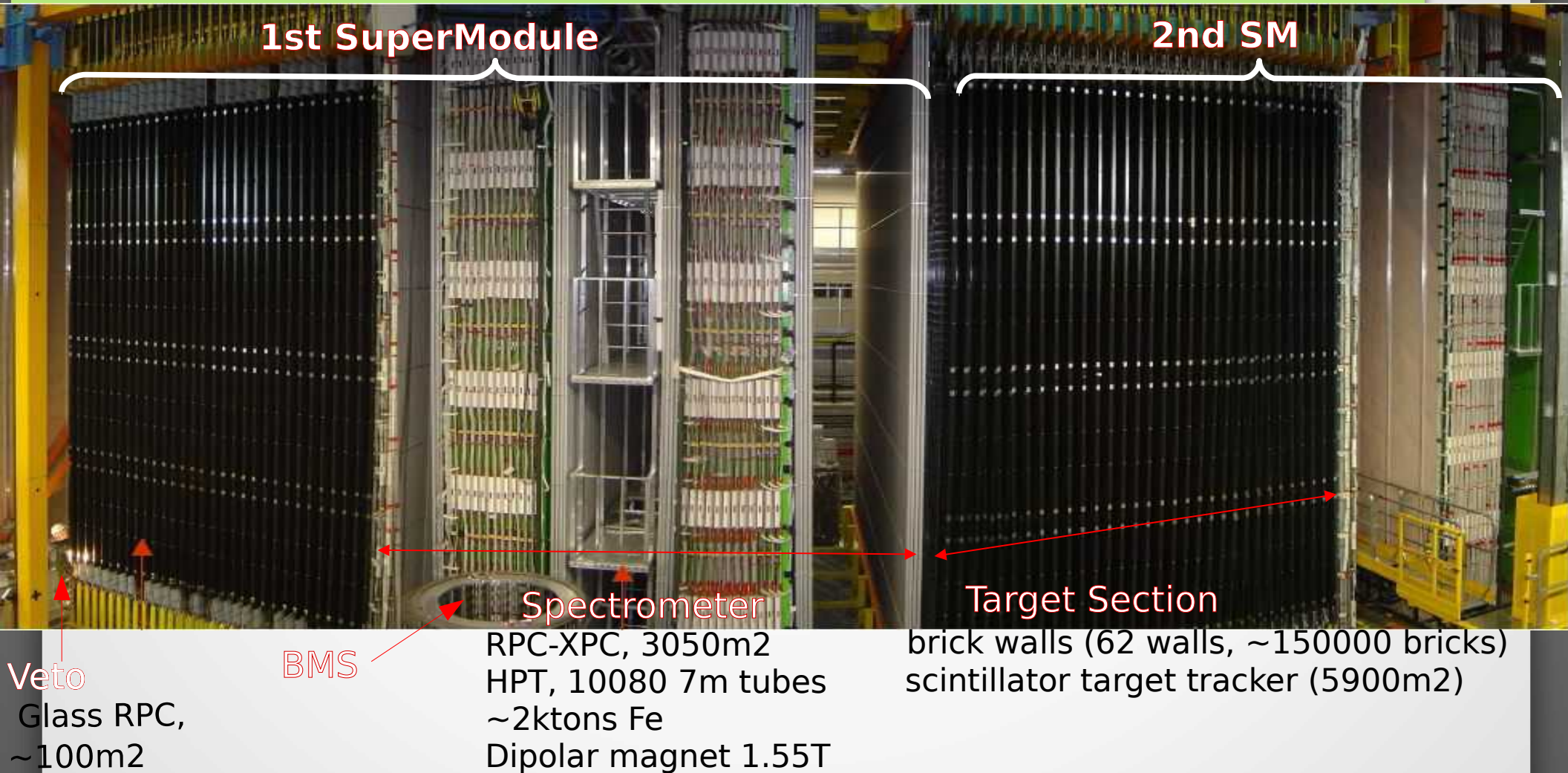
Tracks reconstruction by analysis of ~16 “slices” per emulsion

Identification of “base”-tracks (both emulsion sheets)

Scan back of tracks in successive emulsions of a brick



The OPERA detector



Veto
Glass RPC,
~100m²

BMS

Spectrometer
RPC-XPC, 3050m²
HPT, 10080 7m tubes
~2ktons Fe
Dipolar magnet 1.55T

Target Section
brick walls (62 walls, ~150000 bricks)
scintillator target tracker (5900m²)

T.T. : **trigger**, neutrino interactions localization (**brick finding**), kinematics

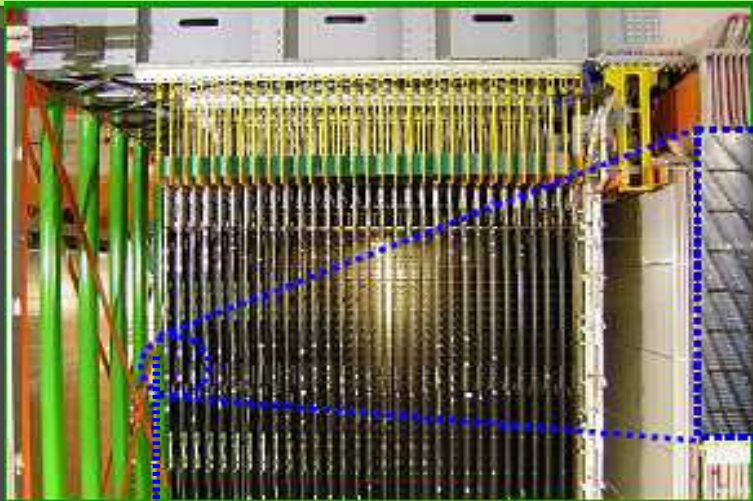
Spectrometer : **μ id.**, charge and momentum measurement

Bricks : **ν vertex** id., decay **kink** search, **kinematics**, **e/π** sep., **e/γ** E meas.

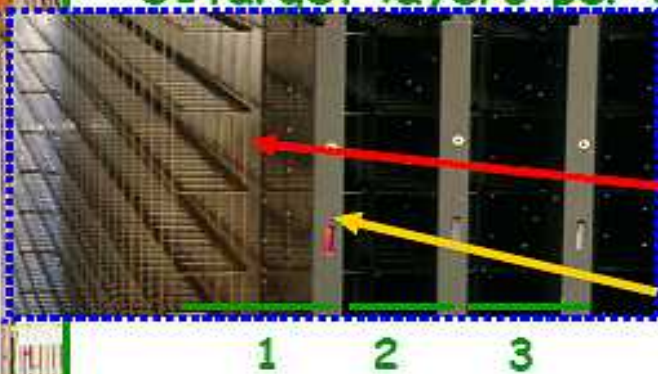
Bricks technology



Another brick in the wall...



The target structure contains the bricks.
31 target layers per supermodule



1 target layer is made of:

1 brick wall (52x64 bricks)

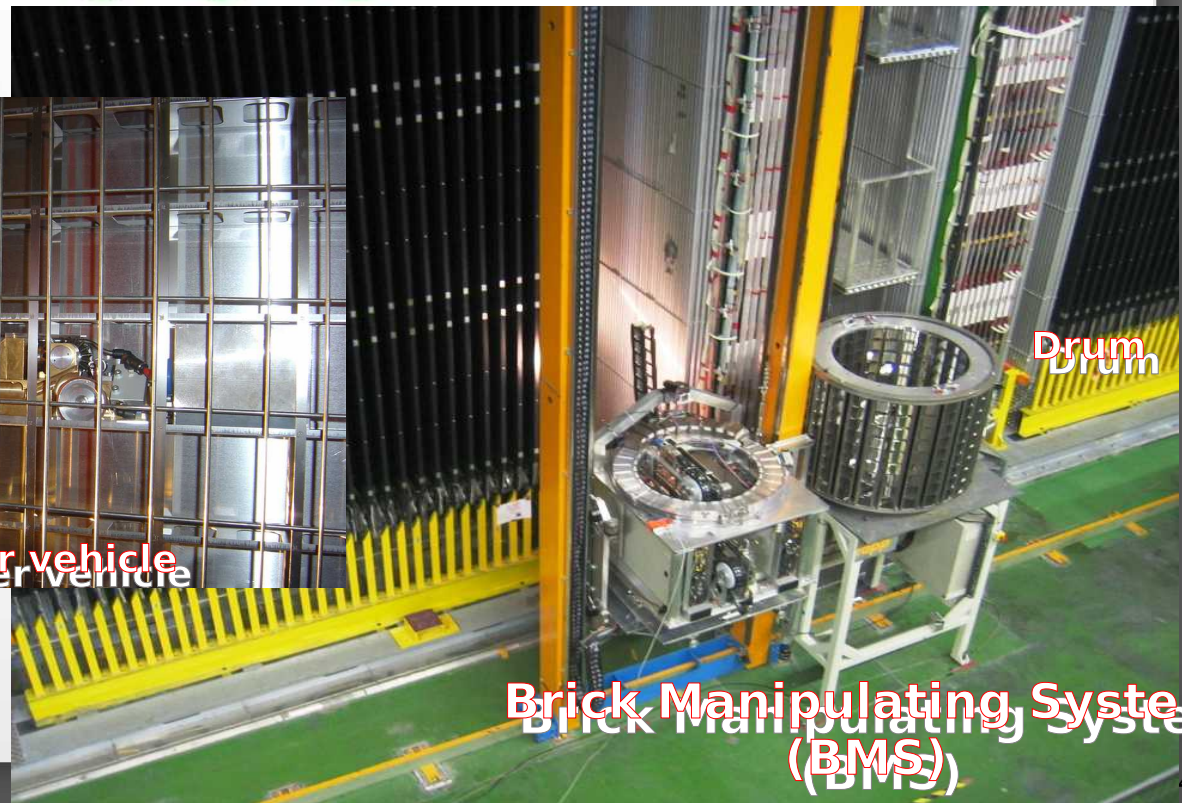
1 scintillator detector plane
(target tracker)



1st brick wall under filling
1st brick wall under filling



Vacuum sucker vehicle



Drum

Brick Manipulating System
(BMS)

OPERA construction



Magnet Assembly in Hall C september 2003

September '03

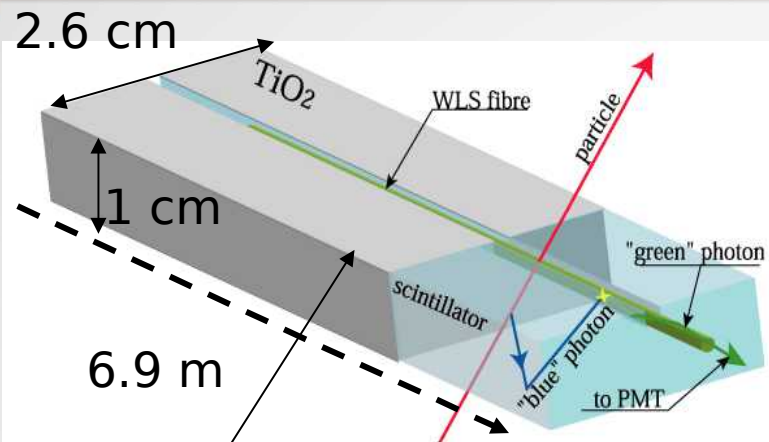


September '04

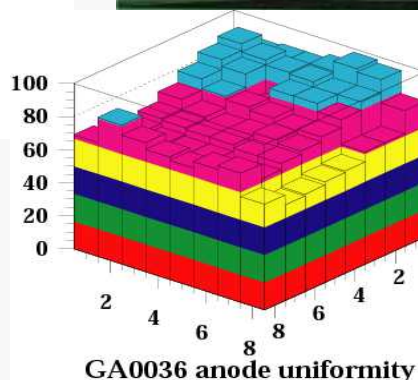
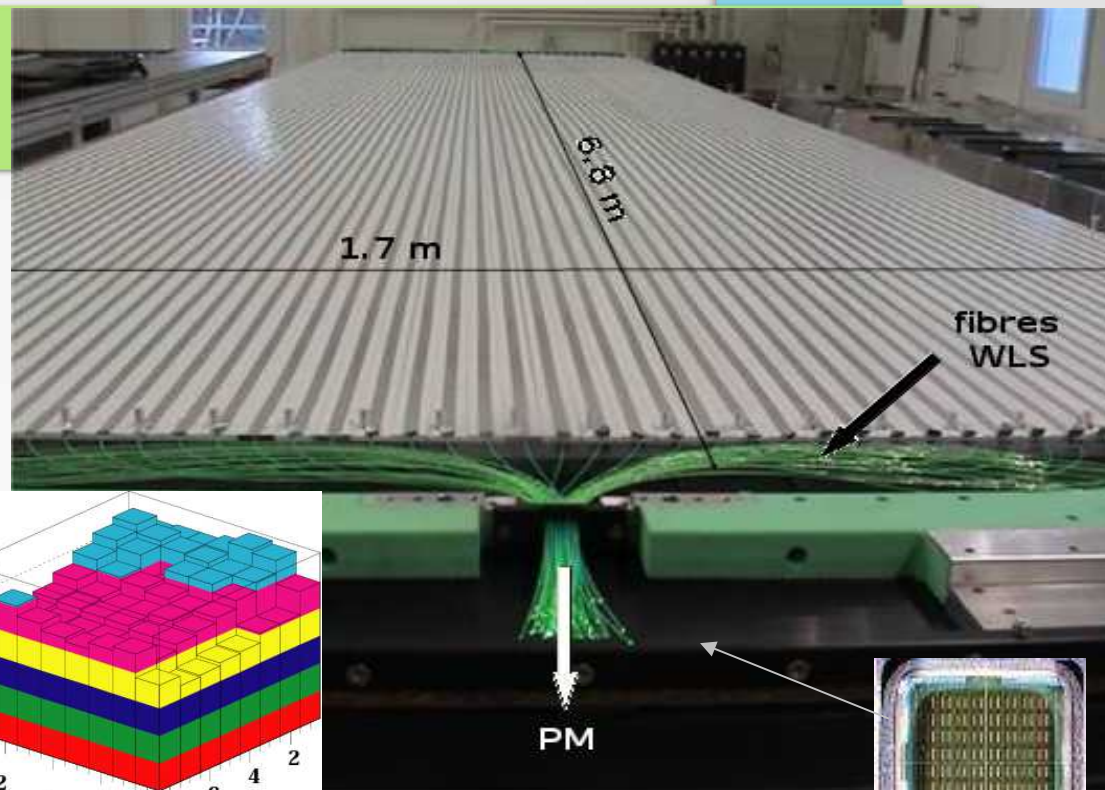


November '05

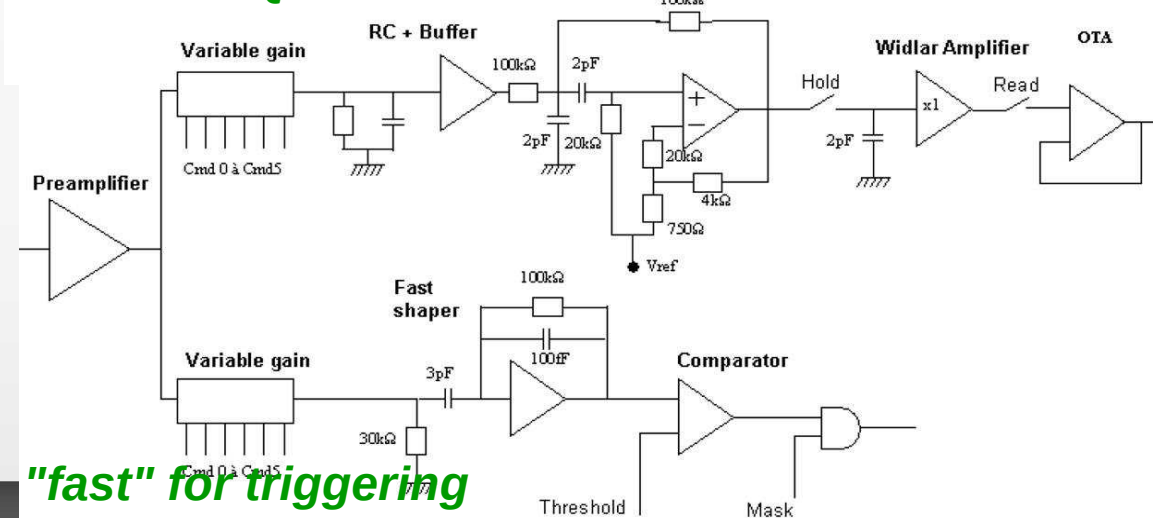
T.T. R/O



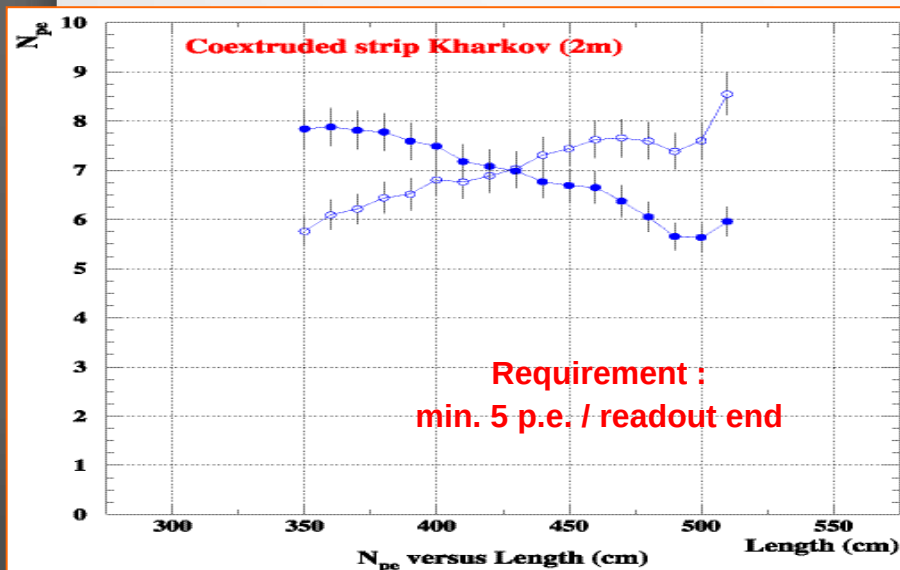
Extruded plastic scintillator strip



"slow" for Q measurement



"fast" for triggering

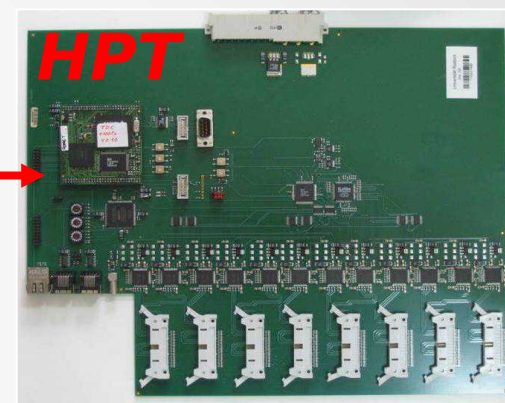


DAQ general features

The distributed DAQ is based on Ethernet. 1200 sensors in a standard Ethernet network (1st HEP application).
The basic “element” of the system is a mezzanine board embedding FPGA, FIFO, μ -processor (AXIS)



R/O : RPC tracker



R/O : drift tubes

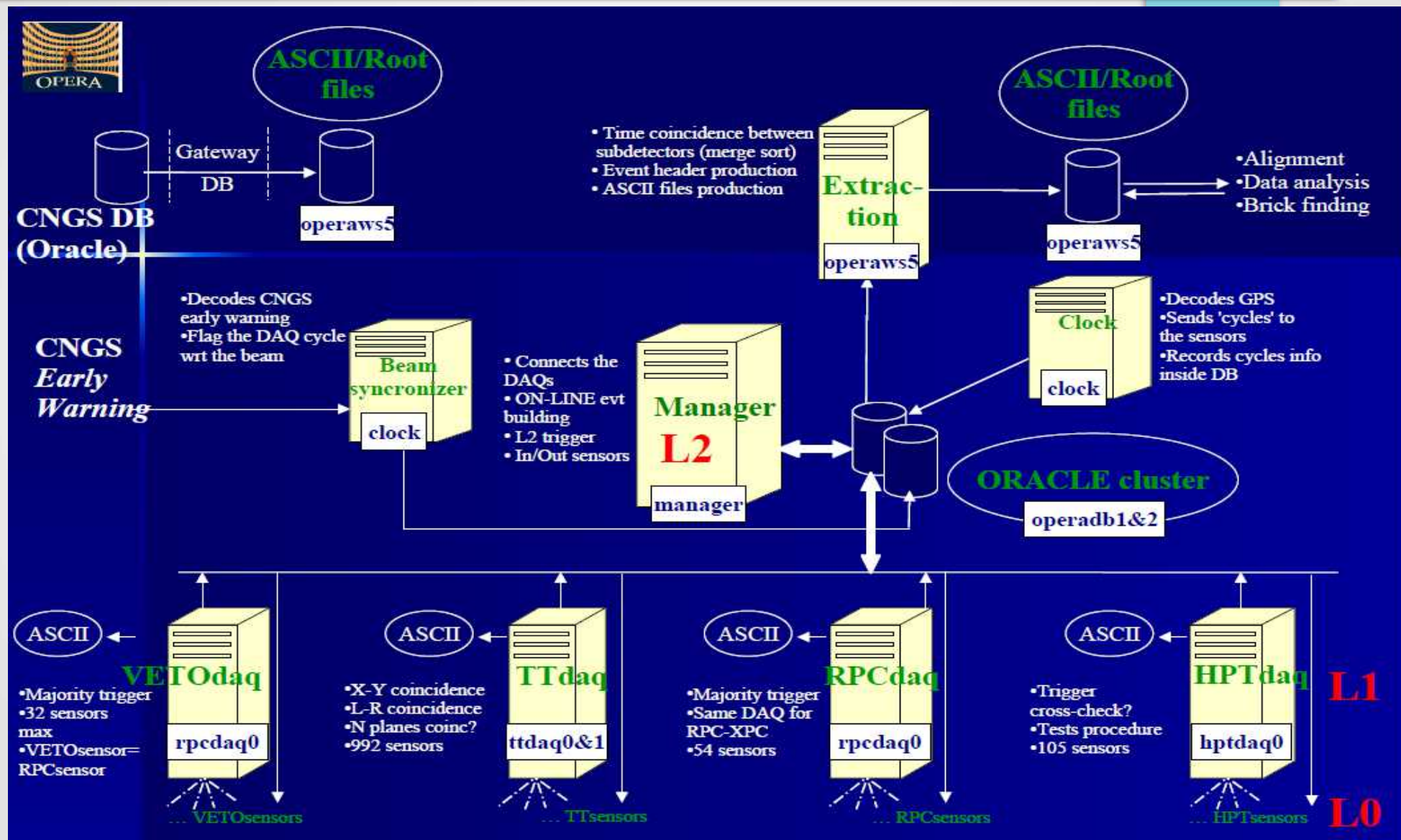


R/O : scintillator + WLS + MaPMT

The client/server protocol used relies on the CORBA standard implemented in C++ with interfaces into postgresQL and Oracle database.

This software is completely object oriented and uses the Interface Description Language (IDL) to describe the distributed objects independantly of the programming language. InterORB protocols guarantee interoperability.

Clock distribution & network architecture



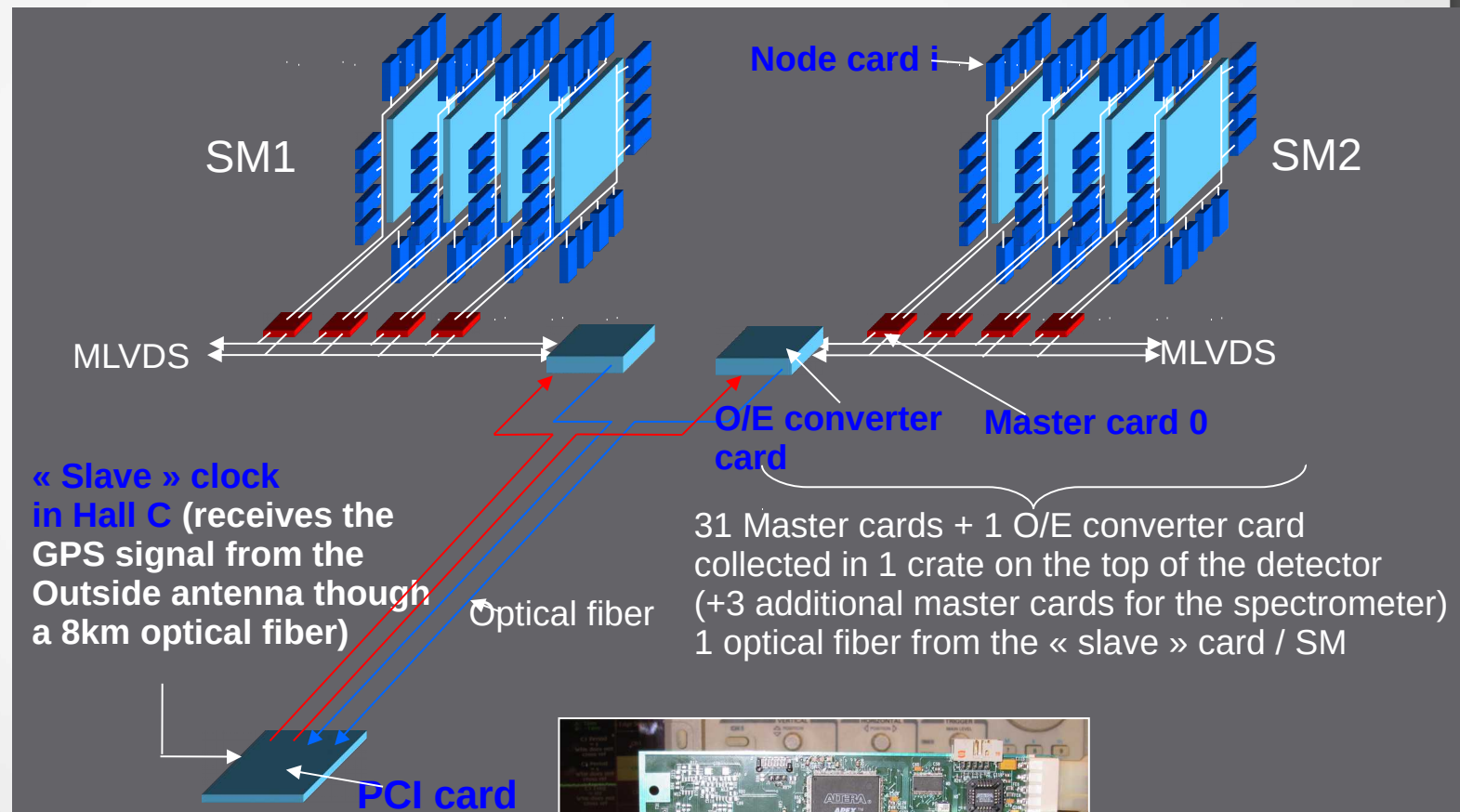
Clock distribution & network architecture

Each individual node runs a local 100MHz clock generated via a common 20MHz clock sent from a precise and stable oscillator.

Dedicated PCI board

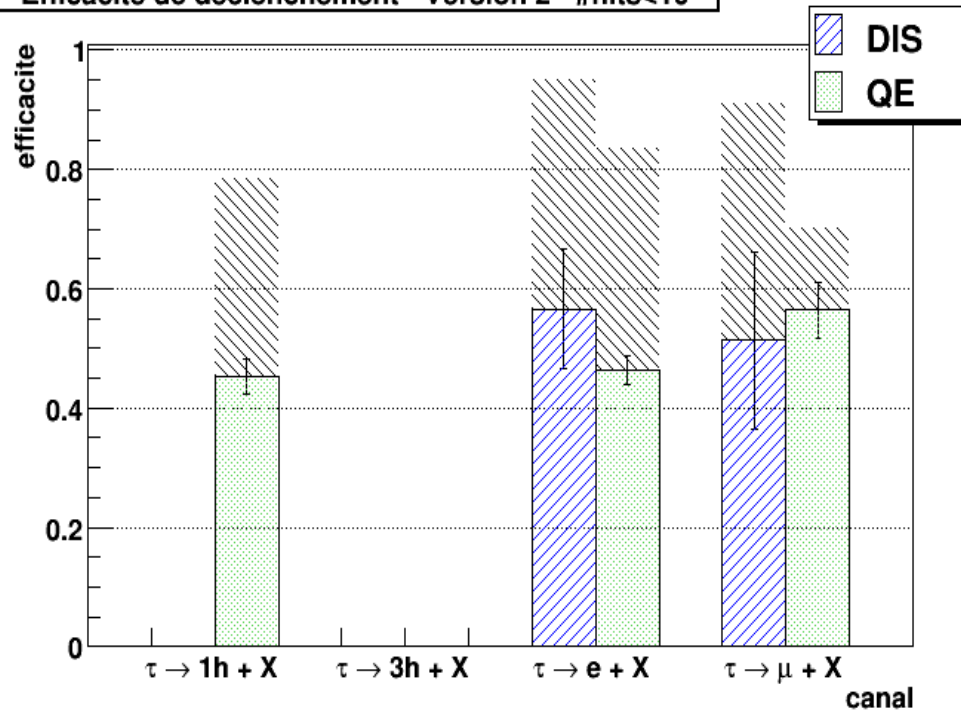
Clock signal locked on the GPS

Commands encoding



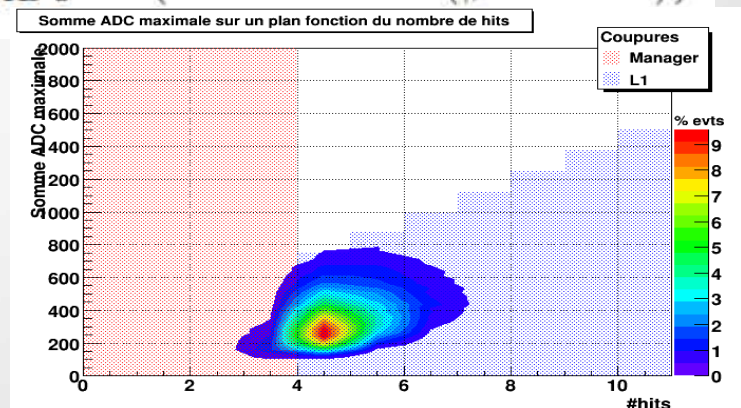
DAQ conditions optimized (T.Brugière thesis)

Efficacité de déclenchement - Version 2 - #hits<10



canal		avant optimisation (%)	après optimisation (%)
$\tau \rightarrow 1h + X$	dis	NA	NA
	qe	25.81 ± 2.63	45.33 ± 3.00
$\tau \rightarrow 3h + X$	dis	NA	NA
	qe	NA	NA
$\tau \rightarrow e + X$	dis	7.73 ± 5.41	56.58 ± 10.04
	qe	31.90 ± 2.24	46.45 ± 2.40
$\tau \rightarrow \mu + X$	dis	40.57 ± 14.57	51.32 ± 14.83
	qe	35.88 ± 4.58	56.41 ± 4.73

$$Somme_{ADC} > (500 + 125 \times (\#hits - 2))$$



DAQ trigger conditions optimized

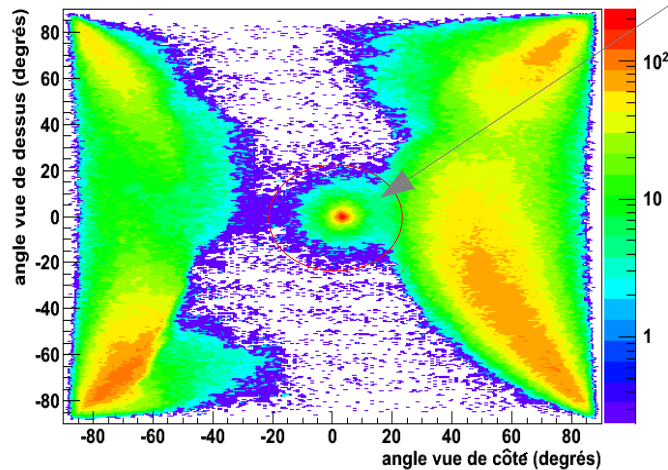
Low multiplicity events trigger conditions upgraded :
 ~15% low multiplicity events in channel $\tau \rightarrow e$ QE
 ~20% low multiplicity events in channel $\tau \rightarrow h$ QE

New efficiency = $99.33 \pm 0.05\%$

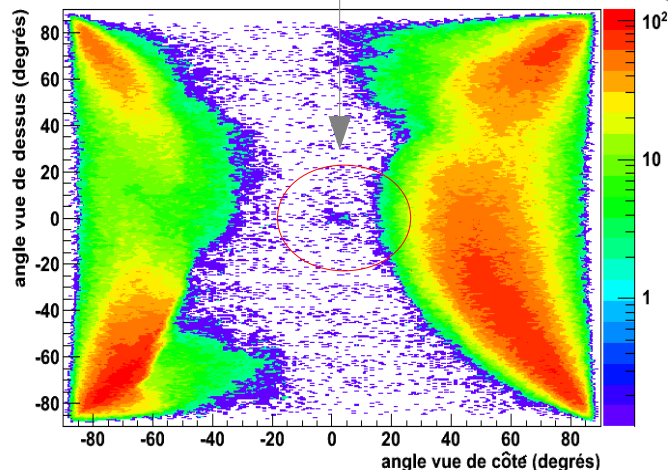
Data Analysis : off-beam physics (T.Brugière thesis)

Beam events

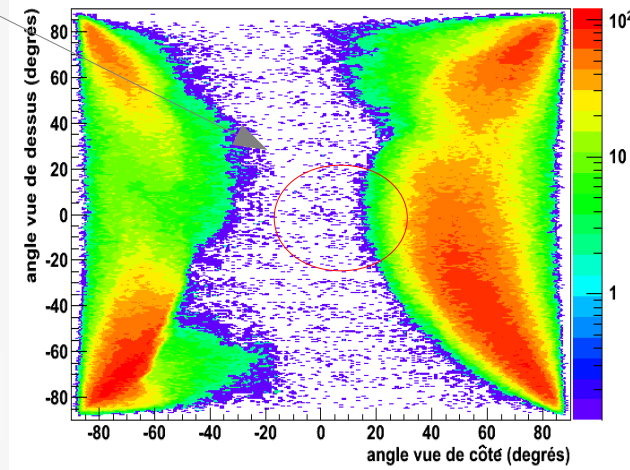
Événements dans le plan (angle vue de côté, angle vue de dessus)



Événements non en temps dans le plan (angle vue de côté, angle vue de dessus)



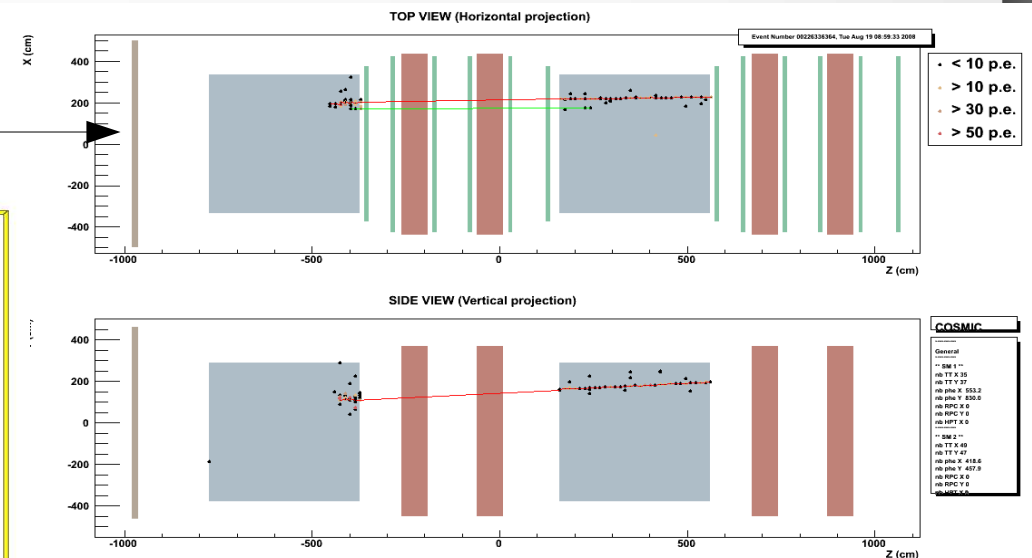
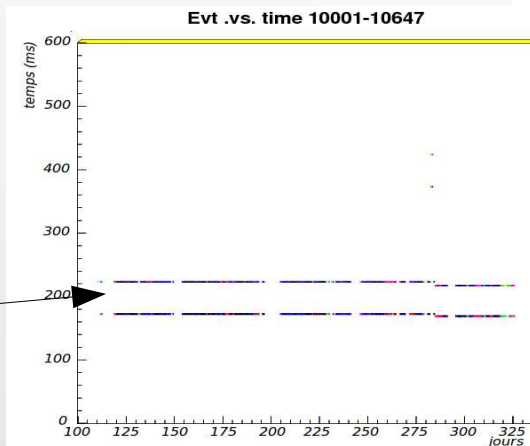
Événements non en temps dans le plan (angle vue de côté, angle vue de dessus) avec le nouveau marquage



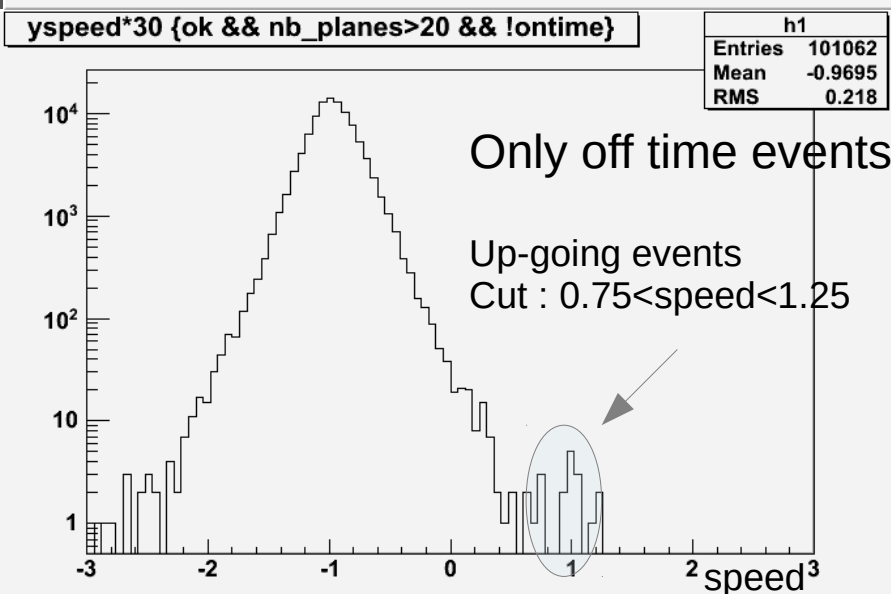
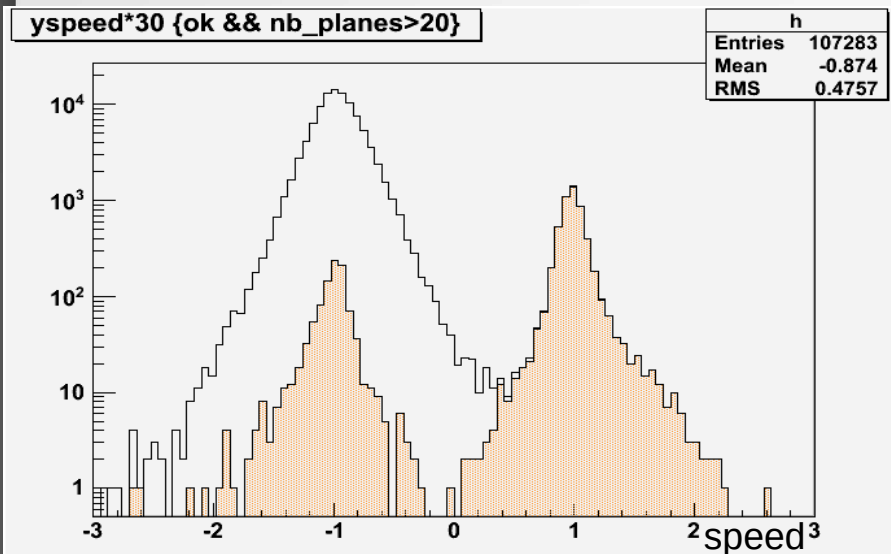
Beam events :

- low X angle
- low Y angle

CNGS-OPERA
time correlation
(event time position
within DAQ cycle)

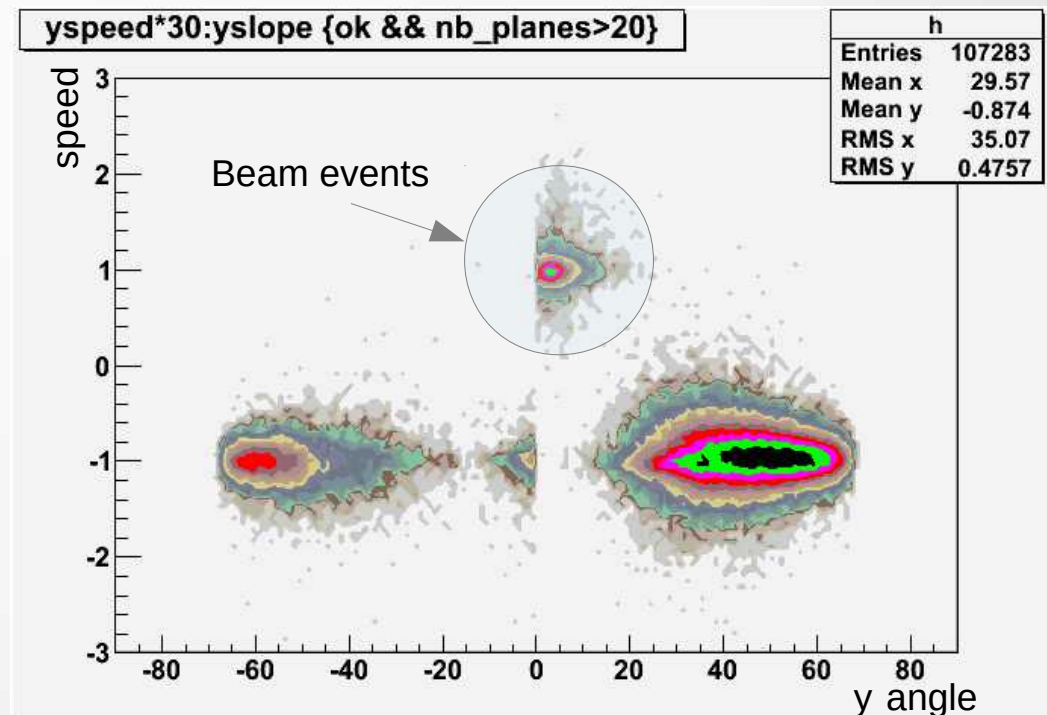


Data Analysis tof analysis (T.Brugière thesis)



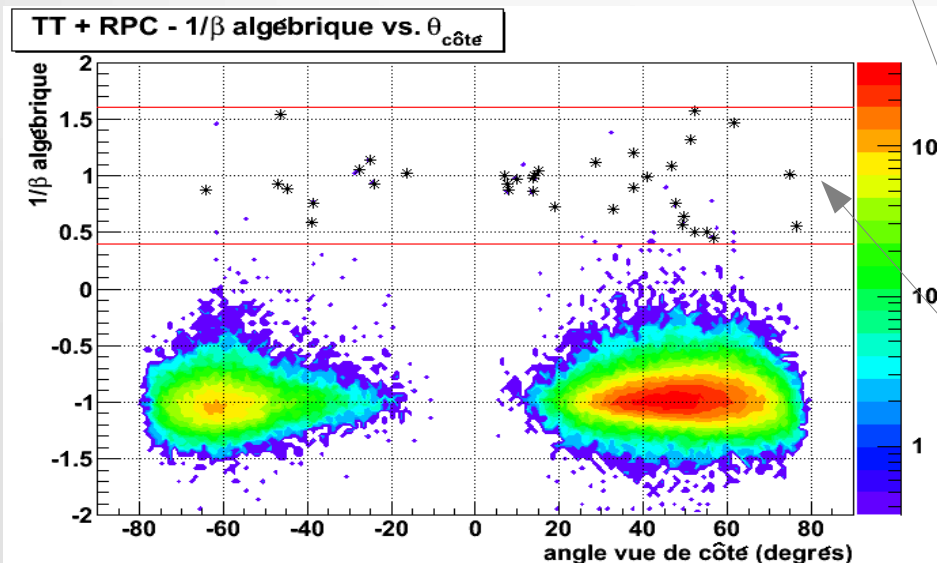
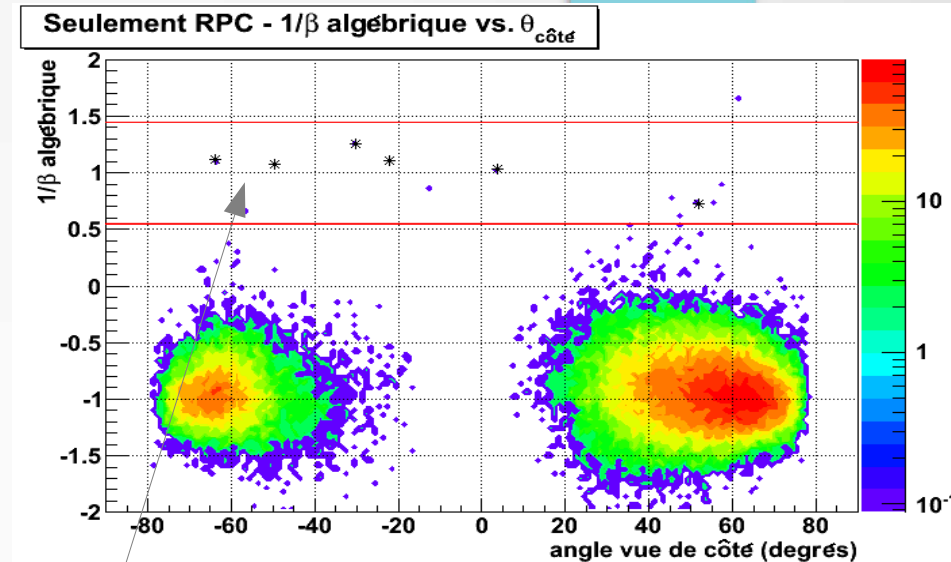
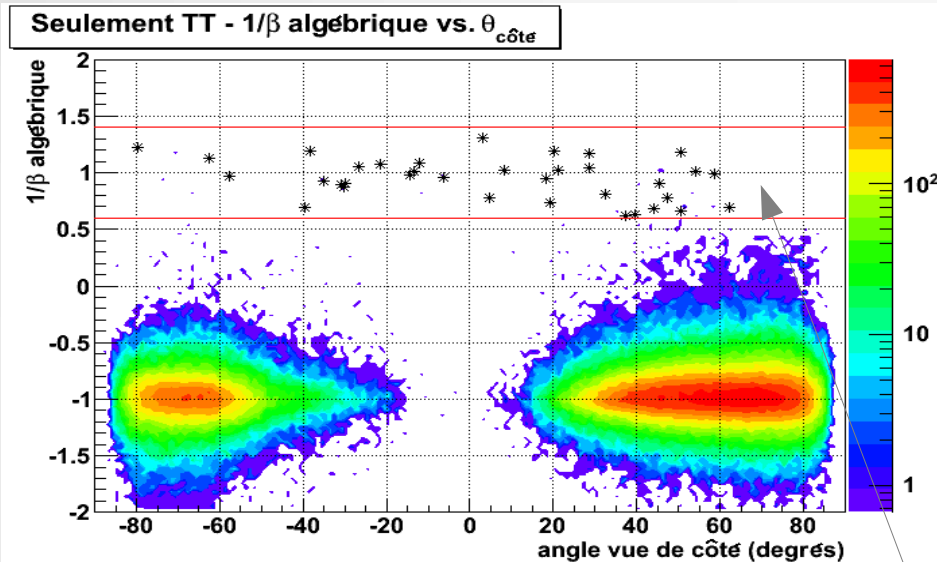
« speed » plots convention :

- -1 peak : down-going particles
- +1 peak : up-going particles



Speed function as angle for side view

Results : up-going candidate events

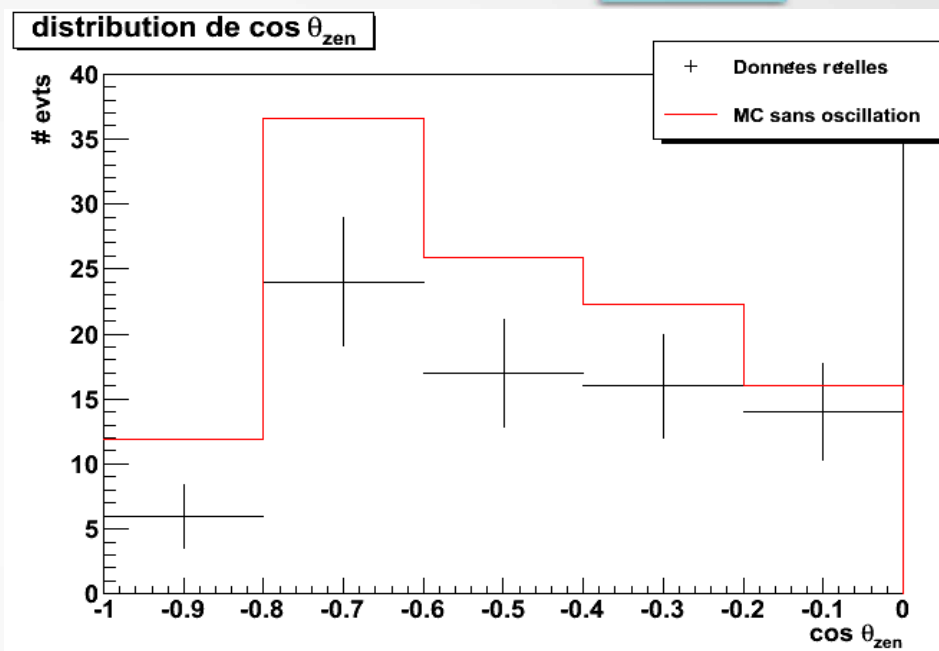
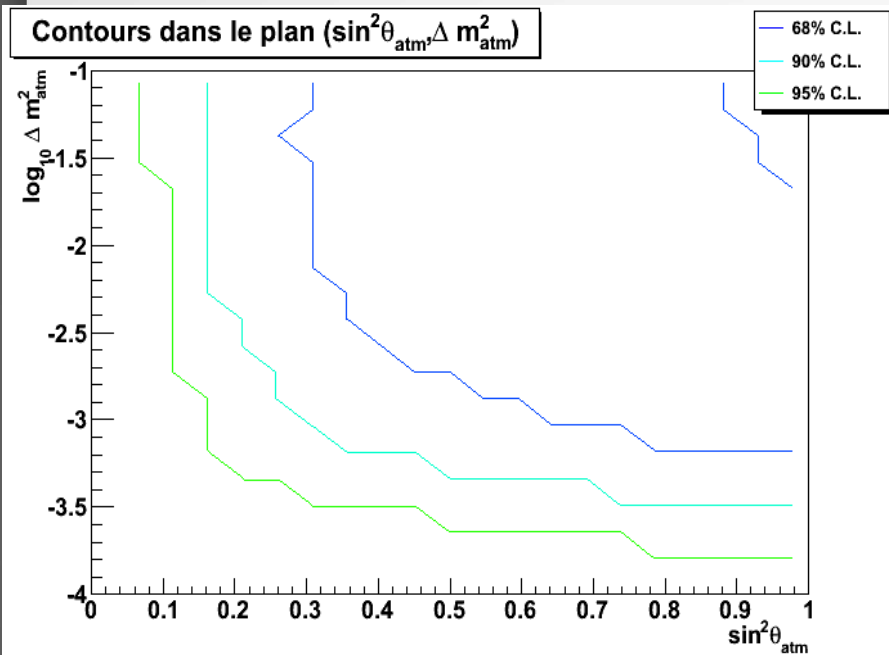


Total number : 77

- TT-only events : 35
- RPC-only events : 6
- TT+RPC events : 36
(reminder : +1 ↔ up-going)

Total effective acquisition time : 1015 days

Data Analysis (Feldman-Cousins method)



$$\chi^2 = \sum_{i=0}^{i<5} \frac{(n_i^{DATA} - n_i^{MC} - b_i)^2}{n_i^{MC}}$$

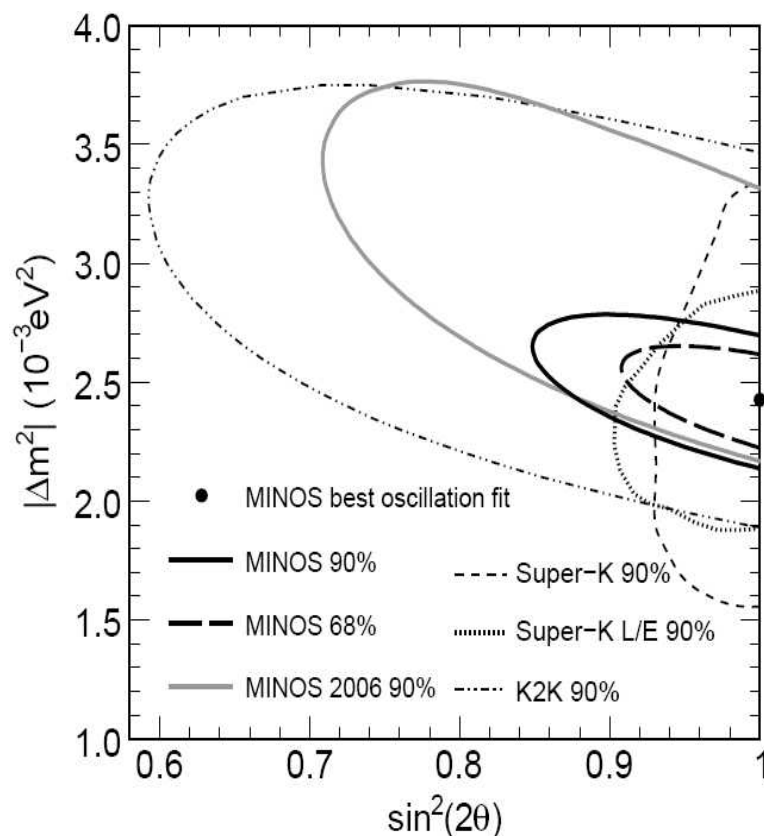
$$\Delta m_{atm}^2 = 3.5 \cdot 10^{-3} \text{ eV}^2$$

$$\sin^2 \theta_{atm} = 1.0$$

→ Data / MC « w/o oscillation »
→ $\cos \theta_{zen}$ distribution

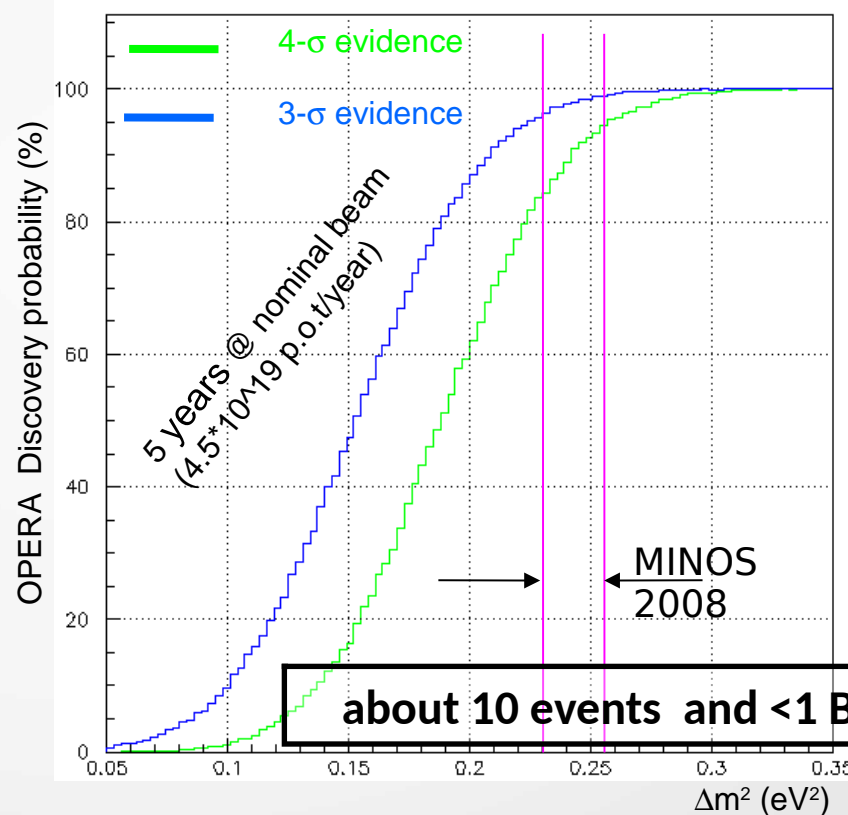
→ Model w/o oscillation rejected at 98.5% C.L.

Beam-physics potential



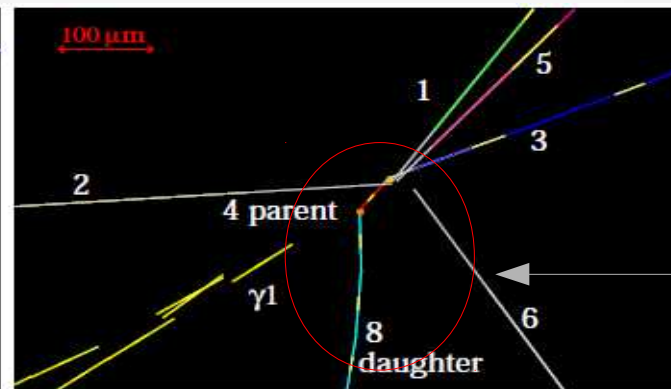
$$|\Delta m^2| = (2.43 \pm 0.13) \times 10^{-3} \text{ eV}^2$$

$$P(\nu_\mu \rightarrow \nu_\tau) \cong \sin^2(2\theta_{23}) \cos^4(\theta_{13}) \sin^2\left(\frac{1.27 \Delta m_{32}^2 L(\text{Km})}{E(\text{GeV})}\right)$$

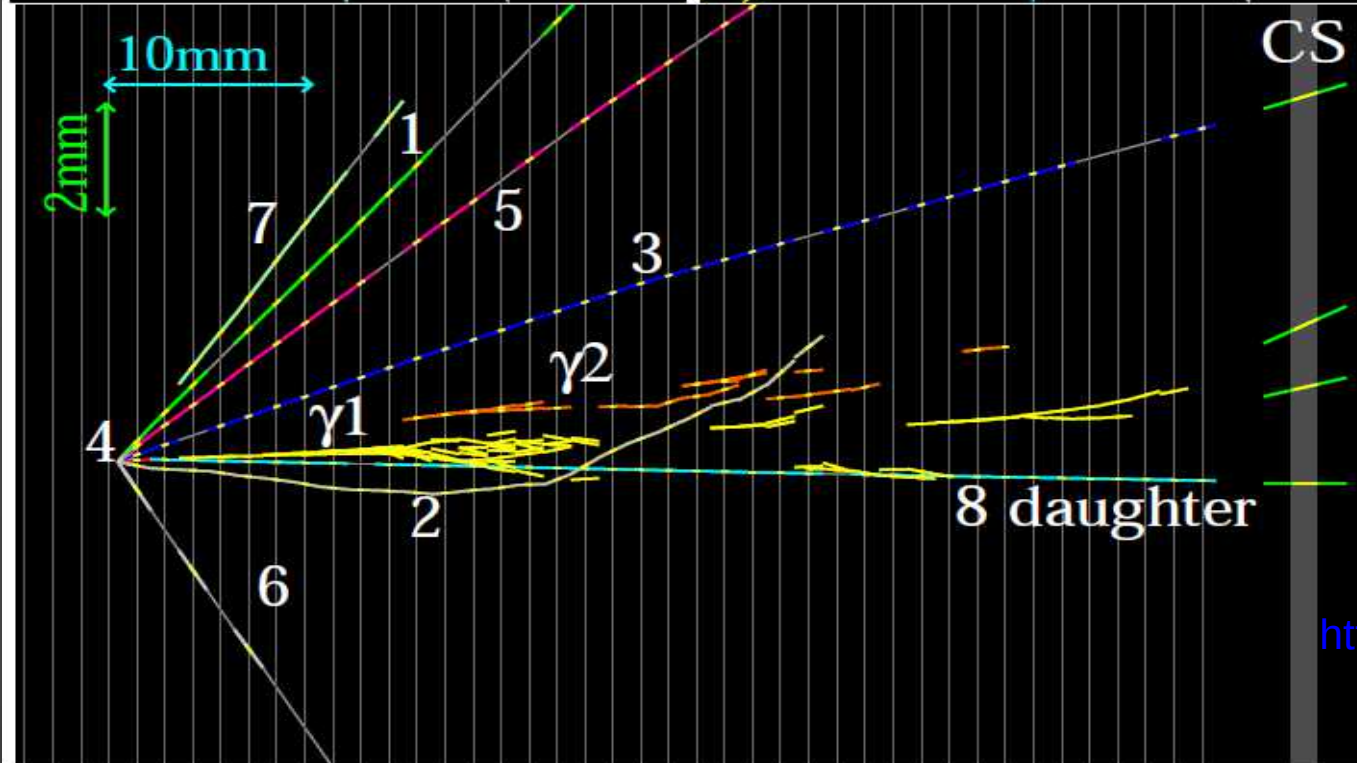


→ Beam optimized to maximize the nbr of ν_τ interactions

First candidate observation



"Kink" topology



First direct observation
of neutrino oscillations

<http://lanl.arxiv.org/abs/1006.1623>

4th candidate detected

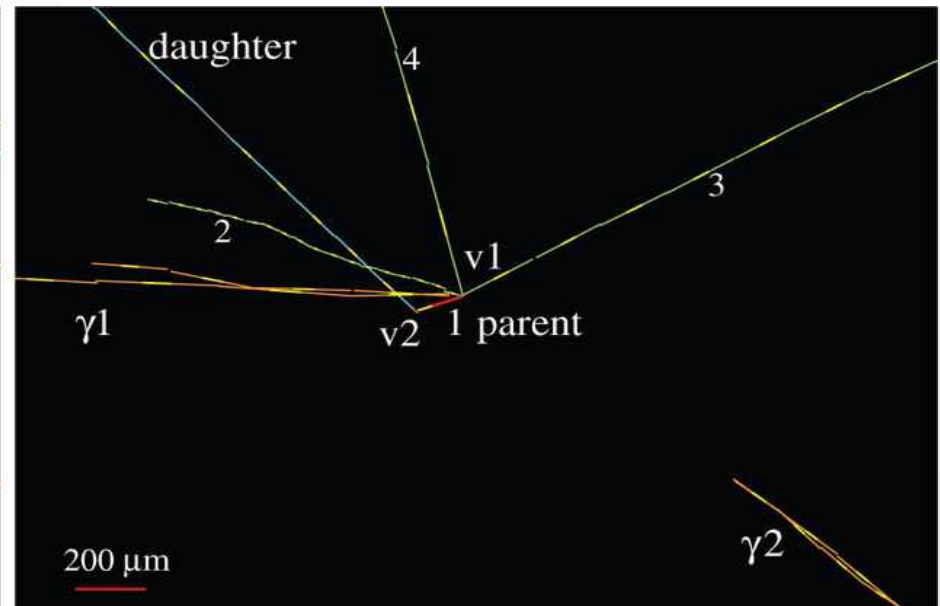
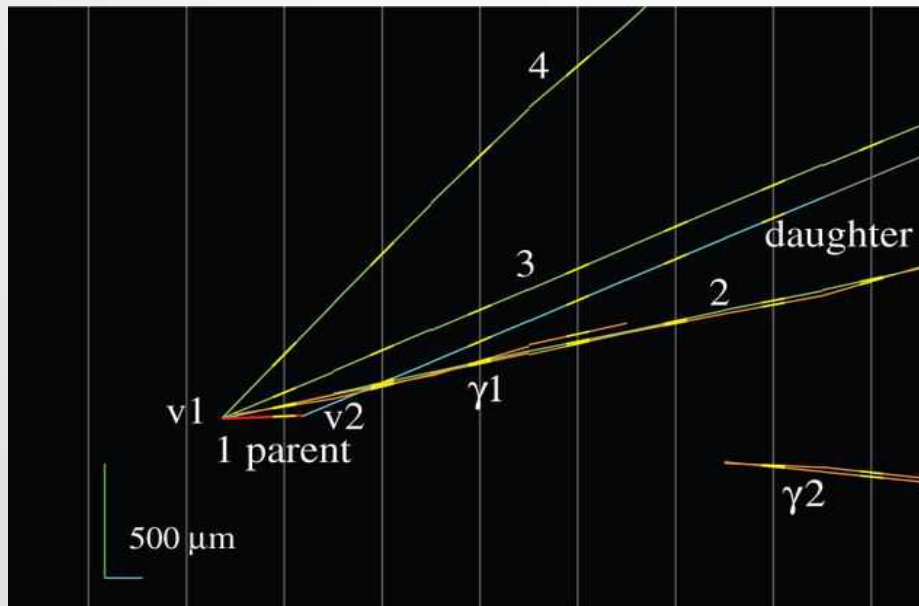
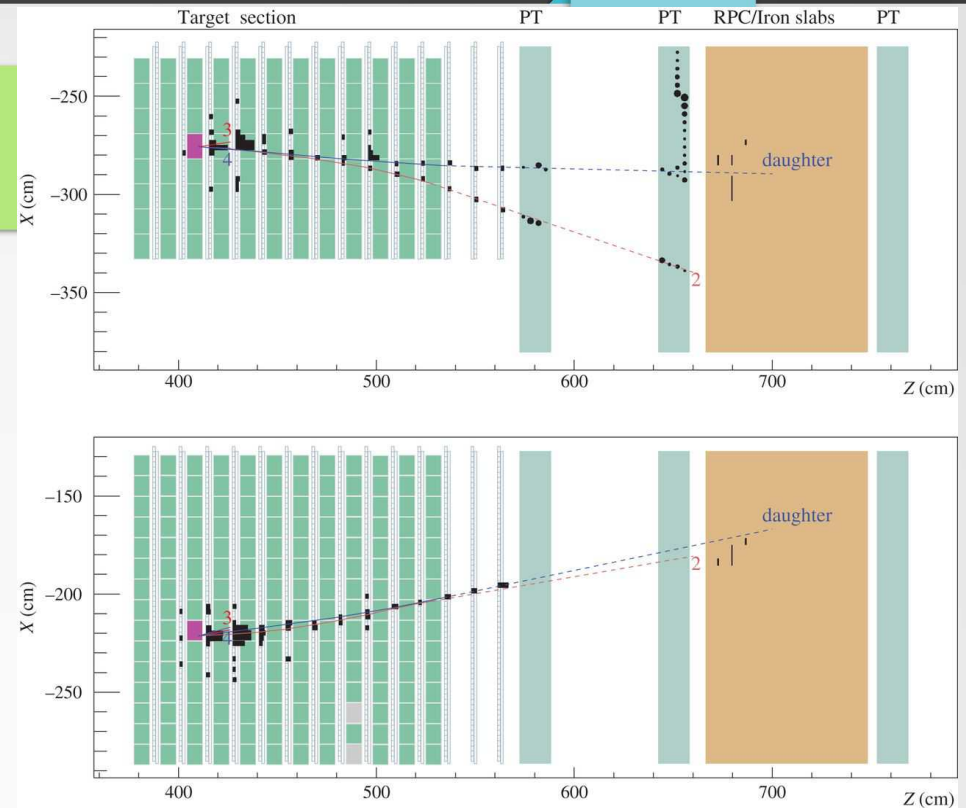
Track 1 is the parent track of a kink topology with an angle of $(137 \pm 4) \text{ mrad}$. This track is the τ candidate.

Track 2 has a momentum of $(1.9 + 0.3 - 0.2) \text{ GeV/c}$

Track 3 has a momentum of $(1.1 + 0.2 - 0.1) \text{ GeV/c}$.

Track 4 is a heavily ionizing particle having $p\beta = (0.4 \pm 0.1) \text{ GeV/c}$. From its range, $(94 \pm 1) \text{ g/cm}^2$, the particle is identified as a proton with a momentum of $(0.7 \pm 0.1) \text{ GeV/c}$.

The kink daughter track has a momentum of $(6.0 + 2.2 - 1.2) \text{ GeV/c}$.

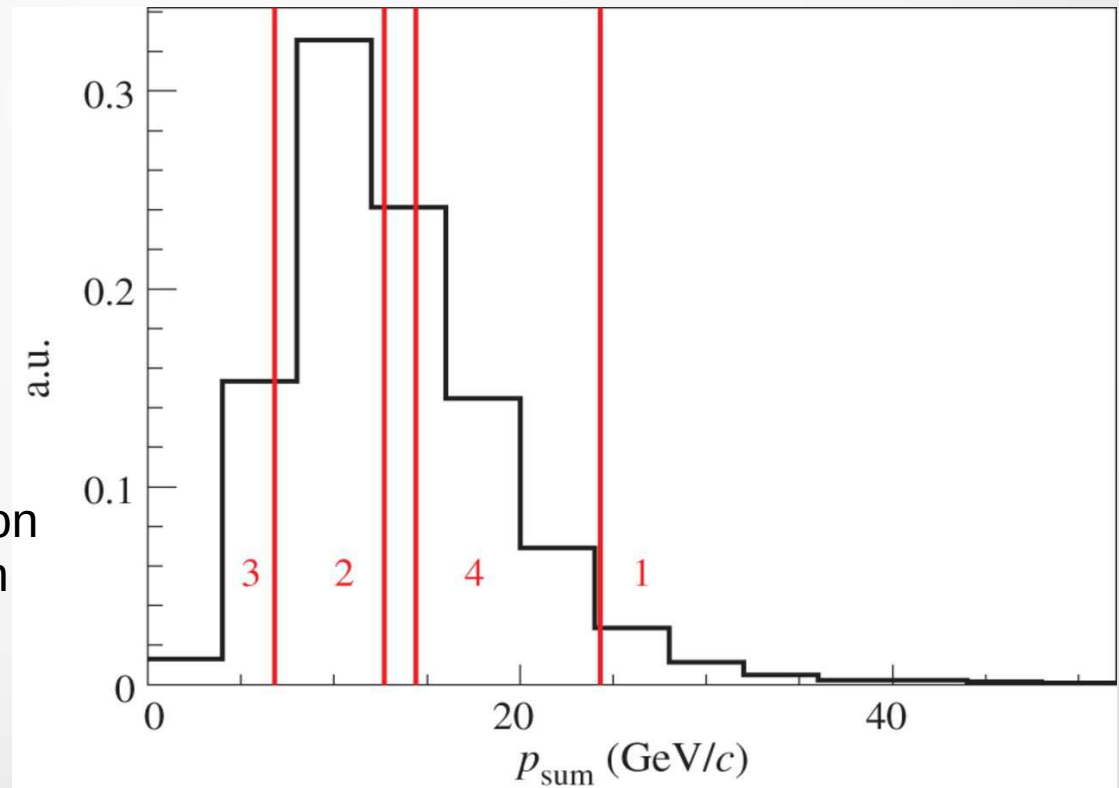


4 candidates detected

OPERA analysis sequence :

- 0μ : 2008-2009 : 2 most probable bricks + 2010-2011 : 1 most probable brick
- 1μ ($p_\mu < 15 \text{ GeV/c}$) : 2008-2009 : 2 most probable bricks + 2011 : 1 most probable brick
⇒ 2 candidates (1h, 3h)
- 1μ ($p_\mu < 15 \text{ GeV/c}$) : 2011-2012 : 1 most probable brick
⇒ + 1 candidate (μ)
- 0μ : 2012 : 1 most probable brick
⇒ + 1 candidate (1h)

Total momentum distribution
of all particles measured in
the emulsions films for
the 4 candidate events



4 candidates detected

Total 5520 events analyzed / 19505 neutrino interactions recorded
(1.8×10^{20} pot vs 2.25×10^{20} pot nominal)

4 observed events, expected background of (0.233 ± 0.041) events
 \Rightarrow 90% C.L. interval of Δm_{23}^2 is $[1.8, 5.0] \times 10^{-3} \text{eV}^2$

Decay channel	Expected signal	Observed	Expected background			
			Total	Charm decays	Hadronic re-interactions	Large-angle muon scattering
$\tau \rightarrow 1h$	0.41 ± 0.08	2	0.033 ± 0.006	0.015 ± 0.003	0.018 ± 0.005	/
$\tau \rightarrow 3h$	0.57 ± 0.11	1	0.155 ± 0.030	0.152 ± 0.030	0.002 ± 0.001	/
$\tau \rightarrow \mu$	0.52 ± 0.10	1	0.018 ± 0.007	0.003 ± 0.001	/	0.014 ± 0.007
$\tau \rightarrow e$	0.62 ± 0.12	0	0.027 ± 0.005	0.027 ± 0.005	/	/
Total	2.11 ± 0.42	4	0.233 ± 0.041	0.198 ± 0.040	0.021 ± 0.006	0.014 ± 0.007

Part – II

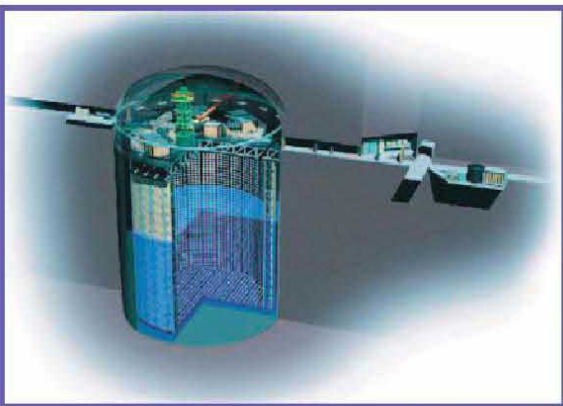
ν oscillations

T2K

T2K : Tokai-To-Kamioka



- Observation of neutrino disappearance (ν_μ) and appearance (ν_e)
- Sensitive to : θ_{13} , δ_{CP} ($\nu_\mu \rightarrow \nu_e$) and θ_{23} ($\nu_\mu \rightarrow \nu_\mu$) + cross-sections
- Run 1-4 : Jan. 2010 – May 2014 (neutrinos). Run 5 – 6 ν and $\bar{\nu}$
- Beam peak energy ~ 0.6 GeV (1st osc. max.), not enough matter effect for MH (degeneracy : $NH + CP > 0 = IH + CP < 0$) \Rightarrow possible combination with NOvA

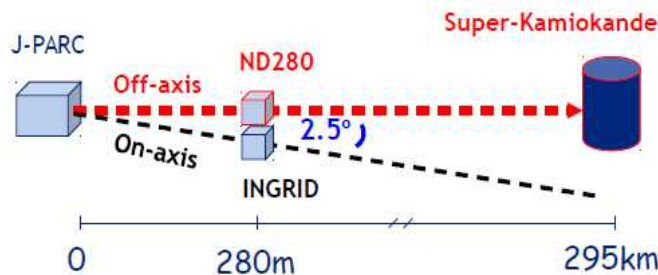


Super-Kamiokande
(ICRR, Univ. Tokyo)

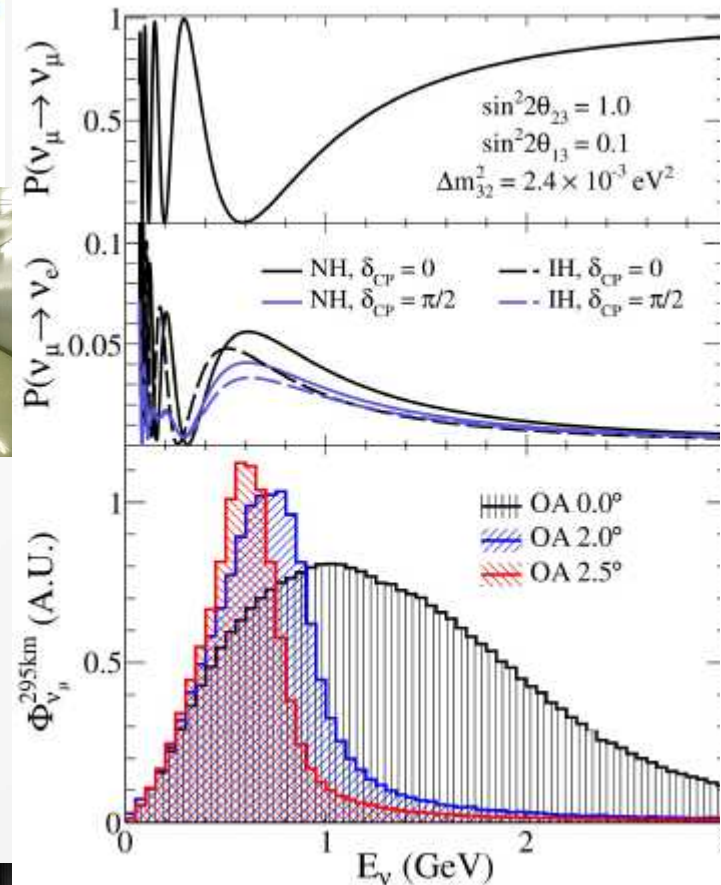
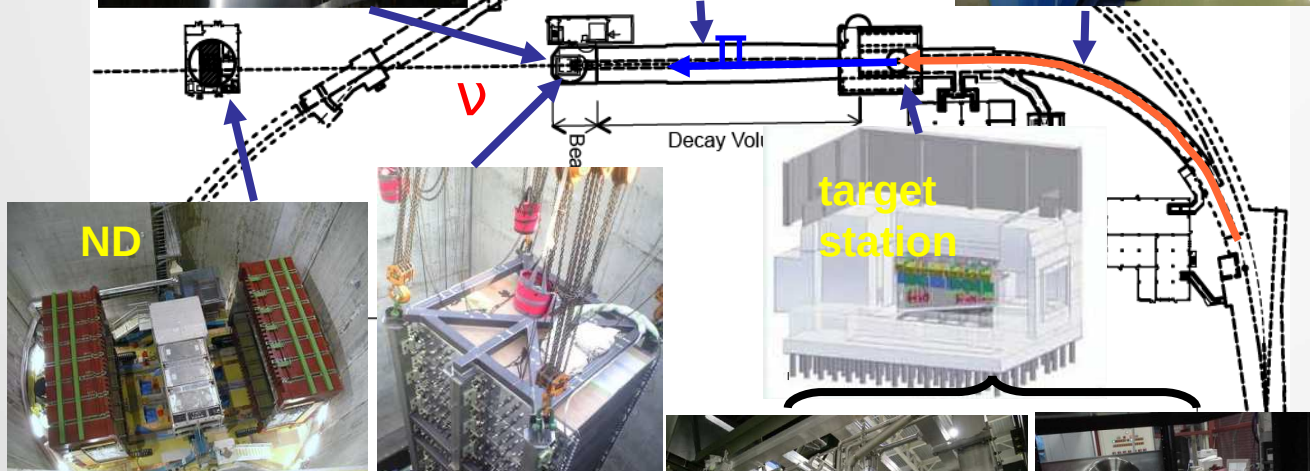
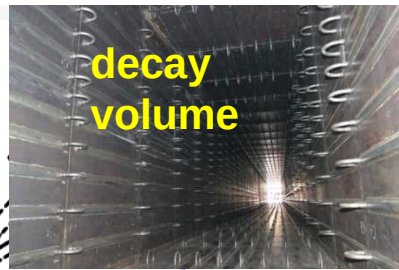
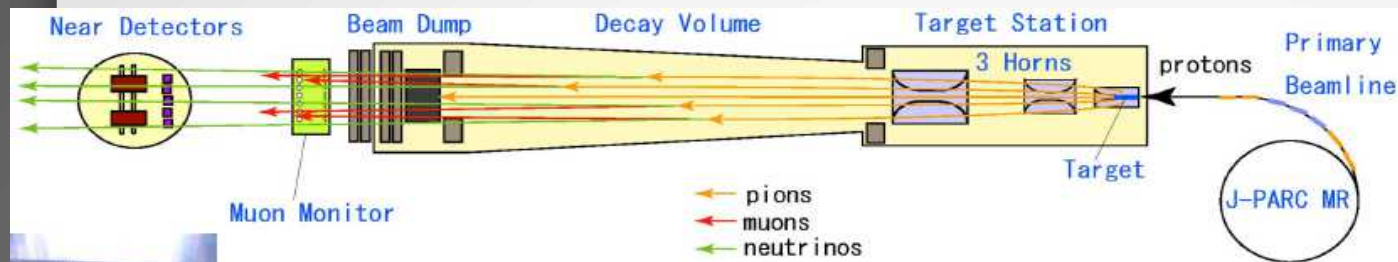


- 2 GeV peak
- 810km baseline
- liquid scintillator in Ash river

J-PARC Main Ring
(KEK-JAEA, Tokai)

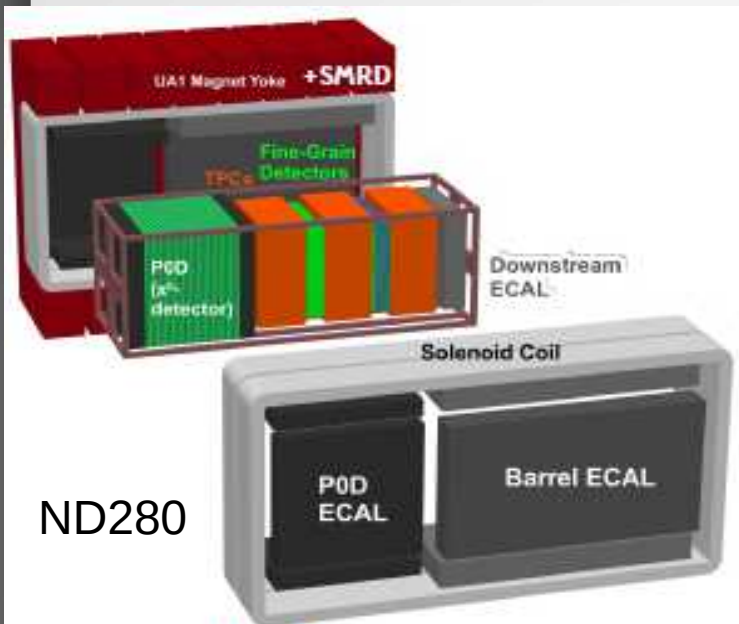


T2K : beam



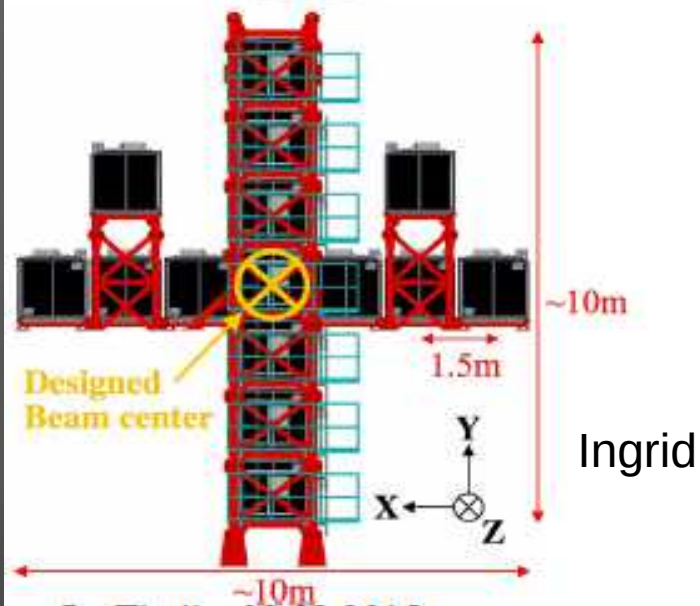
Simulation constrained by NA61/SHINE exp. results

T2K : near detectors



ND280 off-axis near detector:

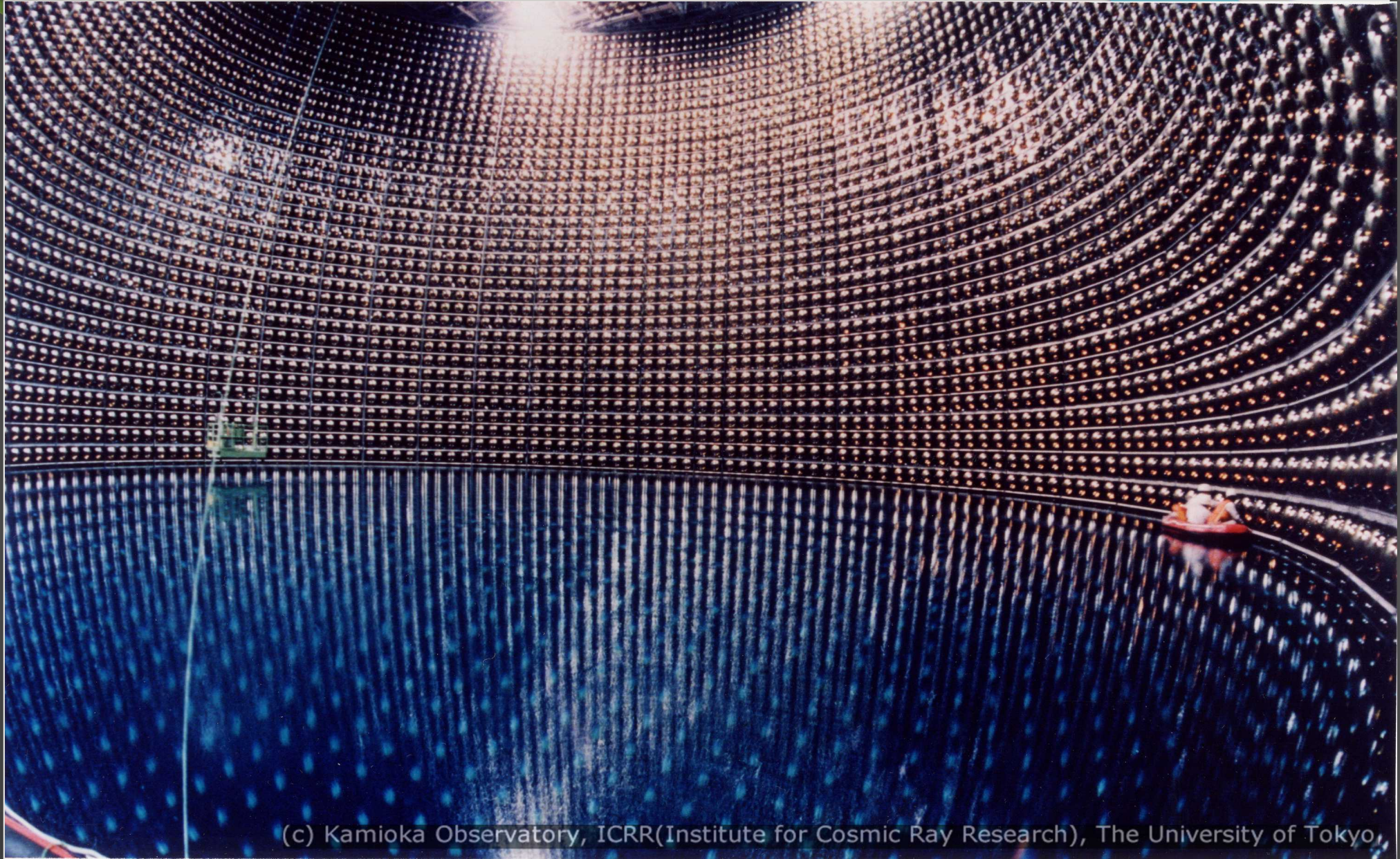
- Several sub-detectors in 0.2T magnetic field: Tracker (TPCs & FGDs), Pizero Detector (P0D), Electromagnetic Calorimeter (ECAL), Side Muon Range Detector (SMRD)
- Measure flux x cross section before the oscillation occurs
- Measure intrinsic ν_e contamination in the beam
- Neutrino cross section measurements
- Short-baseline oscillations (search for sterile neutrinos)



INGRID on-axis near detector:

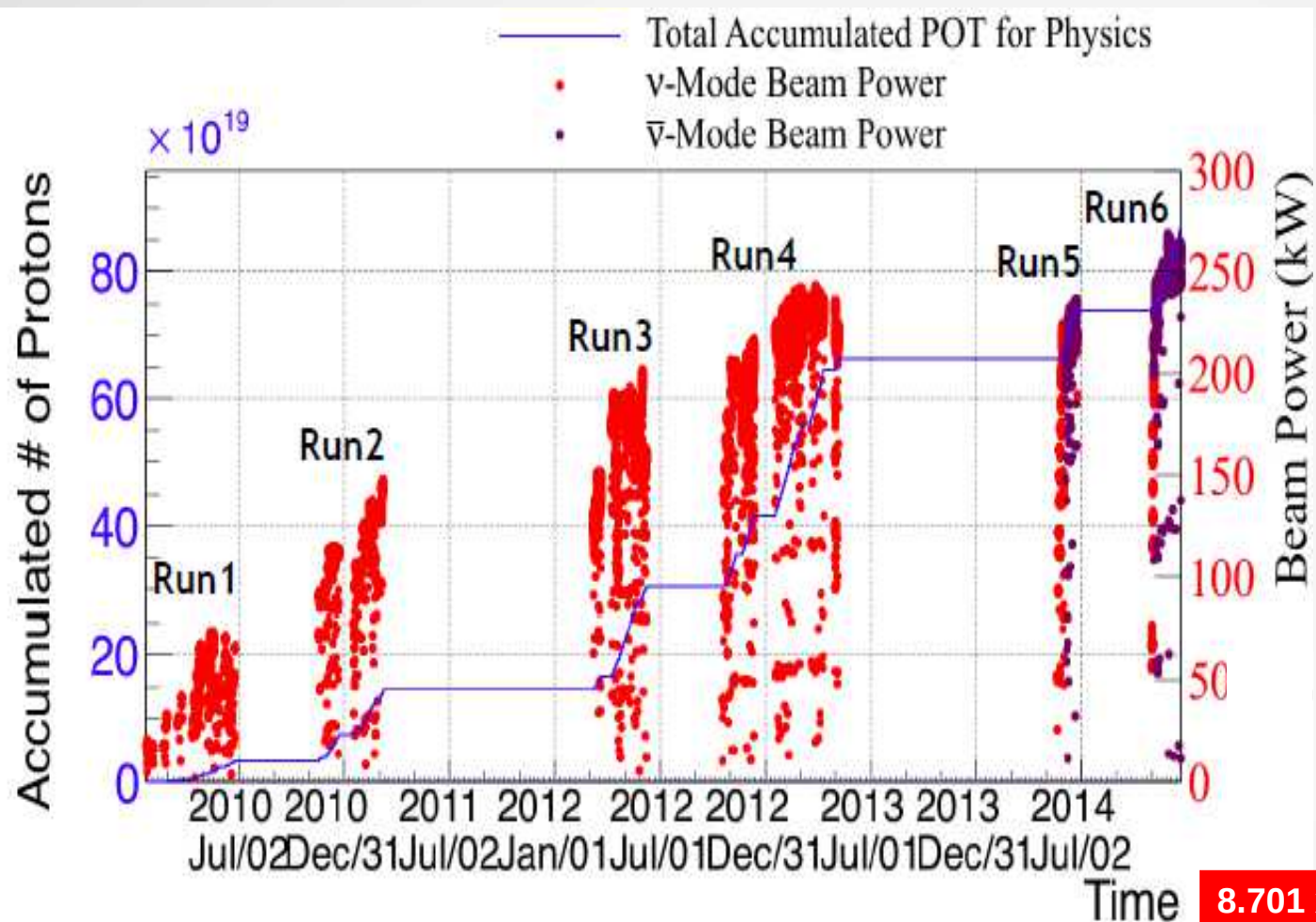
- 16 modules (iron/scintillator sandwich) + additional scintillator-only module (proton module : CCQE cross-section)
- Count neutrinos by reconstructing muons from ν_μ interactions
- Monitor beam rate, direction and stability

T2K : far detector



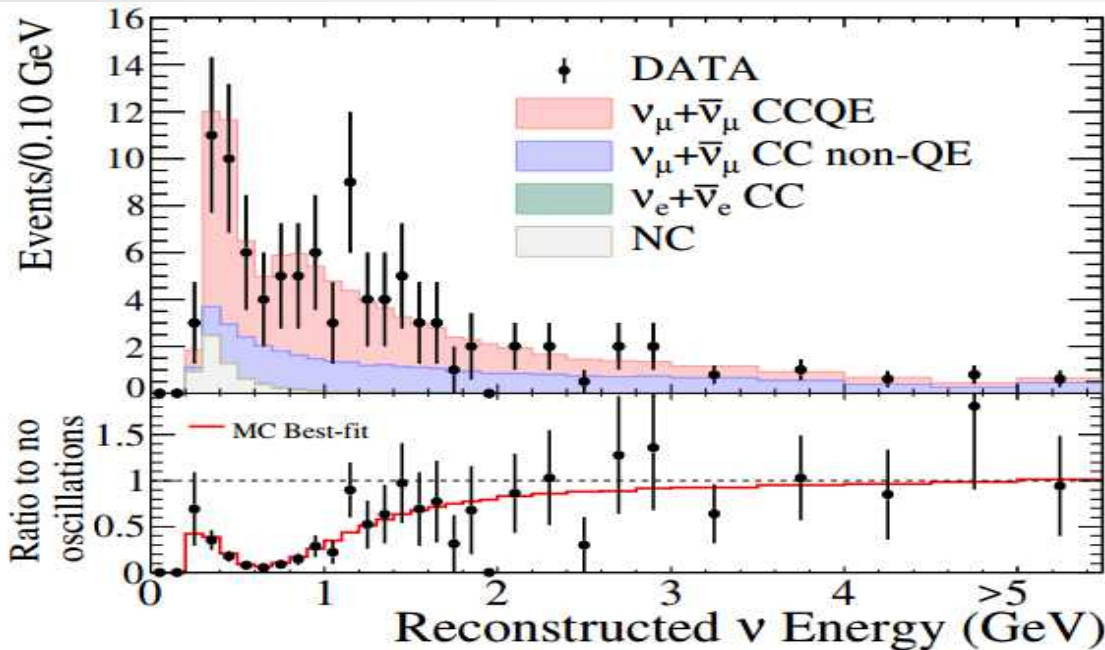
(c) Kamioka Observatory, ICRR(Institute for Cosmic Ray Research), The University of Tokyo,

T2K results : p.o.t.



8.701×10^{20} POT
(80 % ν , 20 % $\bar{\nu}$)
 7.8×10^{21} POT nom.

T2K results : neutrino mode analysis



ν_μ

Disappearance
analysis

$$\sin^2 \theta_{23} = 0.514^{+0.055}_{-0.056} \text{ (NH)}$$

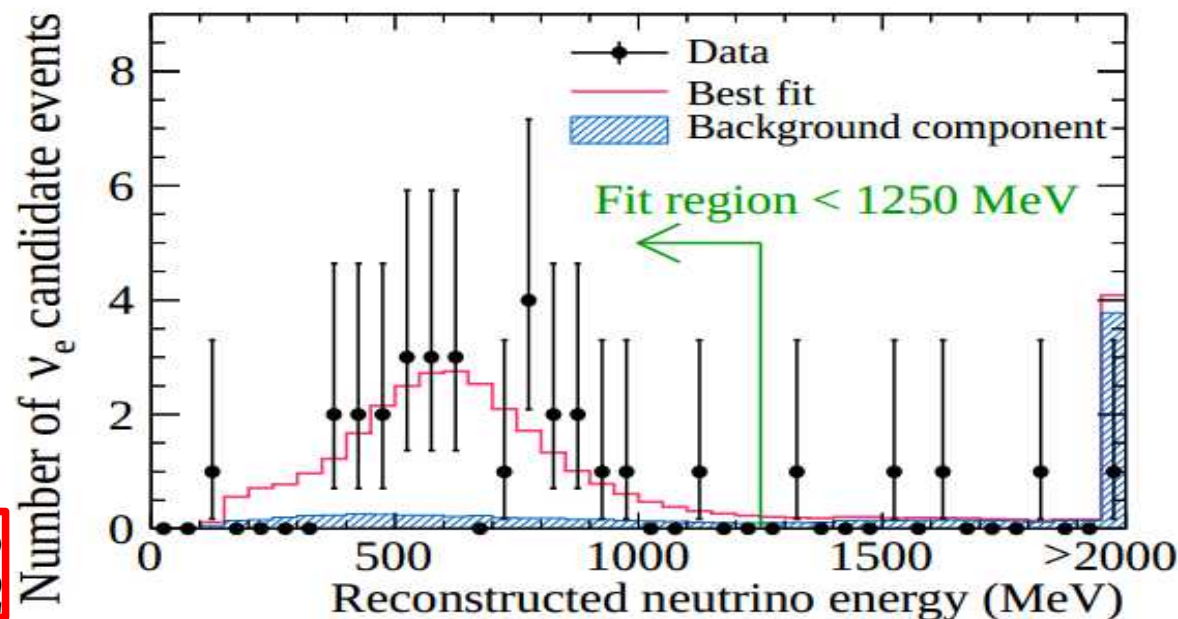
$$\sin^2 \theta_{23} = 0.511 \pm 0.055 \text{ (IH)}$$

ν_e

appearance
analysis

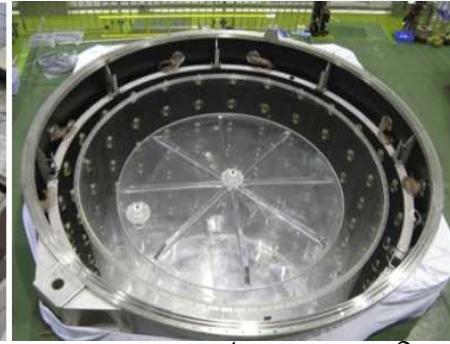
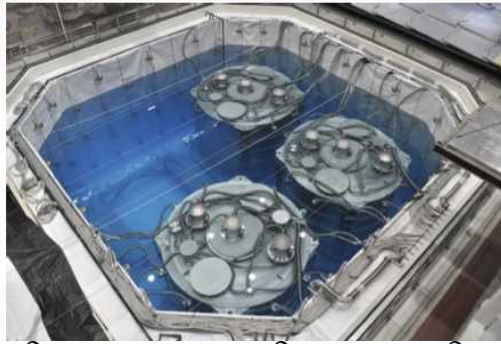
28 candidates
→ 7.3 σ for non-zero θ_{13}

$$\sin^2 2\theta_{13} = 0.140^{+0.038}_{-0.032}$$



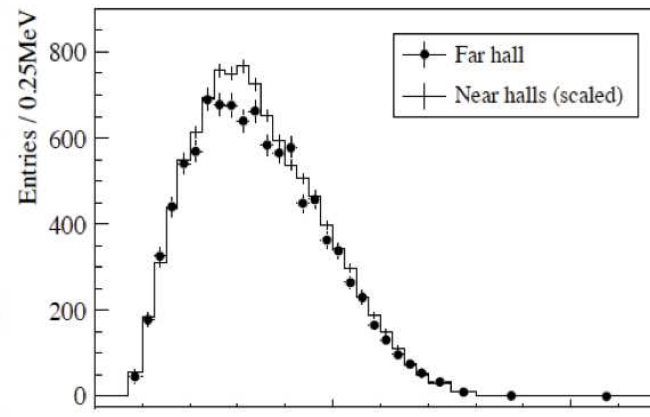
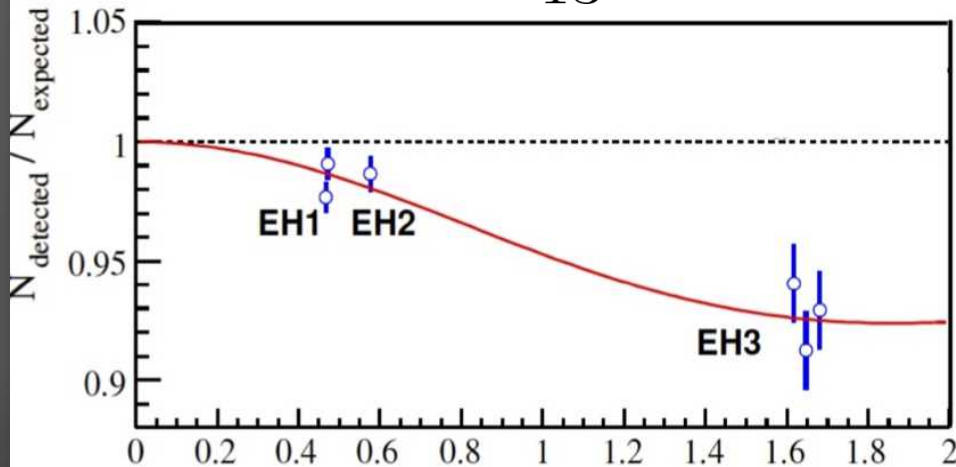
Reactors confirmed... : the Daya-Bay case

- Disappearance of $\bar{\nu}_e$ from nuclear reactors at \sim kilometer baselines
 \Rightarrow relative measurement near/far allows precision measurements of θ_{13}
- 1st meas. : $\theta_{13} = 0$ excluded at 5.2σ after 55 days. Last results : 621 days + 2 A.D.



$$P_{ee} = 1 - \sin^2 2\theta_{13} (\cos^2 \theta_{12} \sin^2 \Delta_{13} + \sin^2 \theta_{12} \sin^2 \Delta_{32}) - \cos^4 \theta_{13} \sin^2 2\theta_{12} \sin^2 \Delta_{21}$$

$$\sin^2 2\theta_{13} = 0.084 \pm 0.005$$



T2K physics potential arXiv:1409.7469

Up-to-date Run 1-4 analyzed : $6,57 \cdot 10^{20}$ pot / $7,8 \cdot 10^{21}$ pot => space for improvement

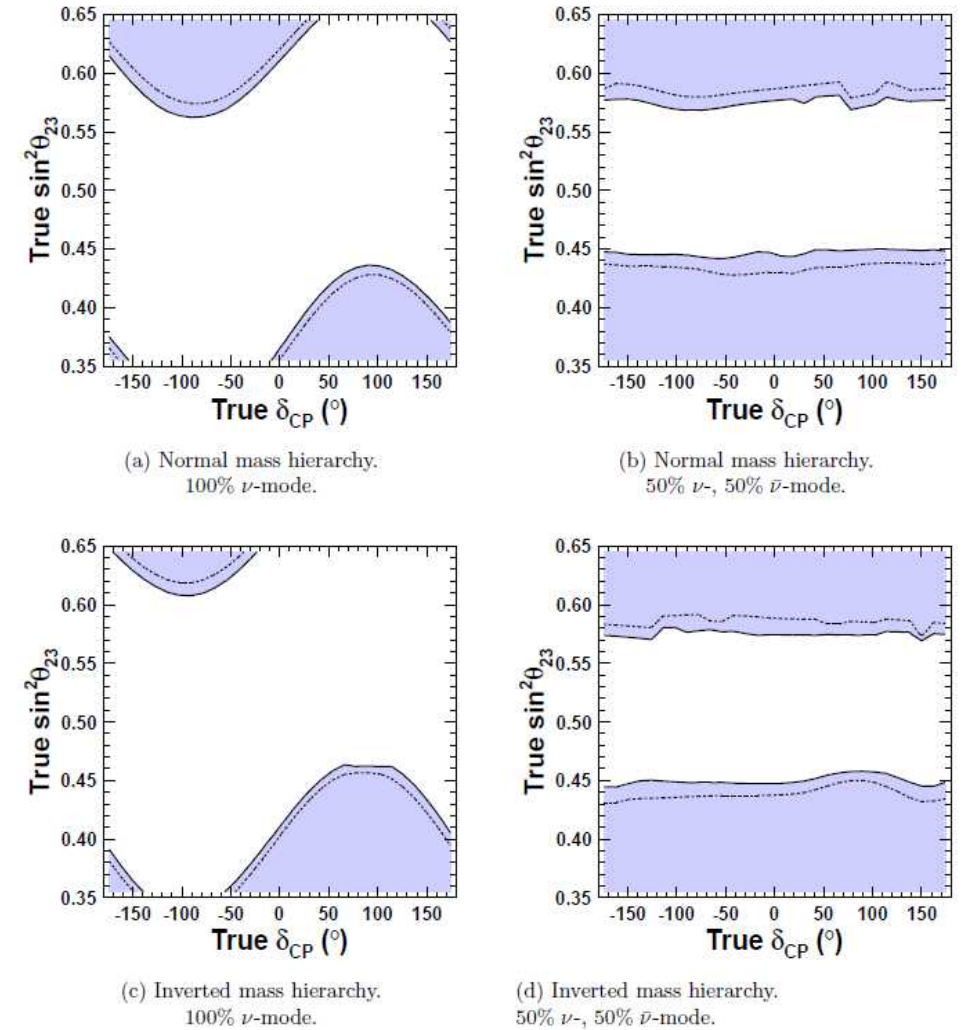
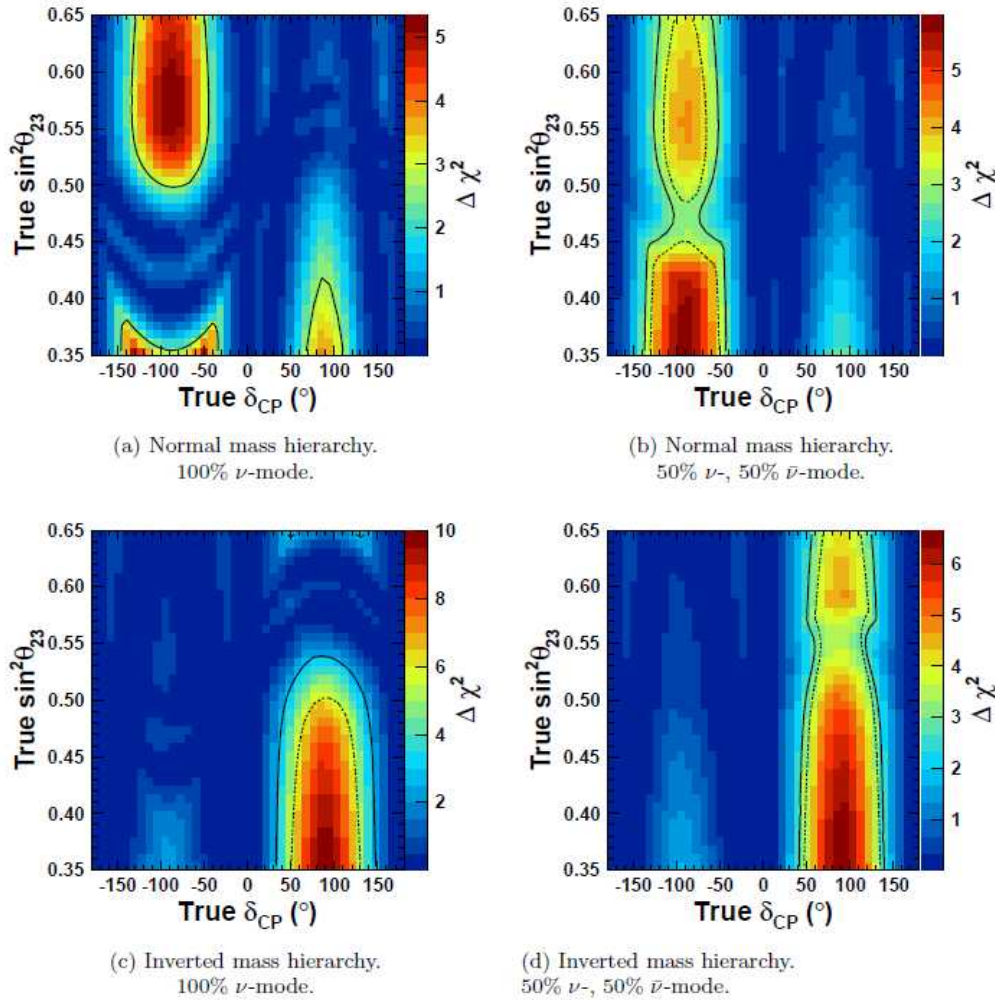
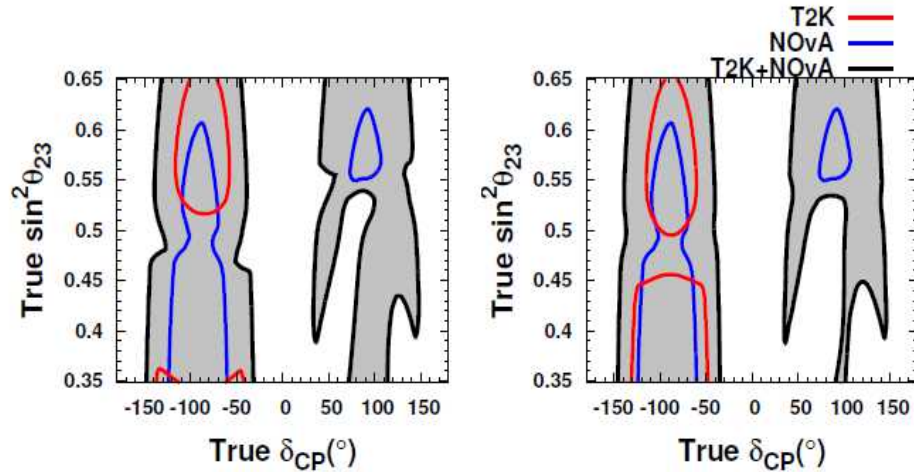


Fig. 7: The expected $\Delta\chi^2$ for the $\sin \delta_{CP} = 0$ hypothesis, in the $\delta_{CP} - \sin^2 \theta_{23}$ plane. The $\Delta\chi^2$ map shown in color is calculated assuming no systematic errors. The solid contours show the 90% C.L. sensitivity with statistical error only, while the dashed contours include the 2012 T2K systematic error. The dashed contour does not appear in (a) because T2K does not have 90% C.L. sensitivity in this case.

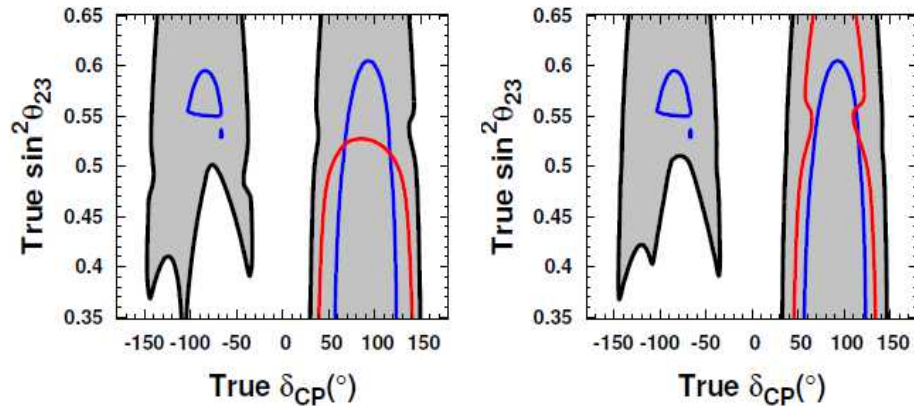
Fig. 11: The region, shown as a shaded area, where T2K has more than a 90% C.L. sensitivity to reject one of the octants of θ_{23} . The shaded region is calculated assuming no systematic errors (the solid contours show the 90% C.L. sensitivity with statistical error only), and the dashed contours show the sensitivity including the 2012 T2K systematic errors.

T2K + NOvA combined : profiting from MH



(a) 1:0 T2K, 1:1 NOvA $\nu:\bar{\nu}$, NH

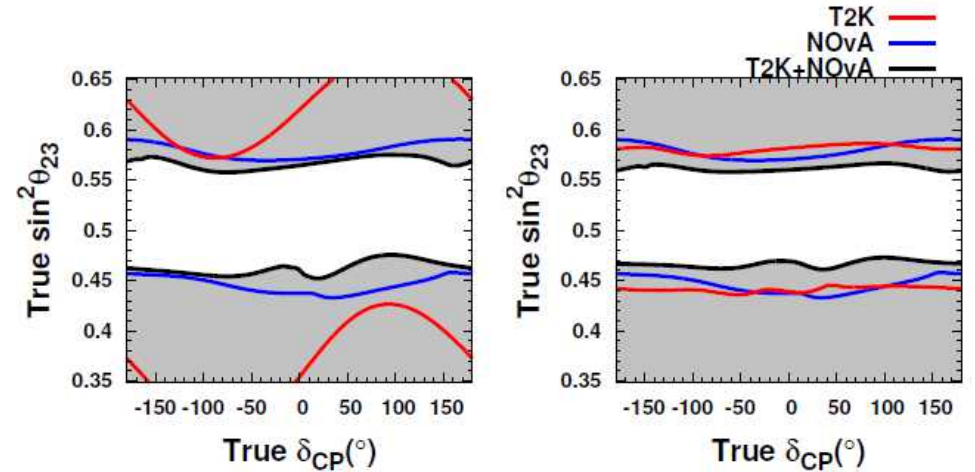
(b) 1:1 T2K, 1:1 NOvA $\nu:\bar{\nu}$, NH



(c) 1:0 T2K, 1:1 NOvA $\nu:\bar{\nu}$, IH

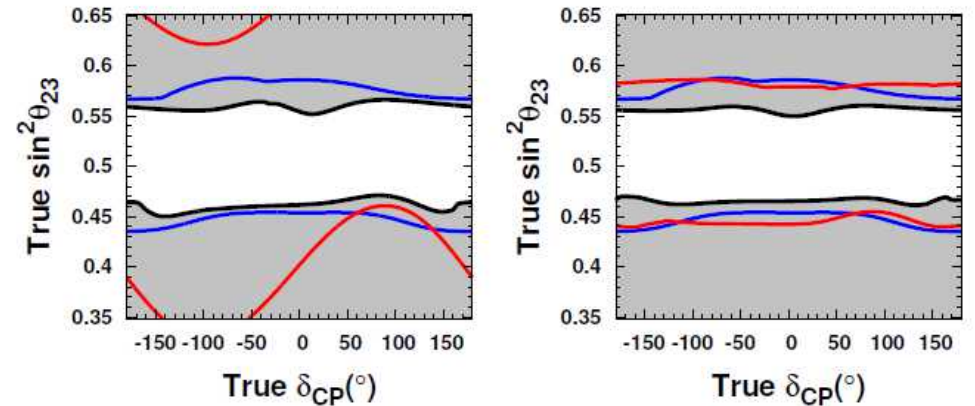
(d) 1:1 T2K, 1:1 NOvA $\nu:\bar{\nu}$, IH

Fig. 17: Regions where T2K (red), NOvA (blue), and T2K+NOvA (black) is predicted to rule out $\sin \delta_{CP} = 0$ at 90% C.L. Points within the gray regions are where $\sin \delta_{CP} = 0$ is predicted to be rejected at 90% C.L. for T2K+NOvA, assuming simple normalization systematics as described in the text.



(a) 1:0 T2K, 1:1 NOvA $\nu:\bar{\nu}$, NH

(b) 1:1 T2K, 1:1 NOvA $\nu:\bar{\nu}$, NH



(c) 1:0 T2K, 1:1 NOvA $\nu:\bar{\nu}$, IH

(d) 1:1 T2K, 1:1 NOvA $\nu:\bar{\nu}$, IH

Fig. 19: Regions for T2K (red), NOvA (blue), and T2K+NOvA (black) where the incorrect octant is predicted to be rejected at 90% C.L. Points inside the gray regions are where the incorrect octant is predicted to be rejected at 90% C.L. for T2K+NOvA assuming simple normalization systematics as described in the text.

T2K cross sections : NEUT simulator

NEUT simulates 7 types of (CC) and (NC) interactions: (quasi-)elastic scattering, single pion production, single photon production, single kaon production, single eta production, DIS, and Coherent pion production.

The Llewellyn Smith model is used as basis for (CCQE) and (NCEL) interactions.

Model of the nucleus : Relativistic Fermi Gas (RFG) by Smith and Moniz.

Dipole axial form factors and vector form factors derived from electron scattering.

Default quasi-elastic axial mass, $M_A^{QE} = 1.21 \text{ GeV}/c^2$

Default Fermi momenta for carbon and oxygen : 217 MeV/c and 225 MeV/c.

Rein and Sehgal model used to simulate neutrino-induced single pion production.

The model assumes the interaction is split into two steps as follows: $\nu + N \rightarrow l + N^*$, $N^* \rightarrow \pi + N'$

The model assigns a 20% branching fraction for pion-less delta decay (PDD) : $\Delta + N \rightarrow N + N$.

The coherent pion production model is described from Rein and Sehgal : $\nu + A \rightarrow l + \pi + X$

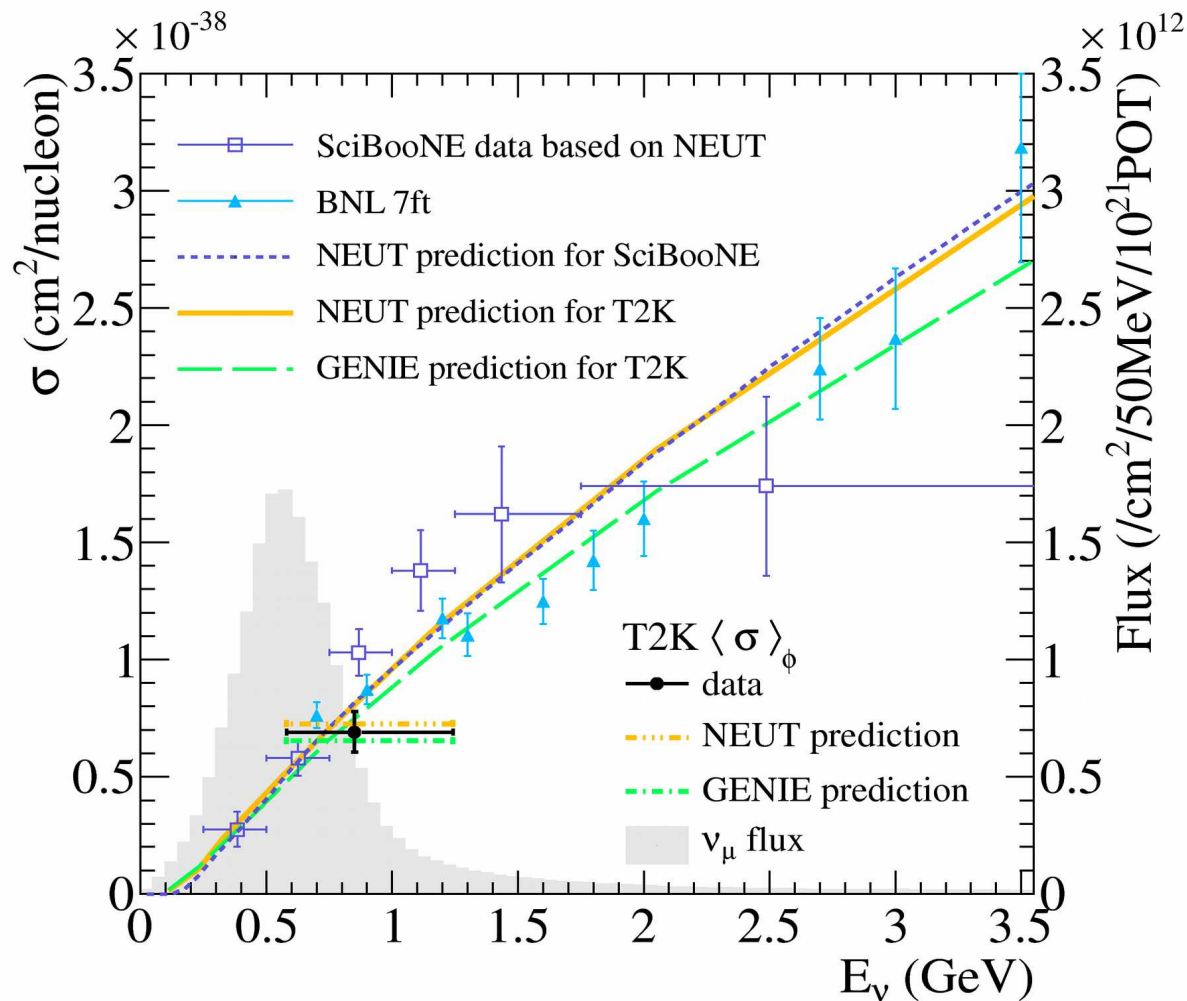
DIS : structure functions from GRV98 parton distribution function with Bodek and Yang corrections for better agreement with experiments in the low- Q^2 region (+ PYTHIA/JetSet for $W > 2 \text{ GeV}/c^2$)

FSI for hadrons : cascade model for pions, kaons, etas, and nucleons (hadron moved from the neutrino interaction point, interaction probabilities computed, steps repeated until all particles are either absorbed or escape the nucleus. The interaction types include charge exchange, inelastic scattering, particle production, and absorption.)

T2K cross sections : results

Measurement of the NuMu inclusive charged current cross section on carbon in the near detector of the T2K experiment

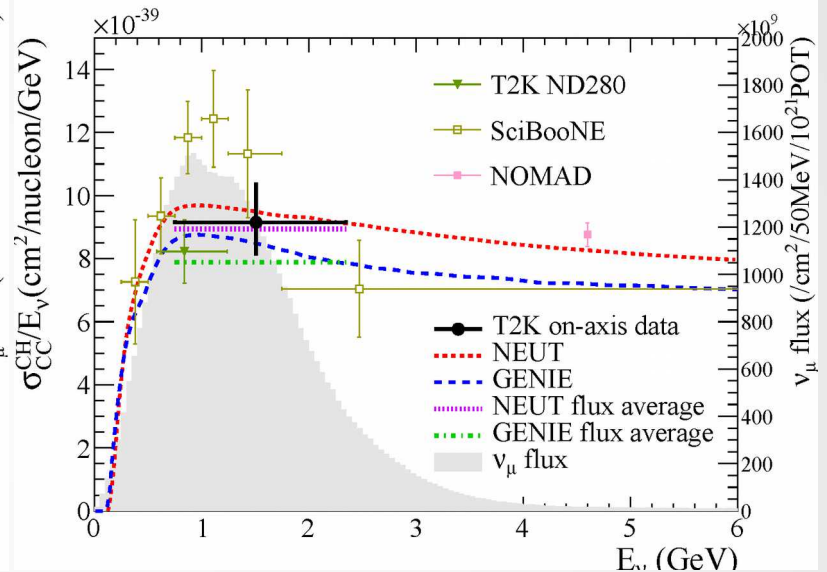
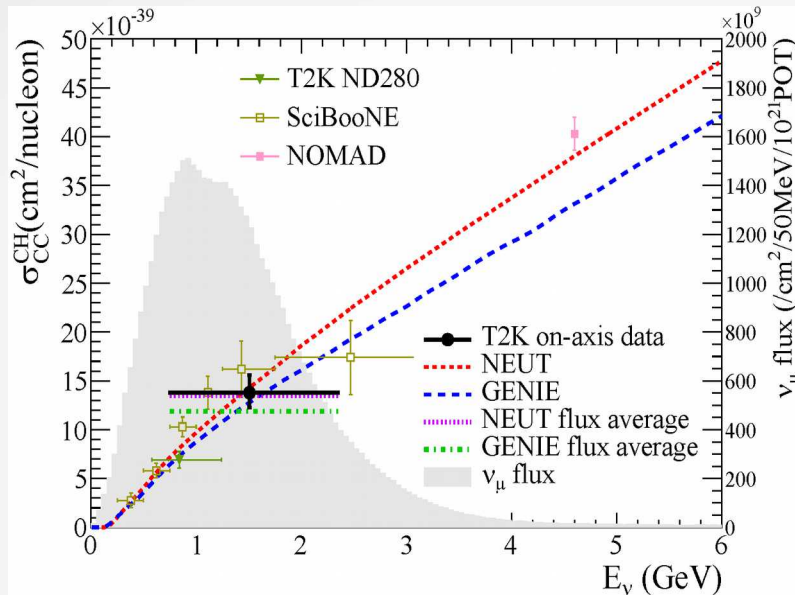
The T2K total flux-averaged cross section with the NEUT and the GENIE prediction for T2K and SciBooNE. The T2K data point is placed at the flux mean energy. The vertical error represents the total (statistical and systematic) uncertainty, and the horizontal bar represent 68 % of the flux at each side of the mean energy. The T2K flux distribution is shown in grey. The predictions for SciBooNE have been done for a C_8H_8 target which is comparable to the mixed T2K target. BNL data has been measured on deuterium.



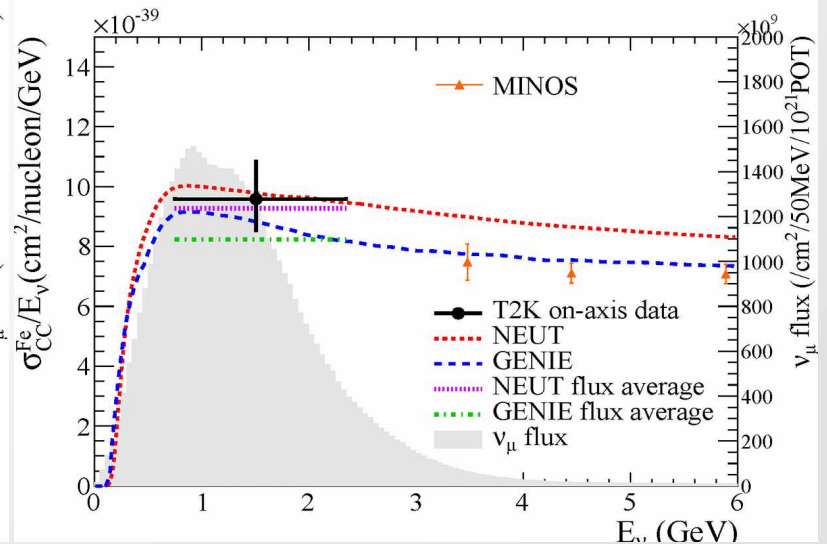
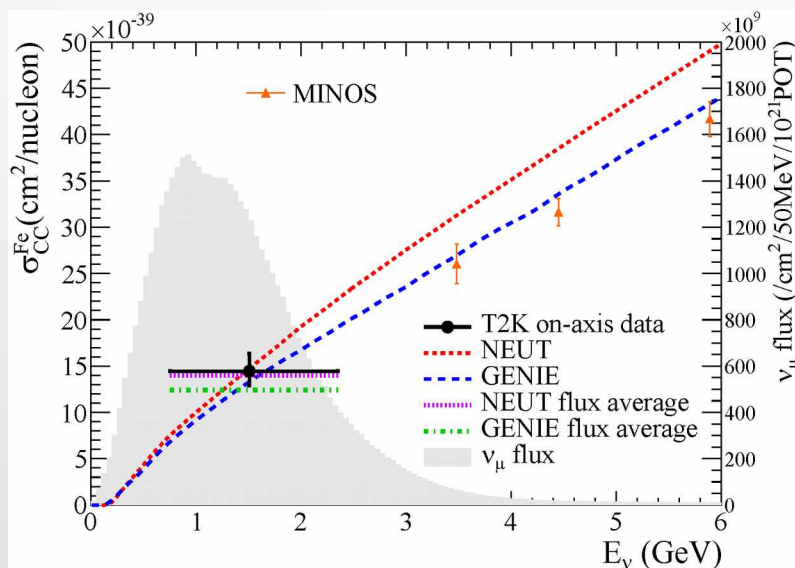
T2K cross sections : results

CC-inclusive cross section with INGRID and Proton Module

CC-inclusive
cross section on CH.



CC-inclusive
cross section on Fe.



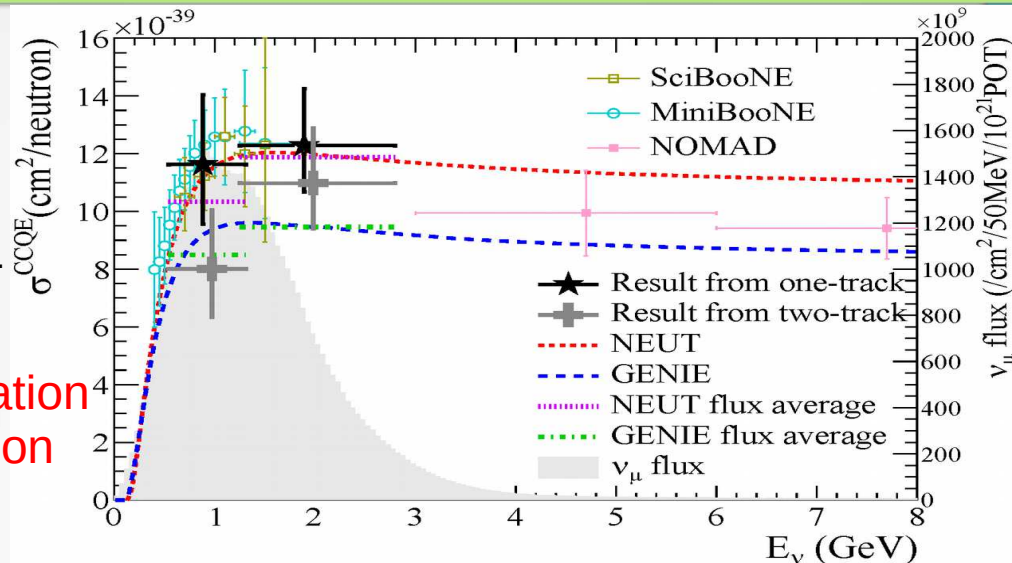
T2K cross sections : results

CCQE cross section with Proton Module

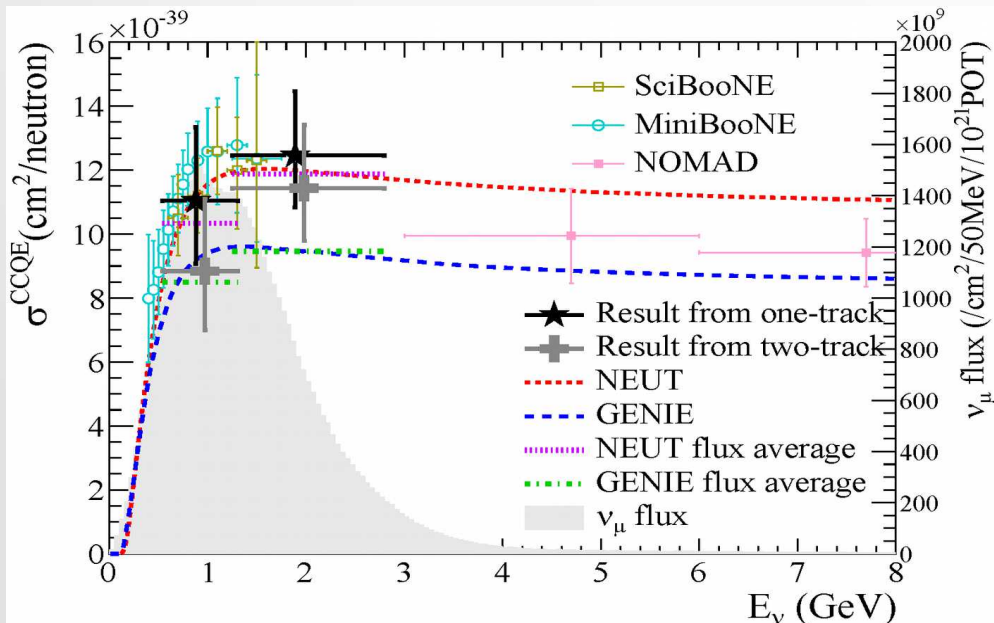
CCQE cross section using default NEUT.

From this analysis :

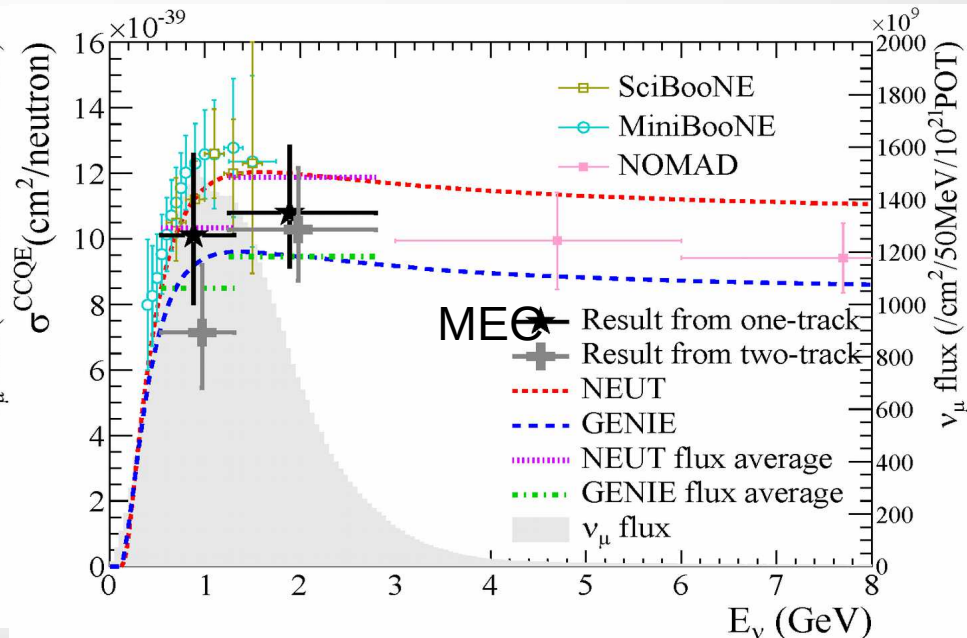
- SF is a better representation
- No definitive conclusion on the existence of MEC...



CCQE cross section using SF



CCQE cross section using MEC

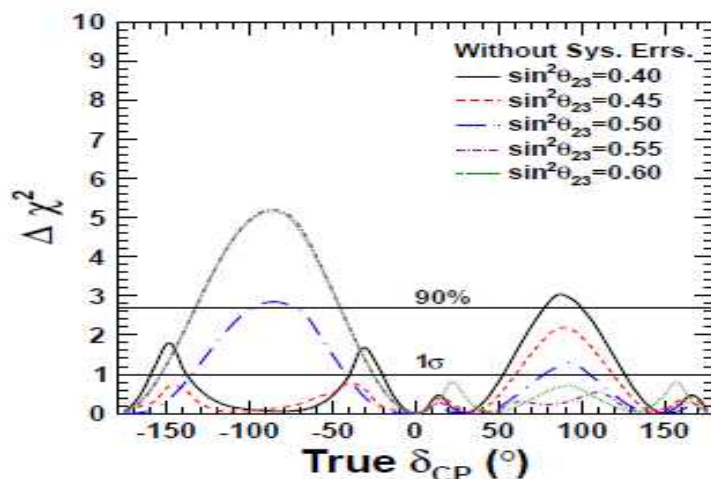


Part – II

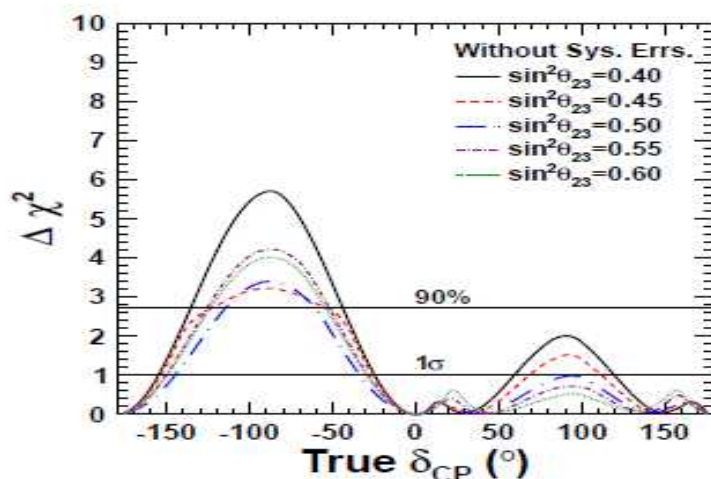
ν oscillations

Beyond : LBNx

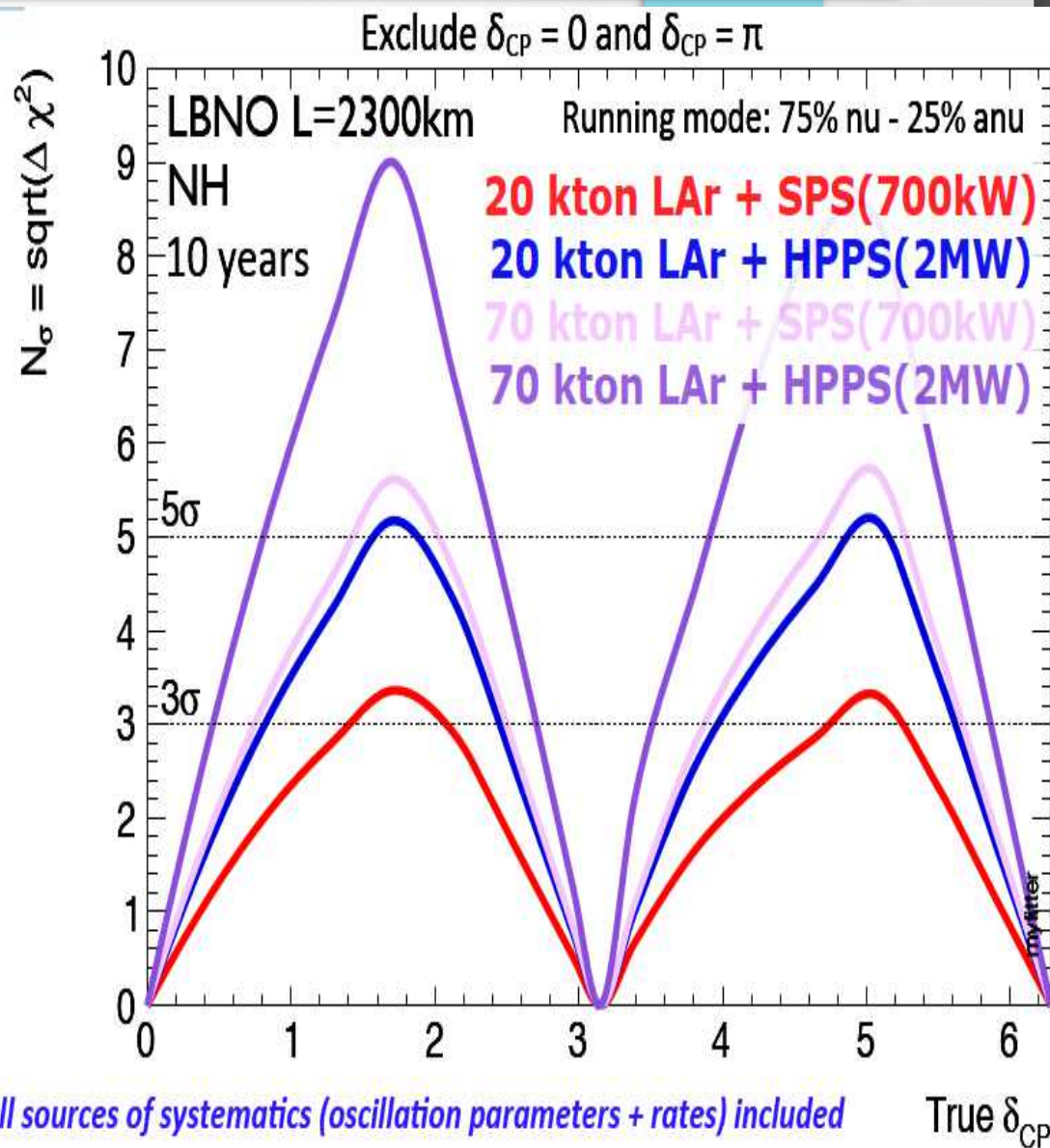
Interlude : from this to next generation



(a) 100% ν -mode, statistical error only.



(c) 50% ν , 50% $\bar{\nu}$ -mode, statistical error only.



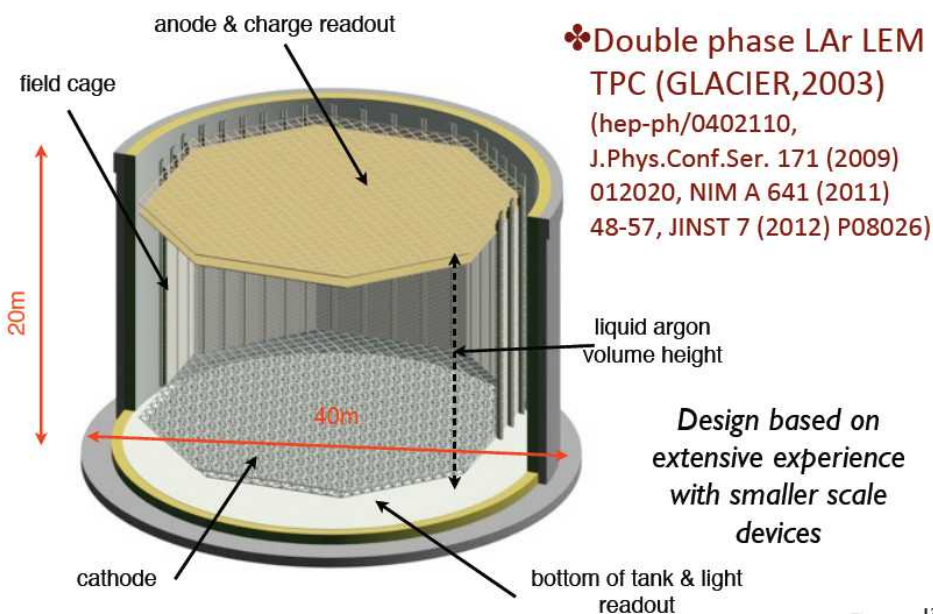
LAGUNA-LBNO : future projects



- What is left to be measured ?
 - Mass hierarchy : sign of Δm_{23}^2
 - CP violation in the leptonic sector : δ_{CP}

$$U = \begin{pmatrix} 1 & 0 & 0 \\ 0 & c_{23} & s_{23} \\ 0 & -s_{23} & c_{23} \end{pmatrix} \begin{pmatrix} c_{13} & 0 & s_{13}e^{-i\delta} \\ 0 & 1 & 0 \\ -s_{13}e^{i\delta} & 0 & c_{13} \end{pmatrix} \begin{pmatrix} c_{12} & s_{12} & 0 \\ -s_{12} & c_{12} & 0 \\ 0 & 0 & 1 \end{pmatrix}$$

Far liquid Argon detector

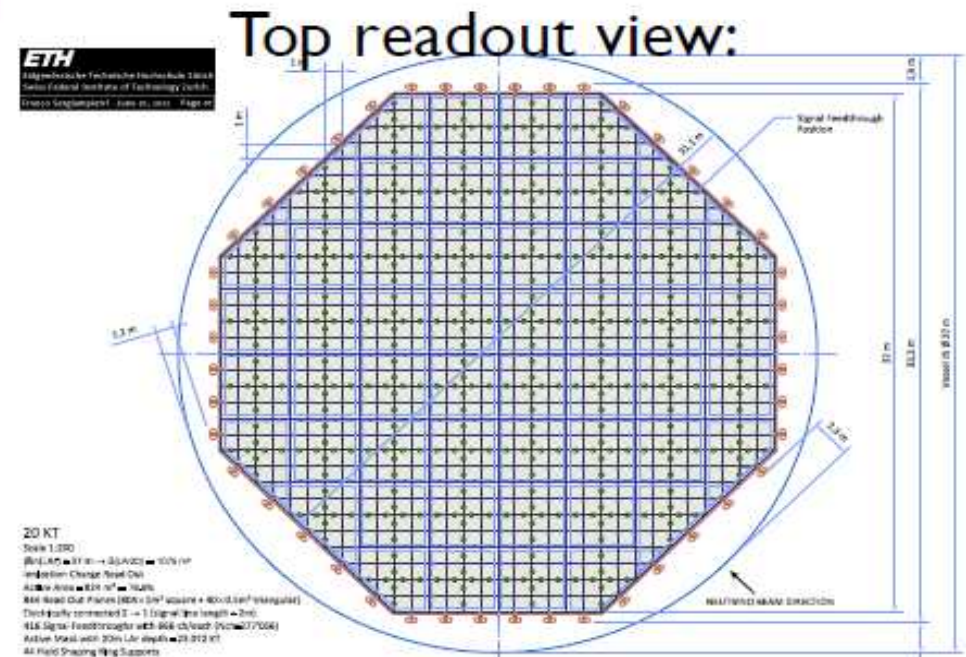
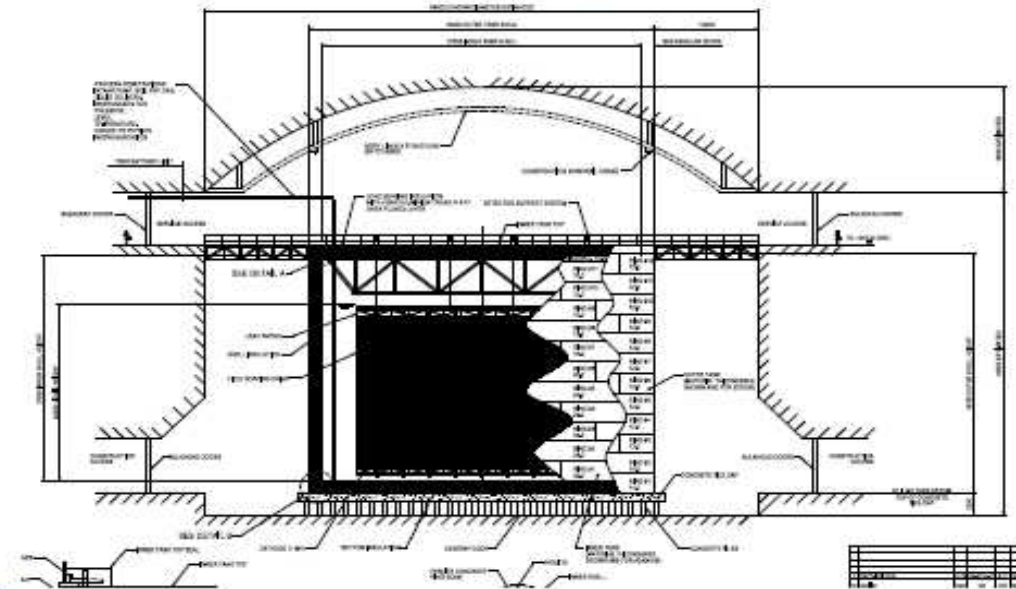


Double-phase liquid argon TPC



GLACIER detector design

- ★ Concept unchanged since 2003: Simple, scalable detector design, from one up to 100 kton (hep-ph/0402110)
- ★ Single module non-evacuatable cryo-tank based on industrial LNG technology
 - industrial conceptual design (Technodyne, AAE, Ryhal engineering, TGE, GTT)
 - two tank options: 9% Ni-steel or membrane (detailed comparison up to costing of assembly in underground cavern)
 - three volumes: 20, 50 and 100 kton
- ★ Liquid filling, purification, and boiloff recondensation
 - industrial conceptual design for liquid argon process (Sofregaz), 70kW total cooling power @ 87 K
 - purity < 10 ppt O₂ equivalent
- ★ Charge readout (e.g. 20 kton fid.)
 - 23'072 kton active, 824 m² active area
 - 844 readout planes, 277'056 channels total
 - 20 m drift
- ★ Light readout (trigger)
 - 804 8" PMT (e.g. Hamamatsu R5912-02MOD) WLS coated placed below cathode
- ★ The concept and the designs are reaching the required level of maturity for submission to SPSC.

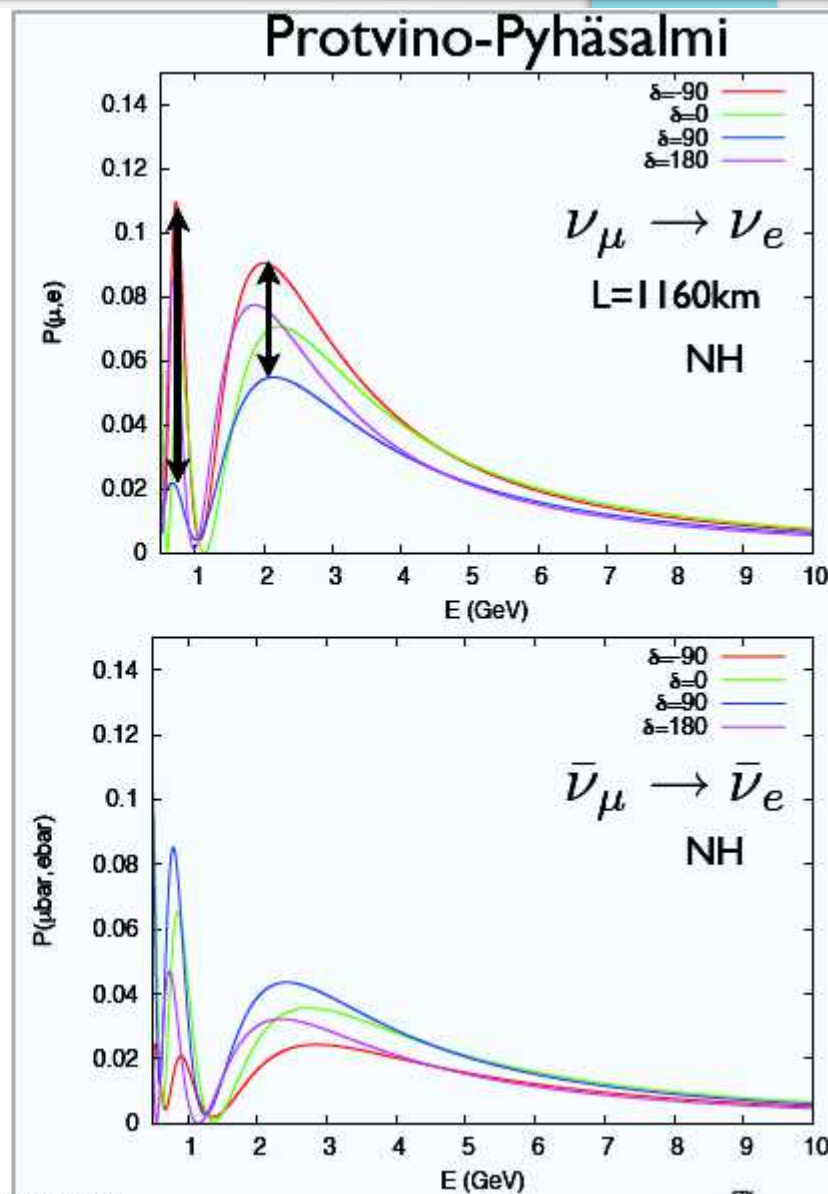
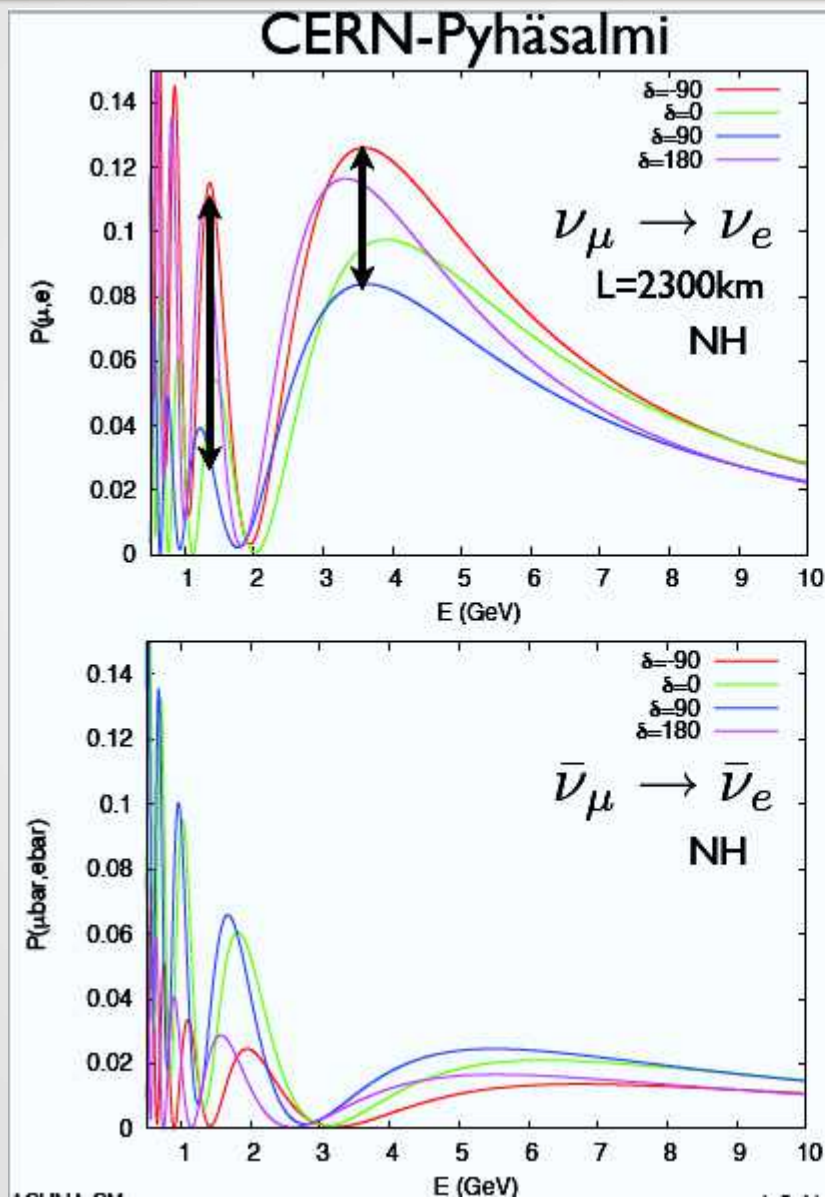


Technical aspects finalized in the LAGUNA-LBNO study as deliverables

including detailed costing → August 2014

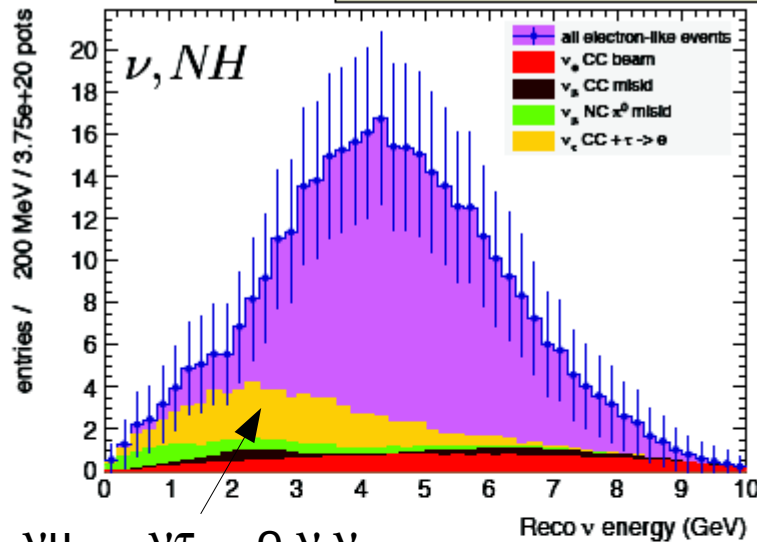
Affordable underground detector

LAGUNA-LBNO : oscillation profiles

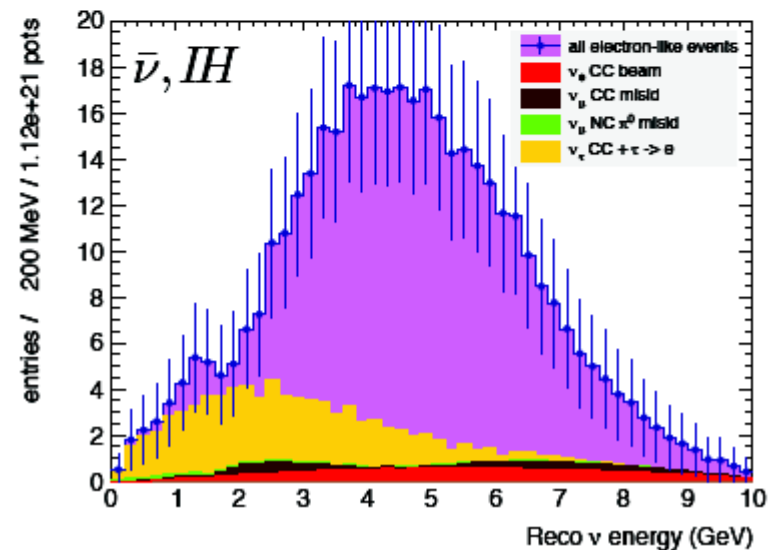
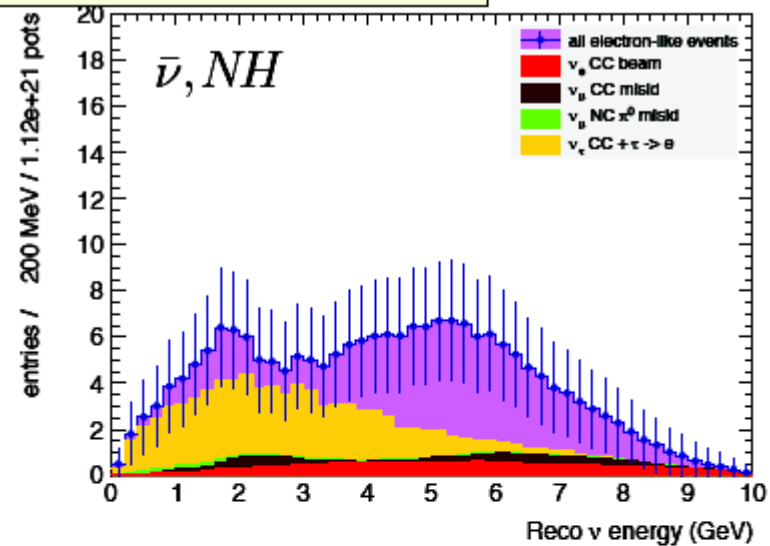
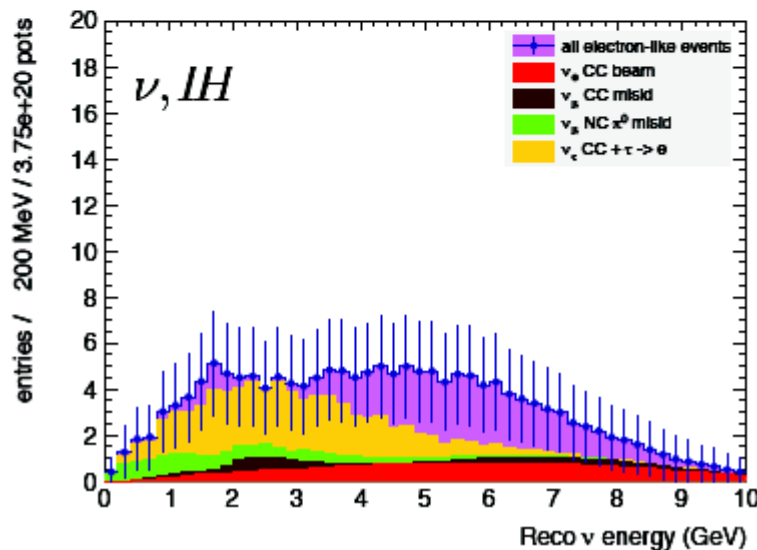


LAGUNA-LBNO : $\nu / \bar{\nu}$ and MH

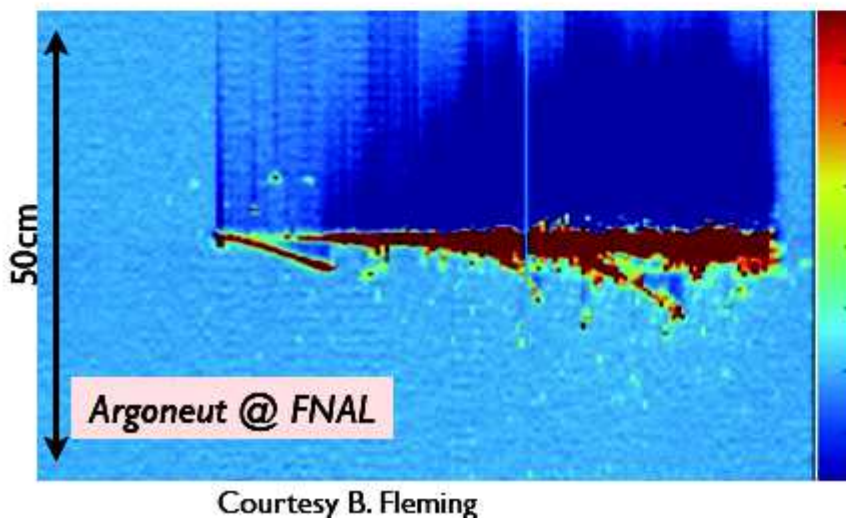
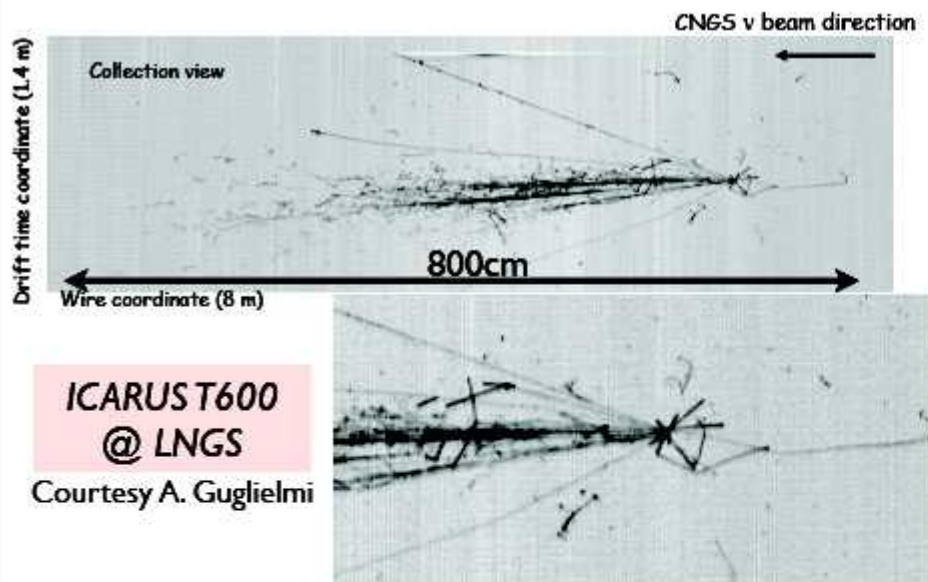
Detector response and resolution included



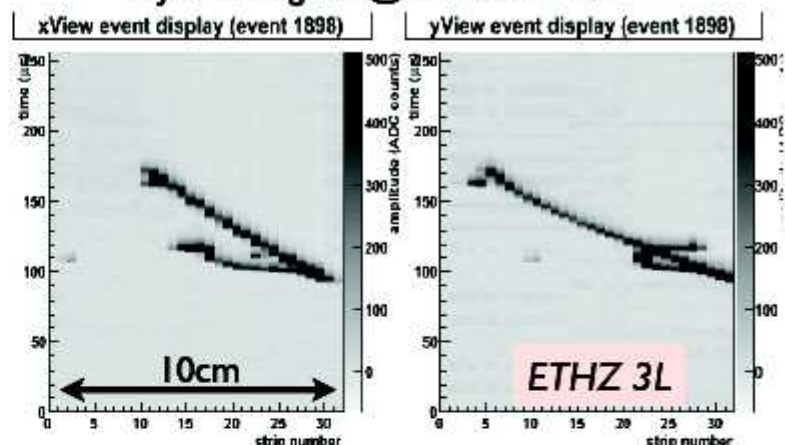
$\nu_\mu \rightarrow \nu_\tau \rightarrow e \nu \nu$



LAr technology : electronic bubble chamber

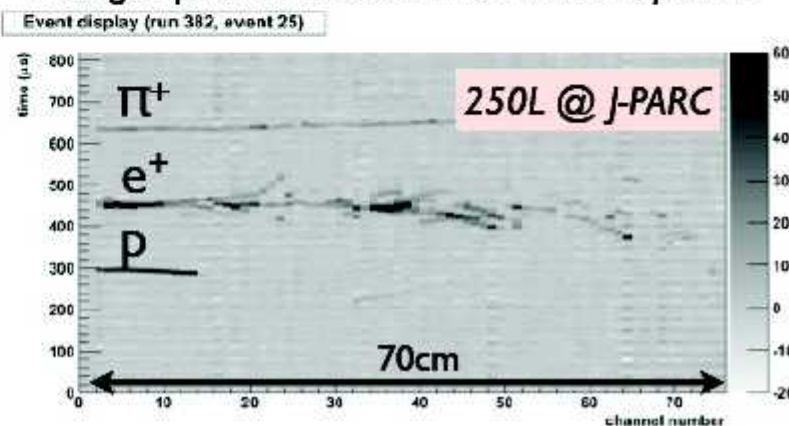


Cosmic track in double phase 3L LAr-LEM TPC with adjustable gain @ CERN-ETHZ



Much improved S/N (>100) compared to single-phase LAr operation (≈ 15)

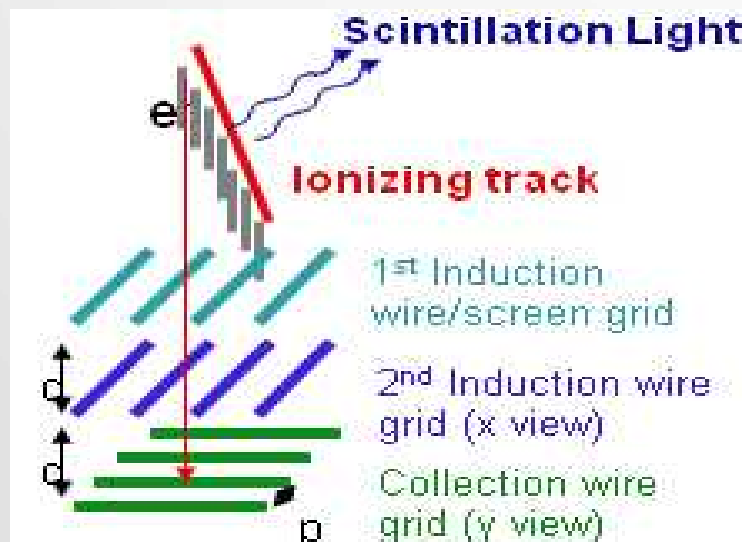
Charged particle beam ≈ 800 MeV/c exposure



The Lar TPC principle (C.Rubbia, 1977)

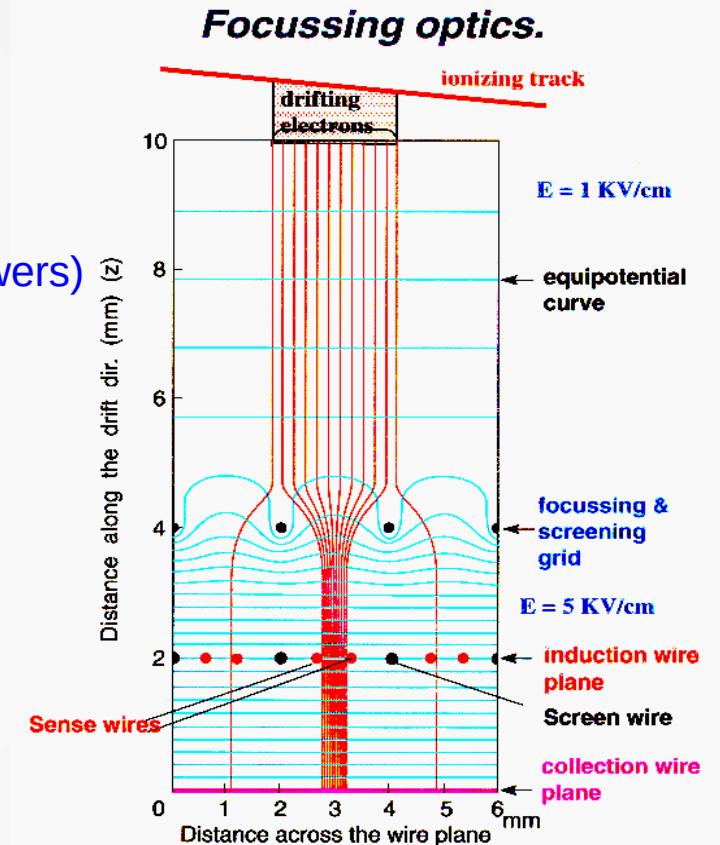
- Homogeneous massive target and ionization detector
→ electronic bubble chamber
- 3D event reconstruction with ~ 1 mm resolution,
- Surface readout of instrumented volume,
- High resolution calorimetry (electromagnetic and hadronic showers)
- Primary ionization in LAr: 1 m.i.p ~ 20000 e⁻ on 3 mm
- Detection of UV scintillation light in LAr (5000 photons/mm at 128 nm) to provide $t = 0$ signal of the event

Ideal detector for neutrino oscillations,
supernovae neutrinos and proton decay



X,Y
Non-destructive
multiple readout
with induction
planes

→ drift requiring < 0.1 ppb O₂ equiv.
impurities

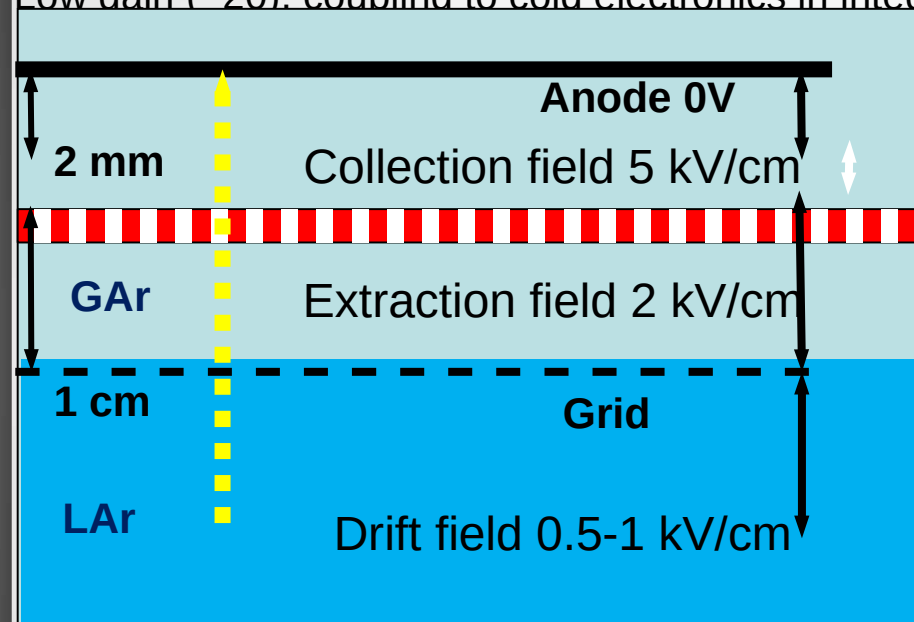


Z = drift time
Drift Field: 0.5-1 kV/cm
Drift time:
2 m/ms @1 kV/cm

Double phase readout

Compensate for long drift: extraction of electrons from the liquid and multiplication with avalanches in pure argon with detectors like LEM (Large Electron Multipliers).

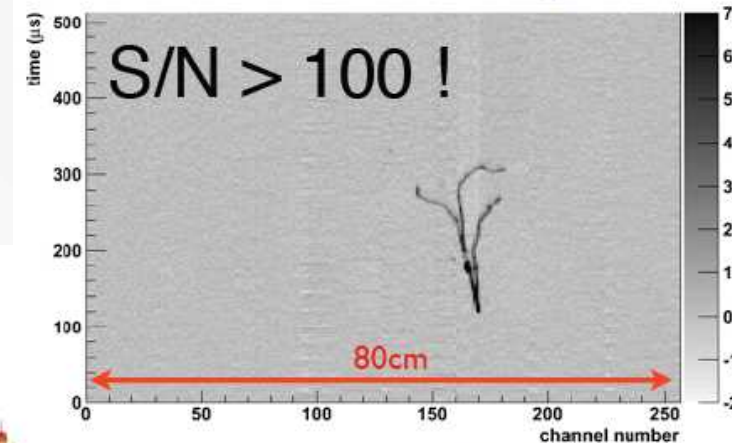
Low gain (~ 20), coupling to cold electronics in integrated modules



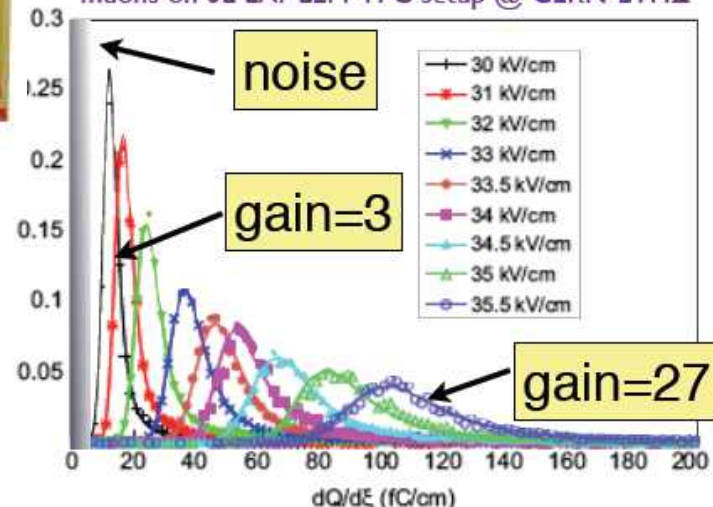
LEM
25-35 kV/cm



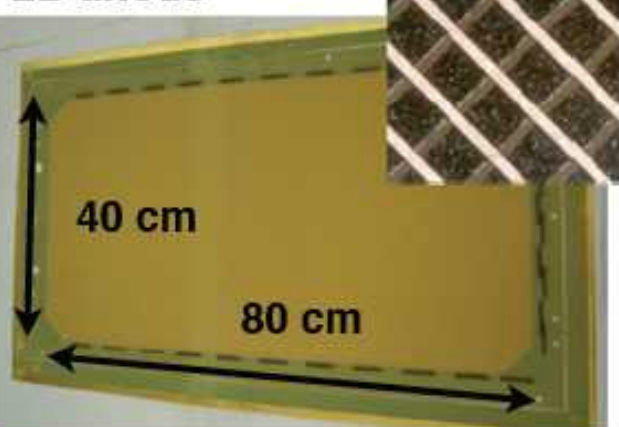
Cosmic Data from 40x80cm² LAr LEM TPC@CERN-ETHZ



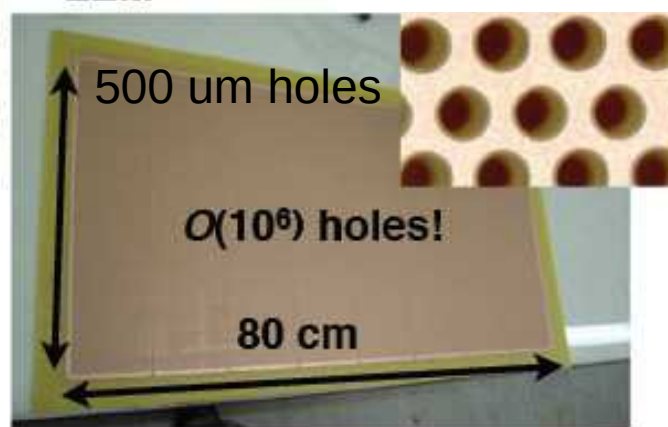
Landau distribution fitted to dE/dx distributions of muons on 3L LAr LEM-TPC setup @ CERN-ETHZ



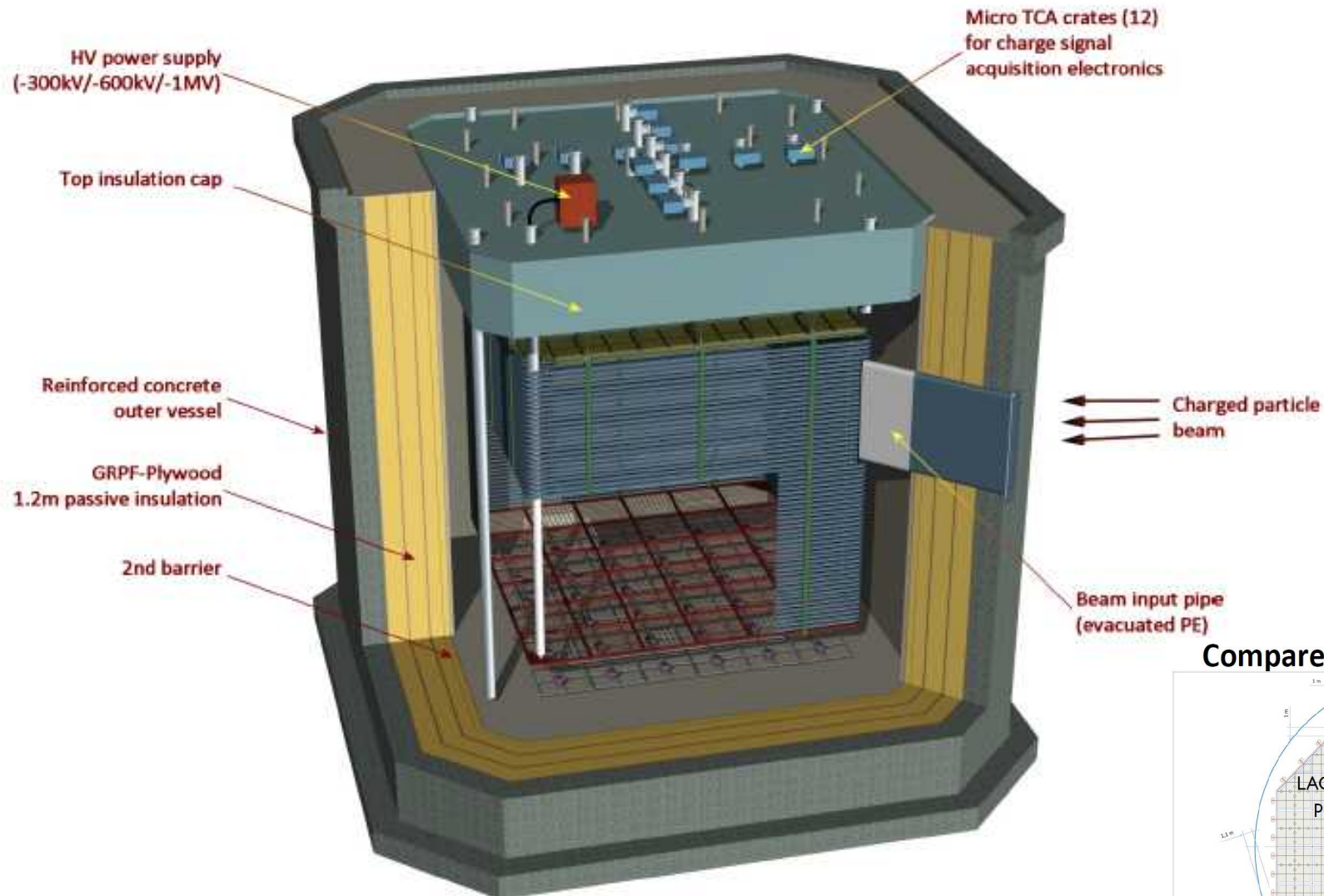
2D anode



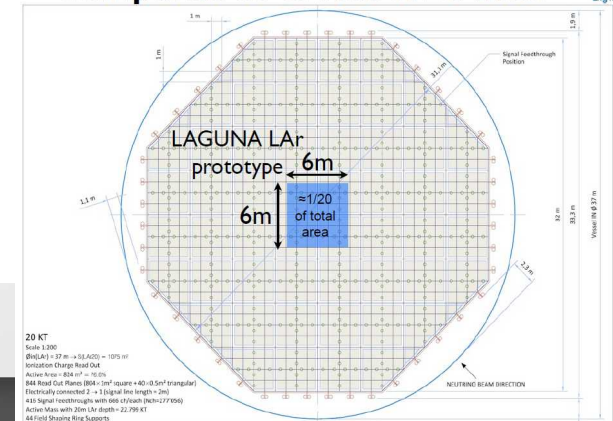
LEM



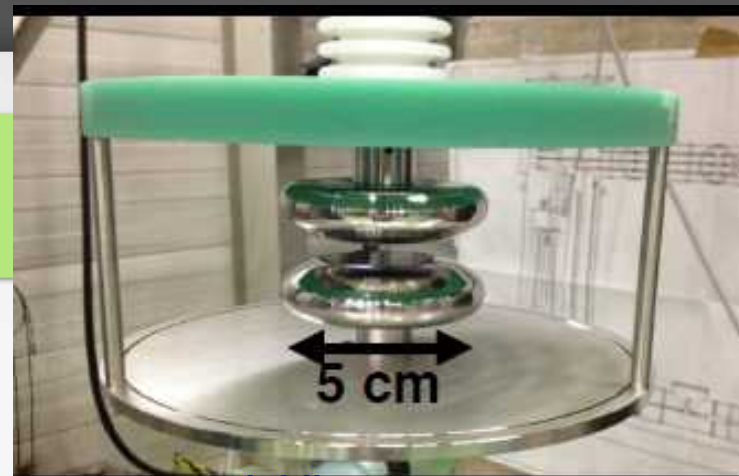
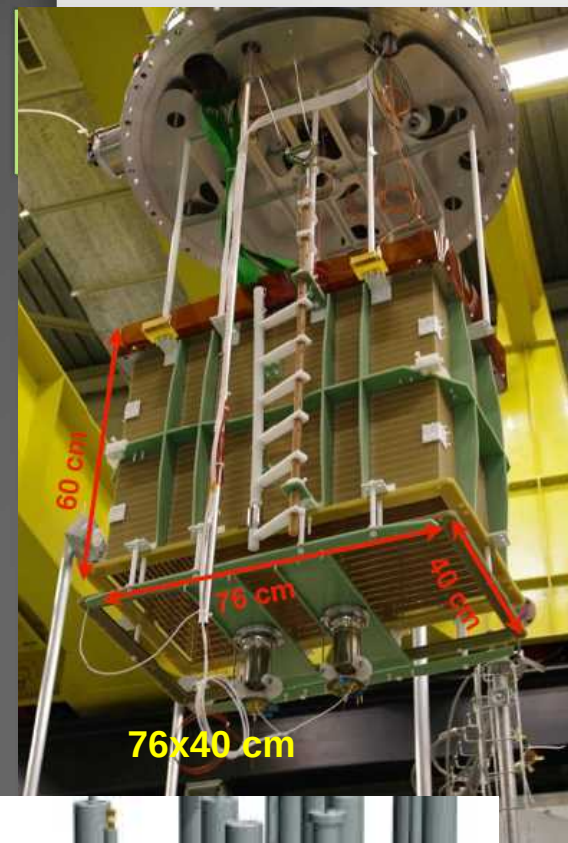
WA105 demonstrator



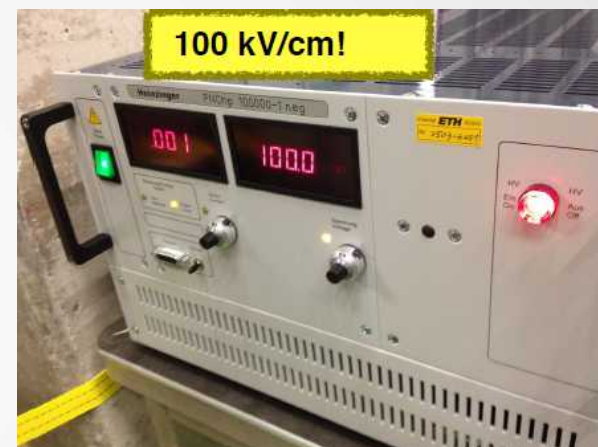
Compared to GLACIER 20 kton



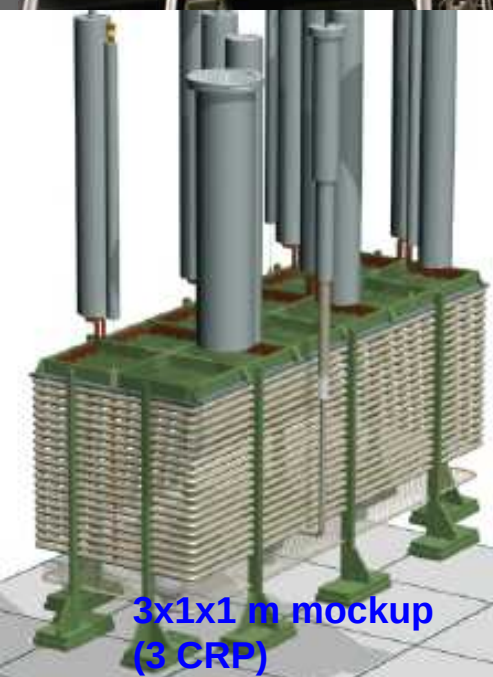
R&D on-going



LAr rigidity test setup



Readout test setup in Lyon



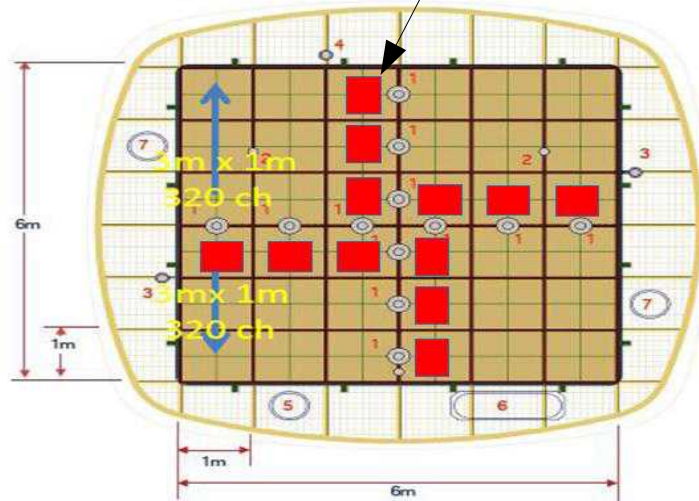
μ TCA-DAQ architecture : proposal



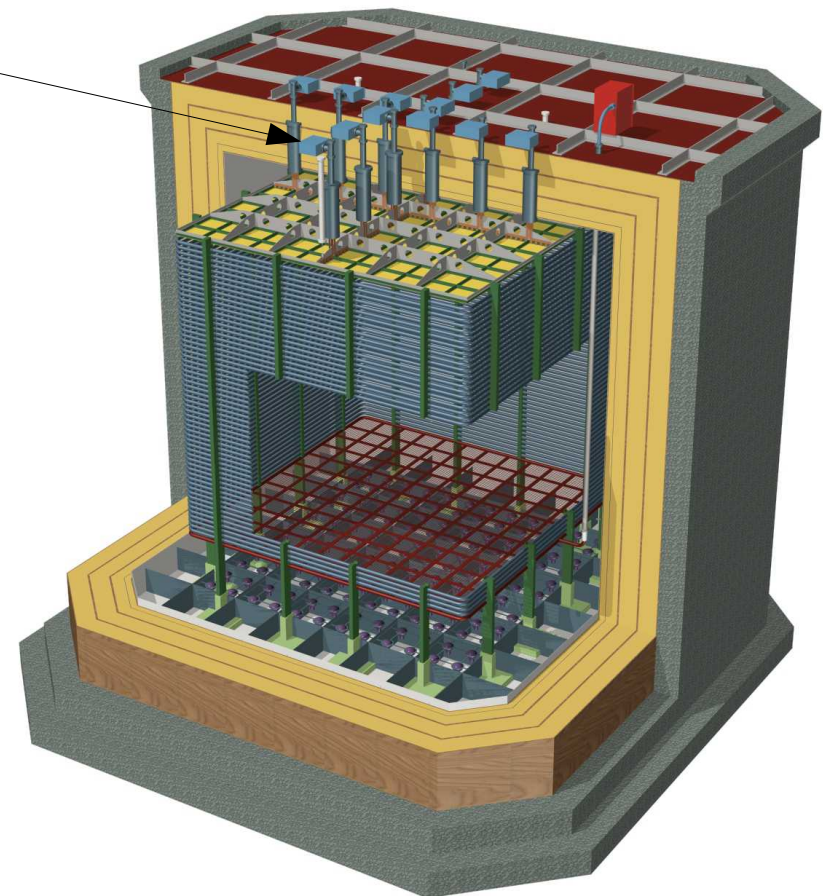
Crates implementation

View from anode with signal (1), suspension (2), HV(3), PMT(4), manhole (5), detail insertion (6), clean room IN/OUT (7) nozzles

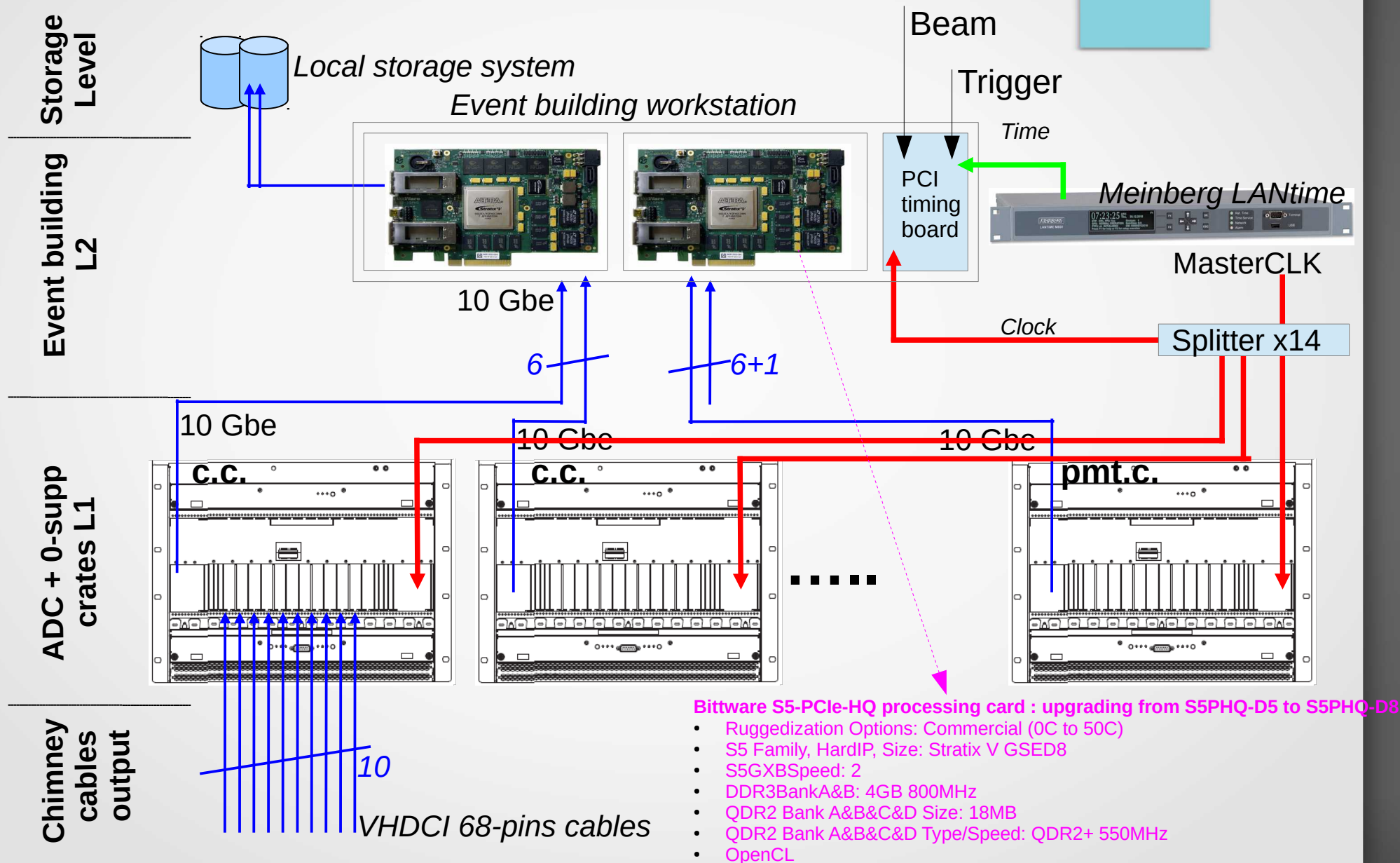
μ TCA.1 option



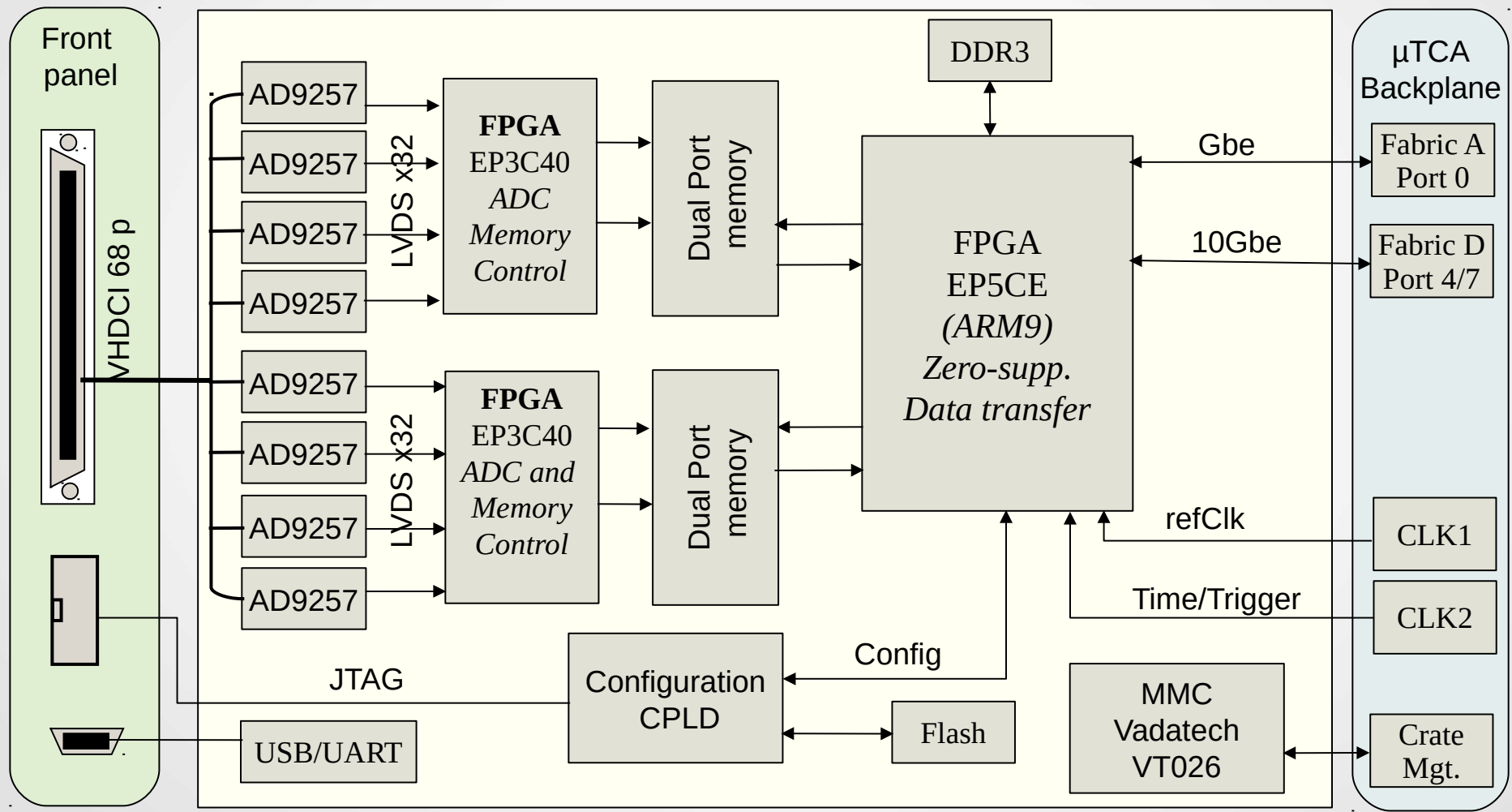
top view



μTCA-DAQ architecture: proposal

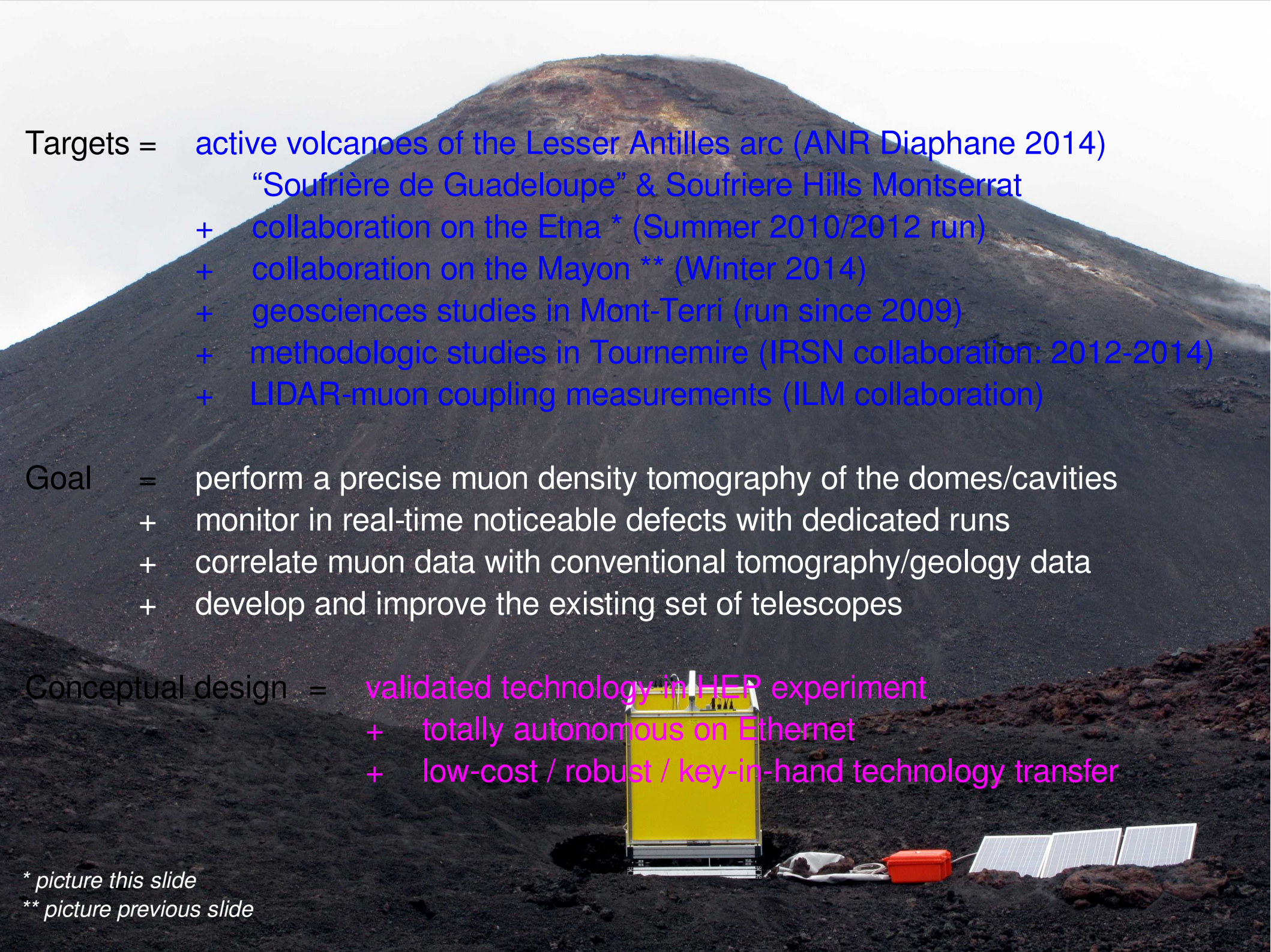


AMC card design : block diagram



Part – III

Imaging with particles



Targets = active volcanoes of the Lesser Antilles arc (ANR Diaphane 2014)
“Soufrière de Guadeloupe” & Soufriere Hills Montserrat
+ collaboration on the Etna * (Summer 2010/2012 run)
+ collaboration on the Mayon ** (Winter 2014)
+ geosciences studies in Mont-Terri (run since 2009)
+ methodologic studies in Tournemire (IRSN collaboration: 2012-2014)
+ LIDAR-muon coupling measurements (ILM collaboration)

Goal = perform a precise muon density tomography of the domes/cavities
+ monitor in real-time noticeable defects with dedicated runs
+ correlate muon data with conventional tomography/geology data
+ develop and improve the existing set of telescopes

Conceptual design = validated technology in HEP experiment
+ totally autonomous on Ethernet
+ low-cost / robust / key-in-hand technology transfer

* picture this slide

** picture previous slide

Volcano hazards

Phreatic eruption and flank collapse are the most likely hazards for La Soufrière (and many volcanoes of this type)

- Phreatic eruption = release of thermal energy contained in the hydrothermal reservoirs (energy is present, we need the trigger)
- Flank collapse may be triggered by internal overpressure, earthquake

Active vent during 1976 phreatic eruption



(c) 1976, M. Bof

... the same in 2010



2010, Q. Gibert

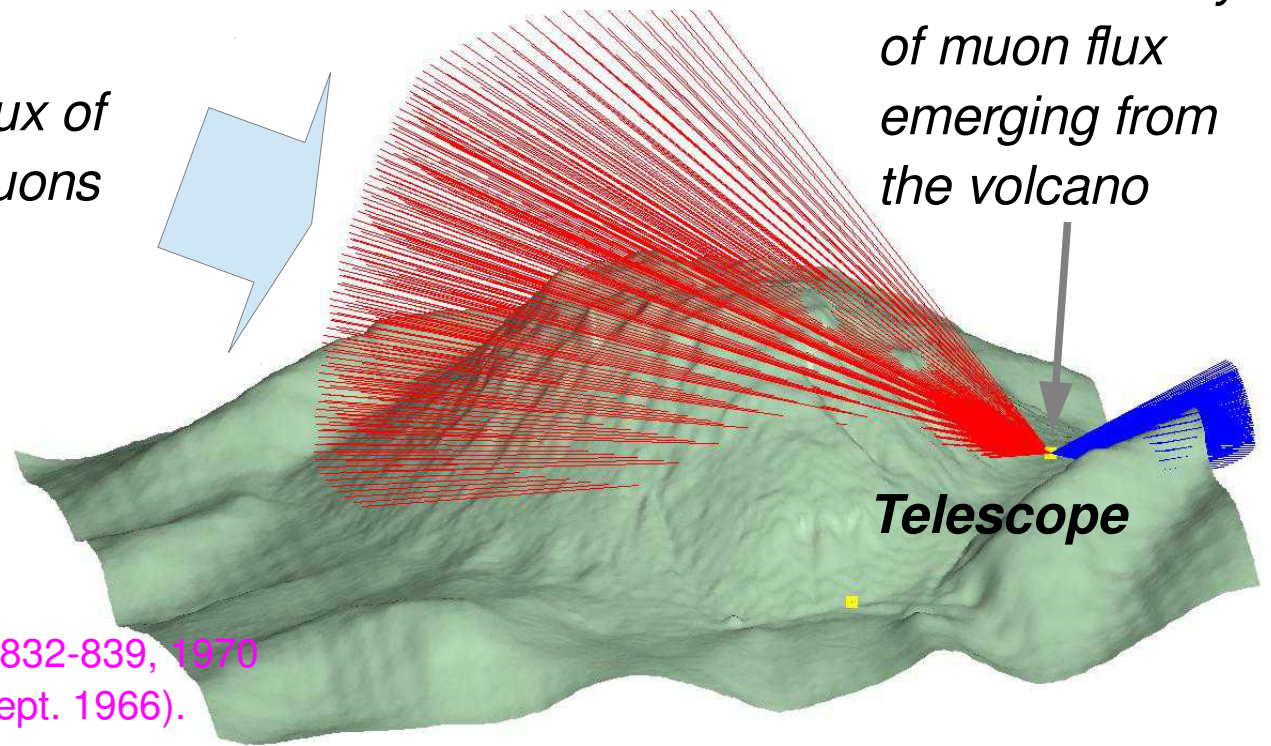
Muon tomography

Measure the flux of muons across the volcano to determine its density structure

- Basic information = opacity $\varrho(L) \equiv \int_L \rho(\xi) d\xi$,

Incident flux of cosmic muons

Data = intensity of muon flux emerging from the volcano



Precursory work:

Alvarez, L.W. et al., *Science*, 167, 832-839, 1970
(see also *Physics Today*, 78-80, Sept. 1966).

Renew of interest:

Nagamine, K. et al., *NIMA*, 356, 585-595, 1995.

Field telescopes

Scintillator strips (1x5x80 cm³) provided by FermiLab

WLS fibers: Bicron BCF-91A

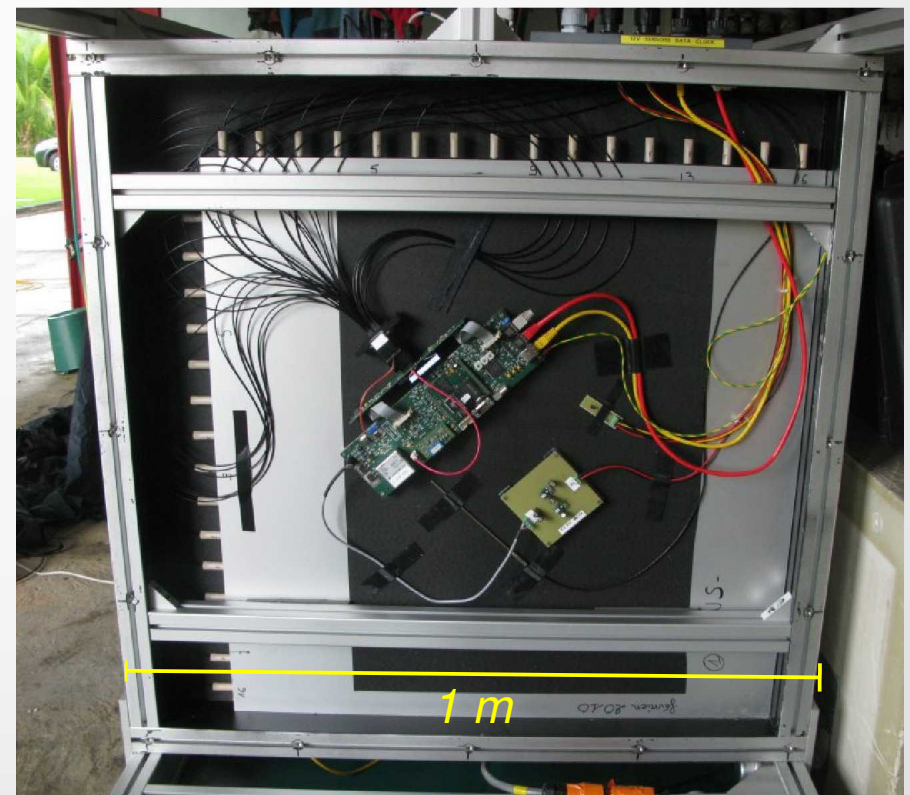
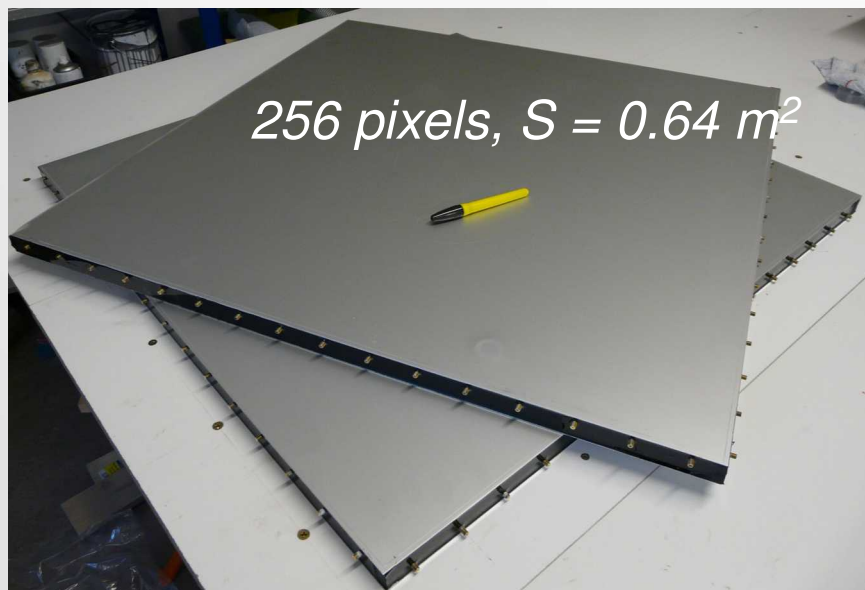
Multichannel PM H8804-200 MOD-5 Hamamatsu

SiPM S10362-13-050C Hamamatsu

Main board: CAMEROP from OPERA

Clock resolution: 1 ns

SiPM Front end developed by IPNL



Field telescopes

Photovoltaic panels, wind turbine, fuel cells

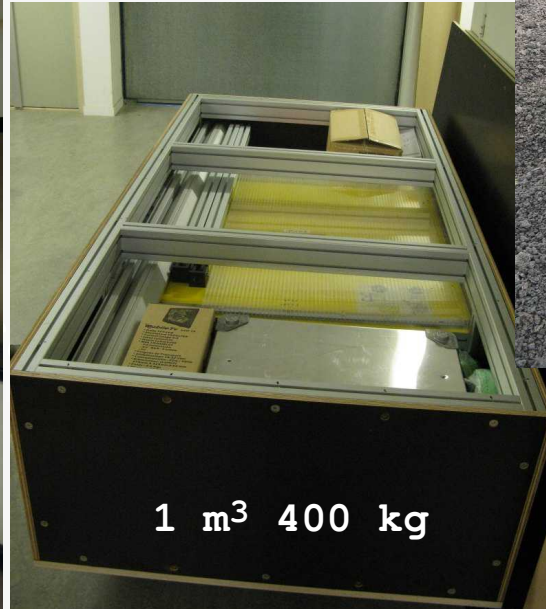
Total mass: 200 to 600 kg (w/ shielding)

Angular aperture/resolution: 30° - 60° / 1° - 2°

Etna, 2012

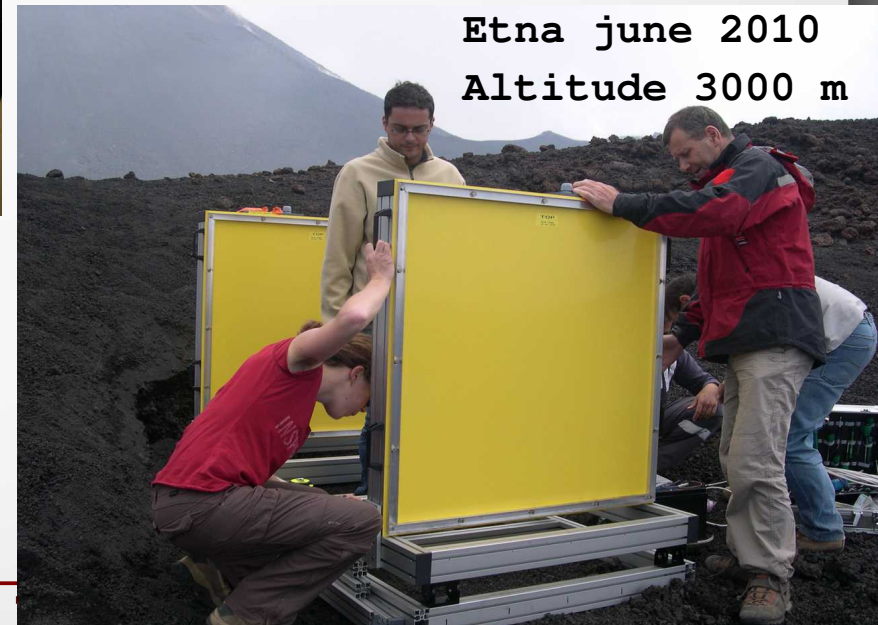


1 m³ 400 kg

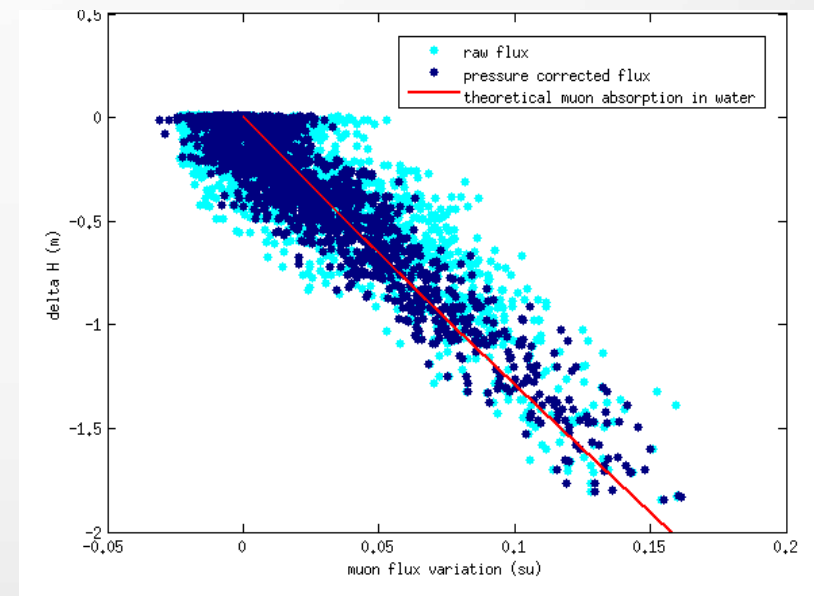
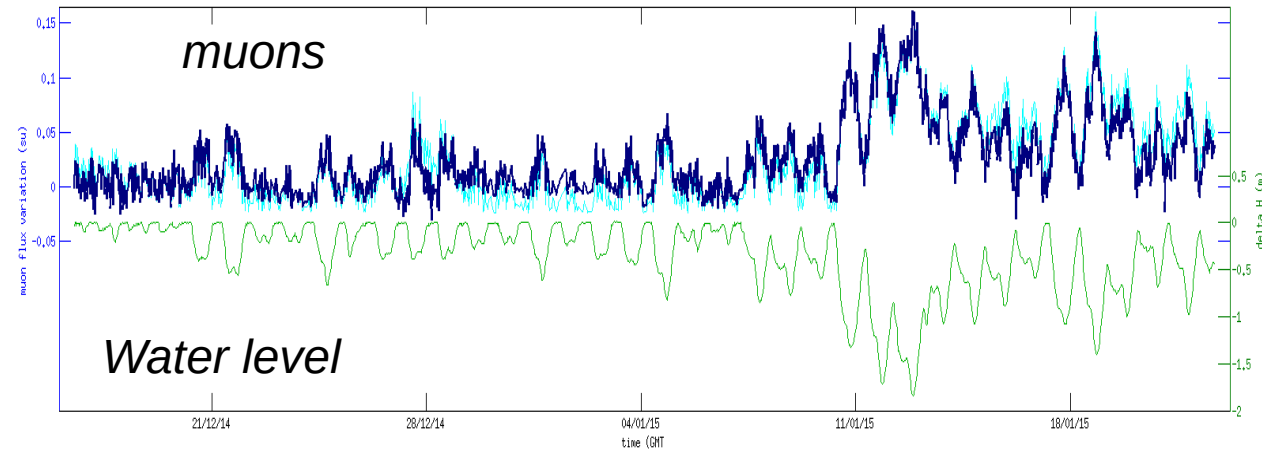
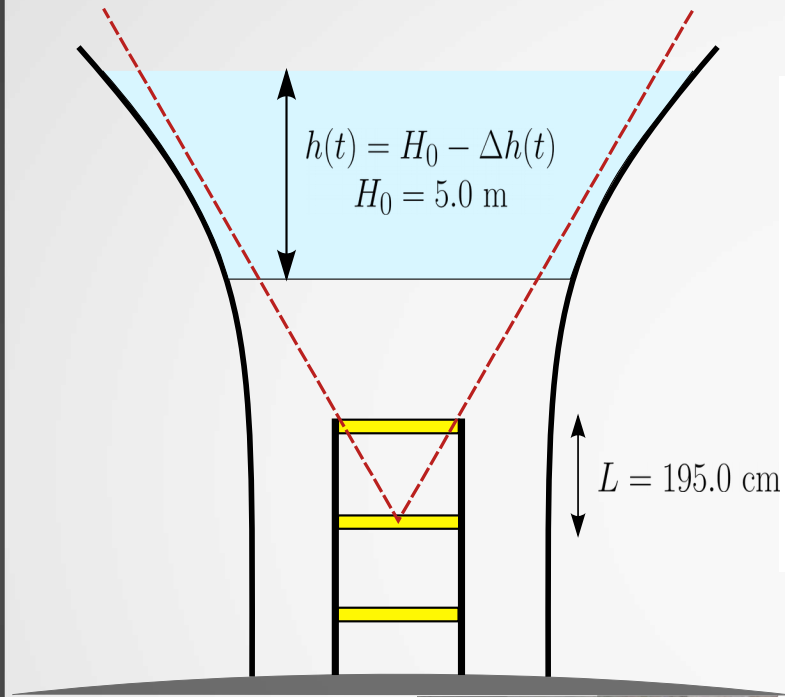


Mayon, 2014

Etna june 2010
Altitude 3000 m

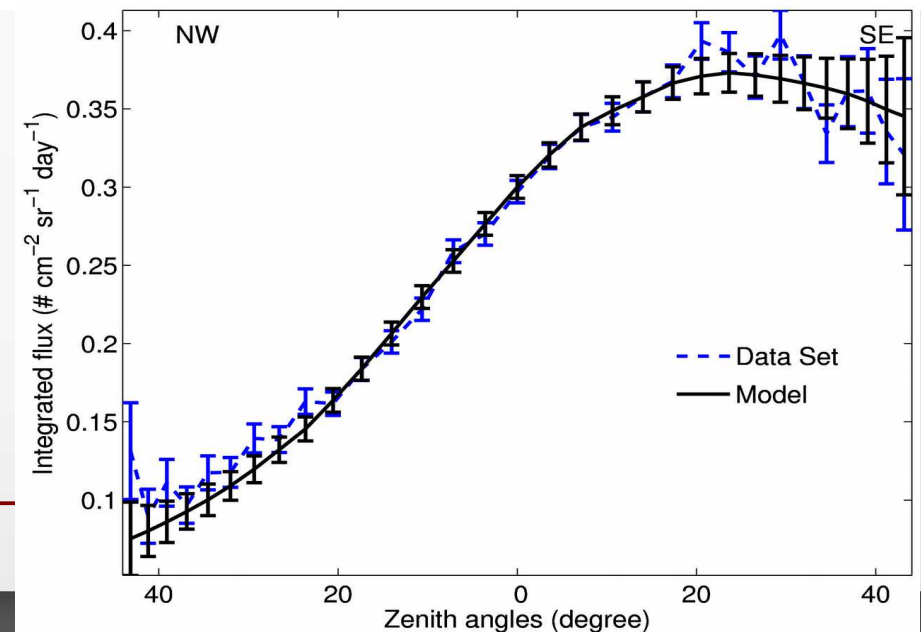
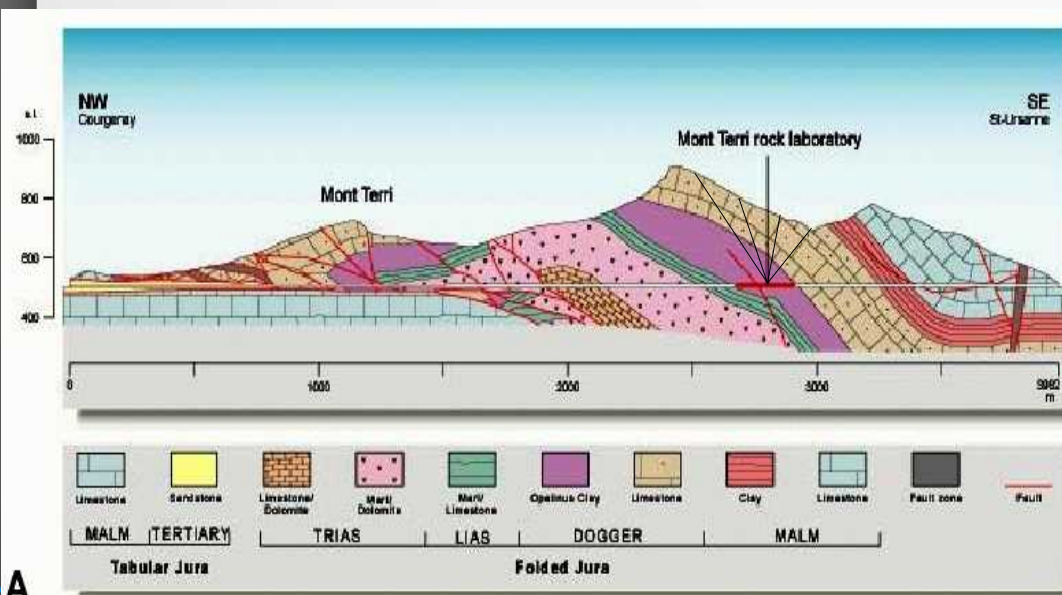
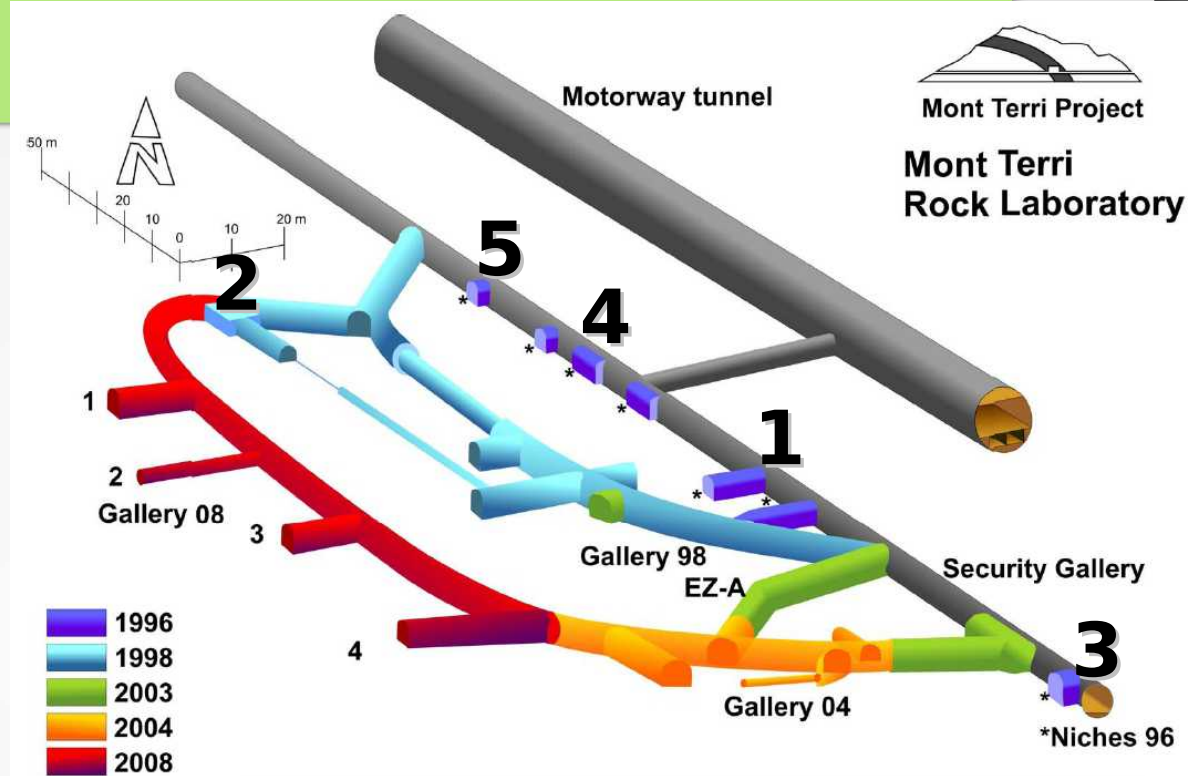


SHADOW experiment



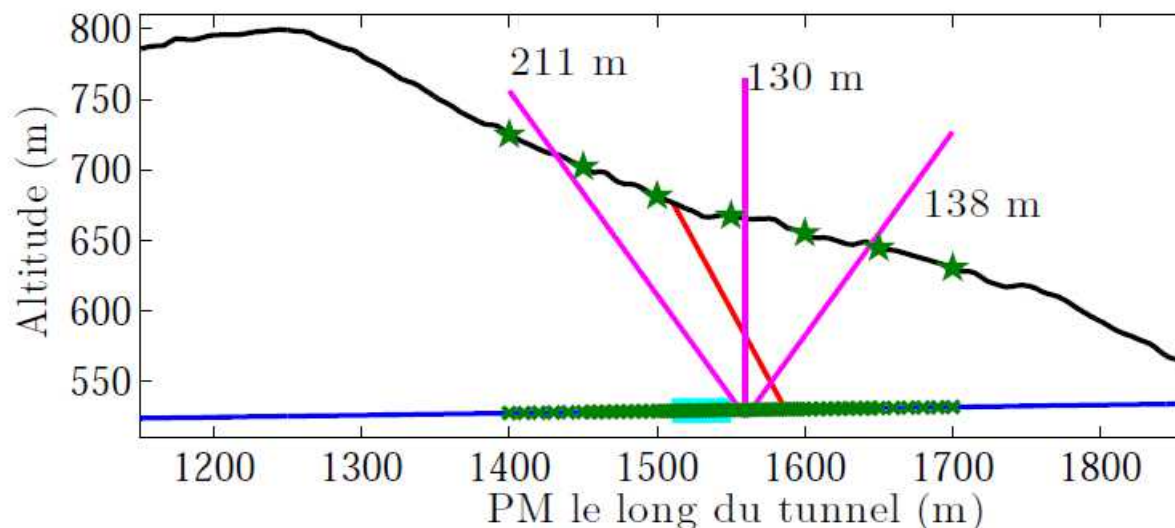
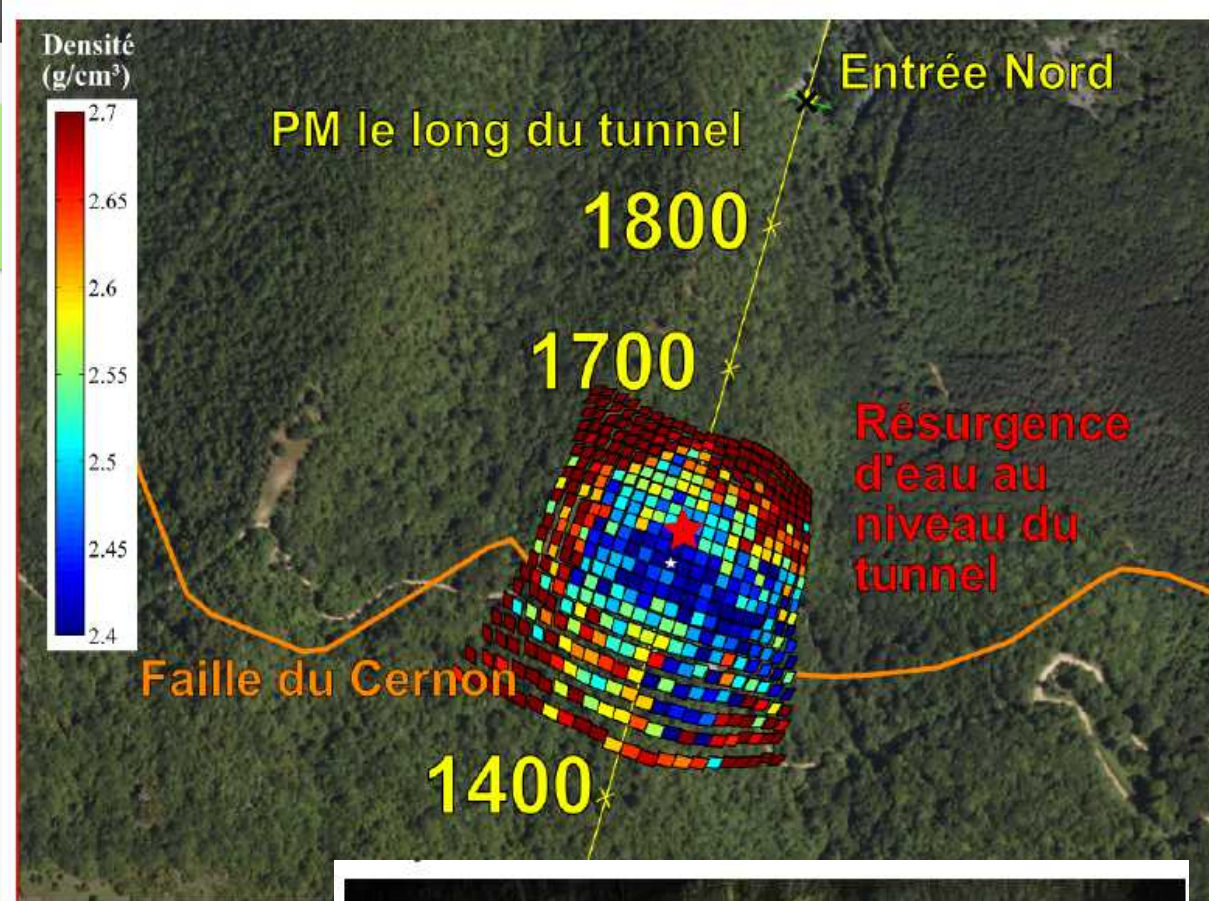
MT laboratory

- "Methodology" measurements for long-term storage studies
 - Simple (and known) geology
 - "Silent" environment w.r.t. parasitic radiations, noise, downstream flux etc
 - Imaging the interfaces between various geological layers :
- $\rho_{\text{limestone}} = 2.7 \text{ g/cm}^3$ / $\rho_{\text{clay}} = 2.45 \text{ g/cm}^3$
- Different measurements on different locations

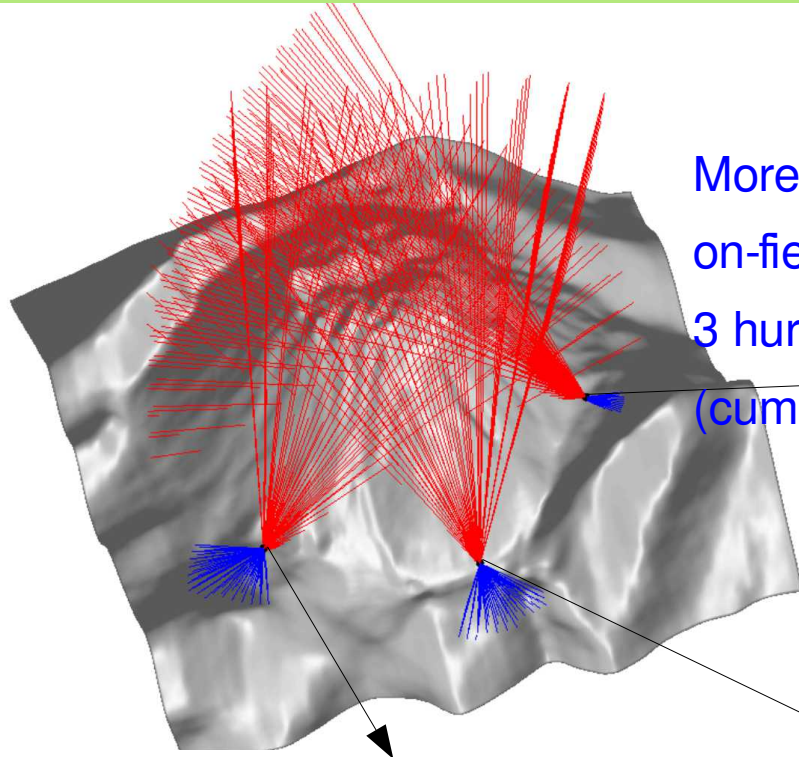


Tournemire IRSN

- "Methodology" measurements
- Simple (and known) geology
- One of the experiment conducted under a fault (Cernon)

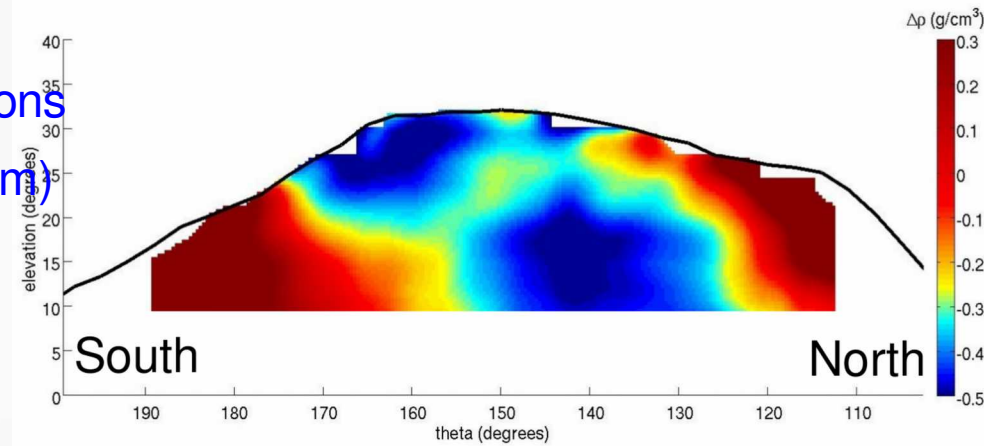


Soufrière structural imaging

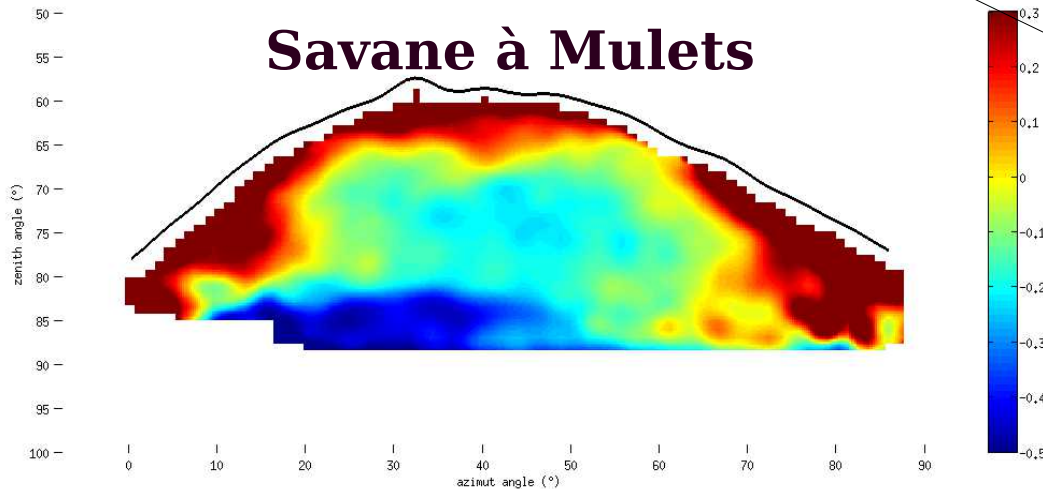


More than 3.5 years of
on-field operation
3 hurricane seasons
(cumul rain = 10 m)

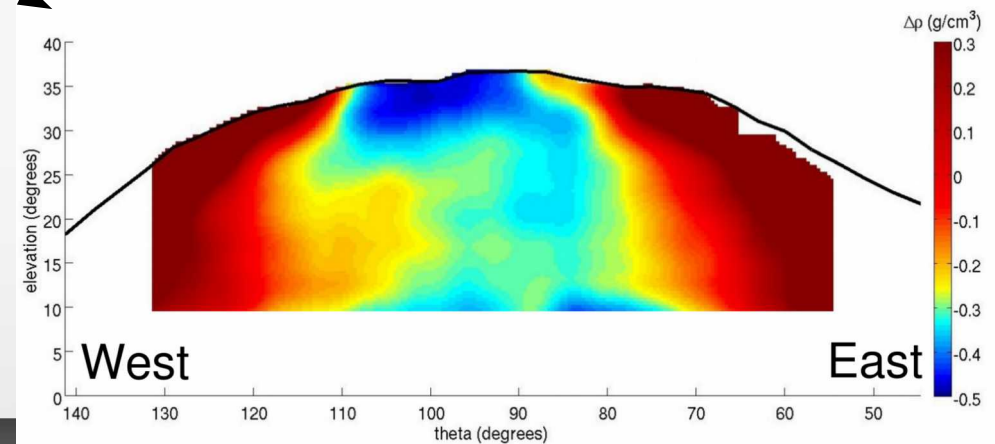
Rocher Fendu



Savane à Mulets



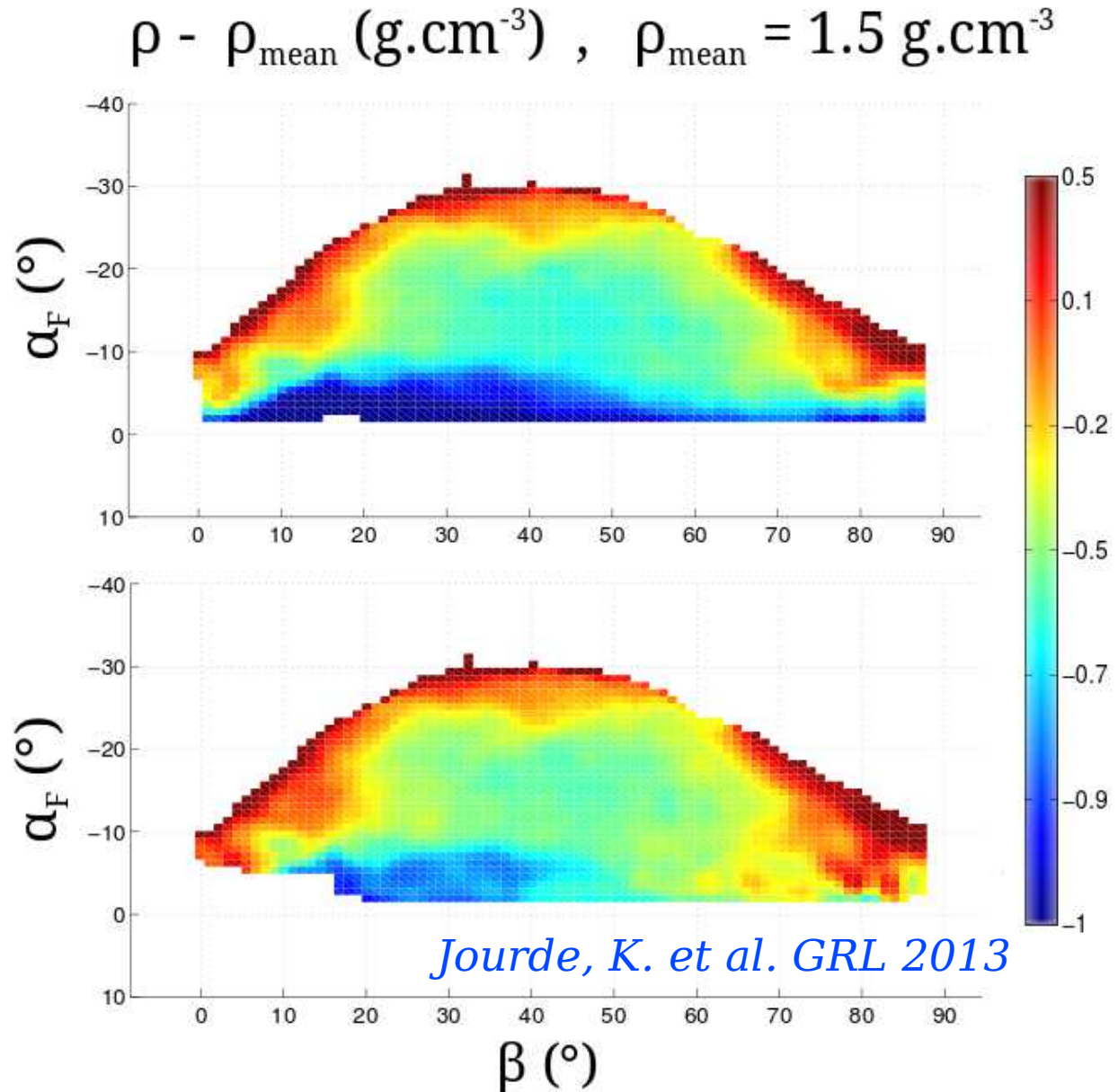
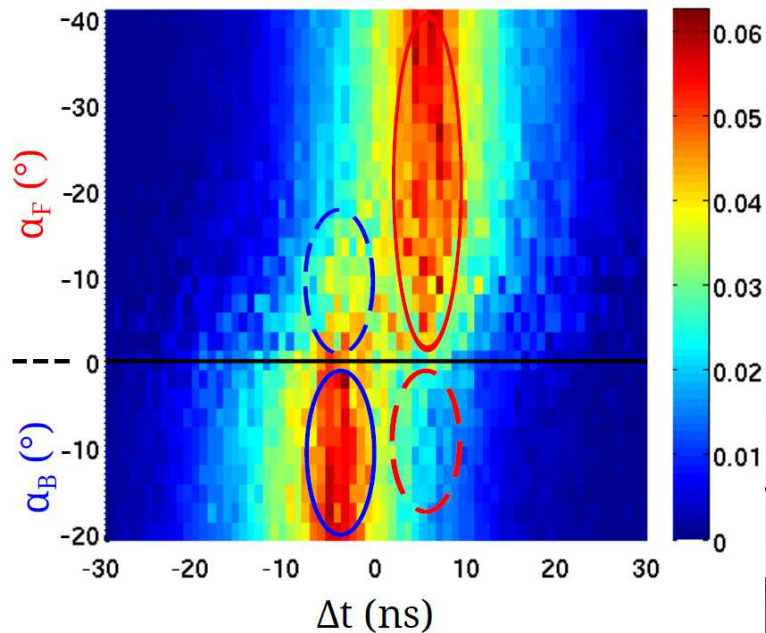
Ravine Sud



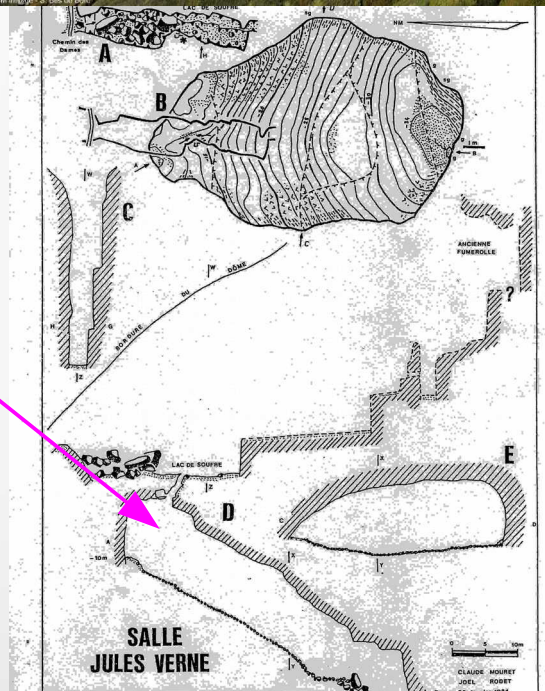
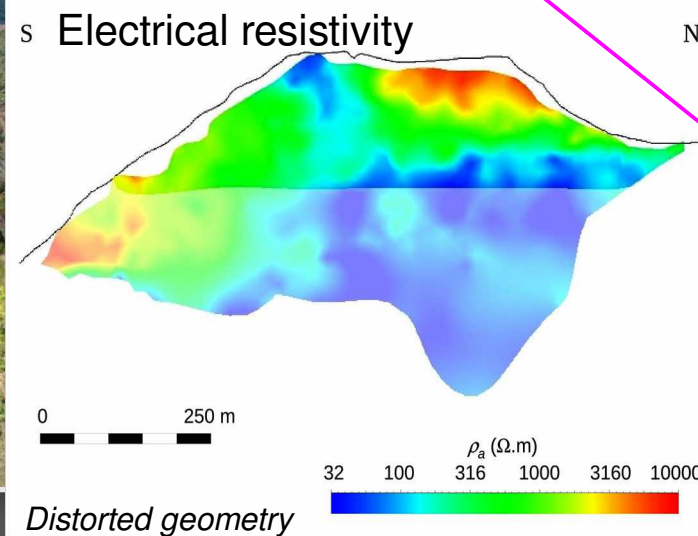
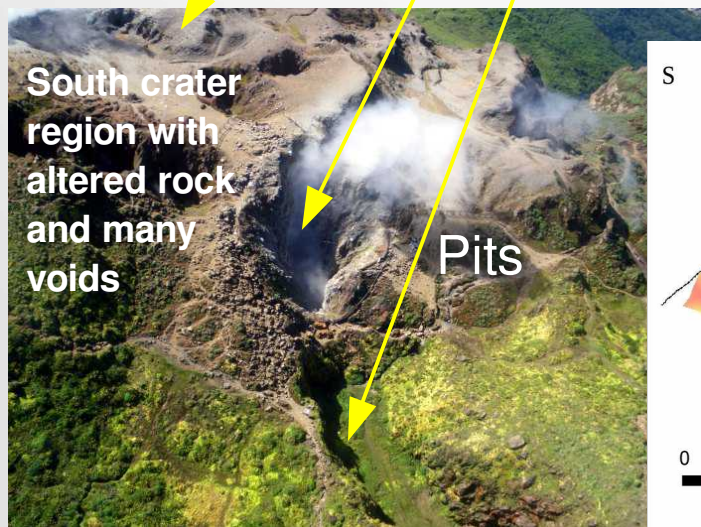
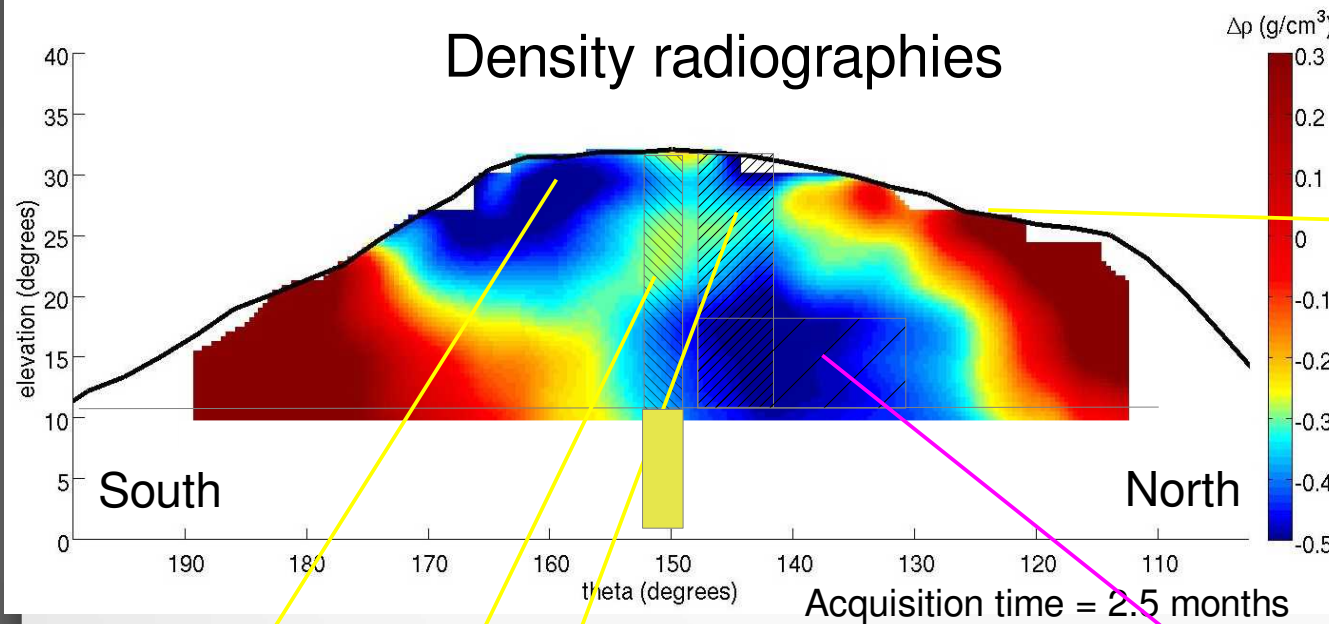
TOF measurements

The **high precision clock** allows a TOF analysis to disentangle particles coming either from **the front or the rear** of the telescope

A particle upward-flux was enhanced on the Savane à Mulets site permitting to **correct the low density region** above the horizon.

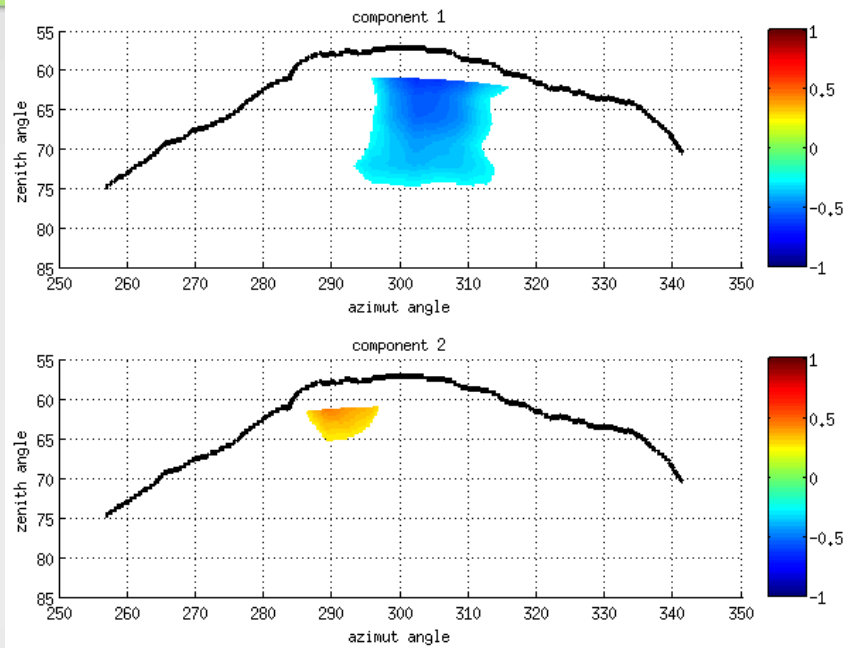


Soufrière structural imaging

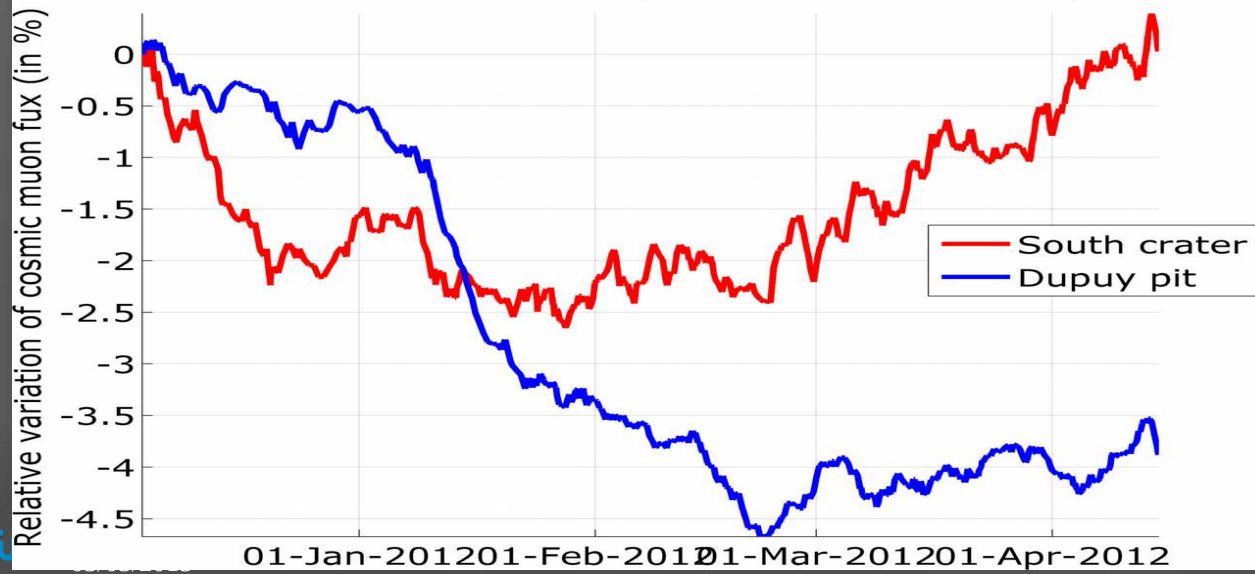


Low density region might be the Spallanzani cave described in ancient texts.
No more accessible.

Dynamic monitoring



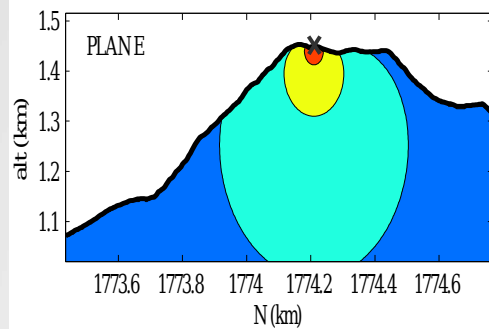
Rocher Fendu location (East side of lava dome)



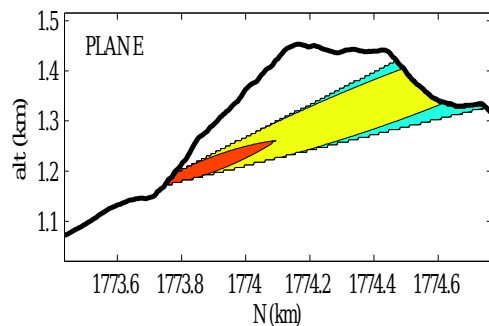
Correlation between activity at the top and increase of the measured muon flux (compatible with a decrease of the water level in the volcano)

Coupling with gravimetry

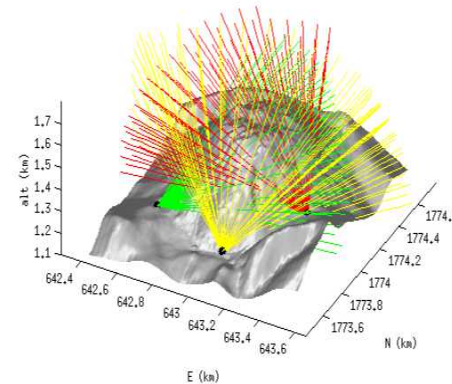
gravimetry acquisition kernel, G



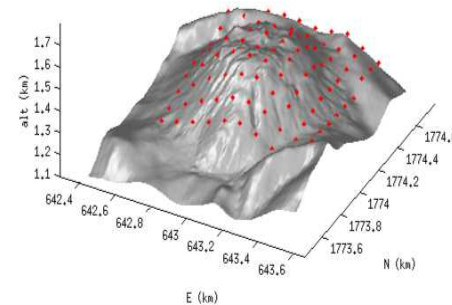
tomography acquisition kernel, M



tomography coverage



gravimetry coverage



Tomography and gravimetry are linear problems that are function of density:

$$\begin{pmatrix} \rho \\ g \end{pmatrix} = \begin{pmatrix} M \\ G \end{pmatrix} \cdot \rho$$

M and G are the acquisition kernels. The inverted density reads:

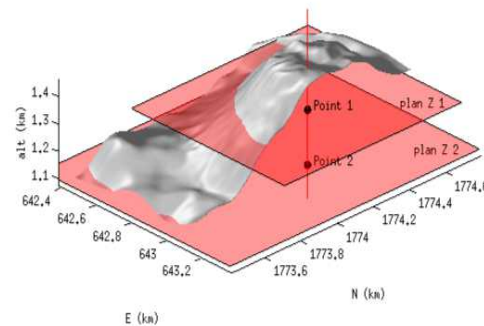
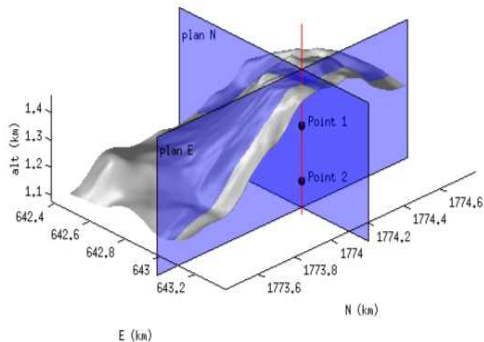
$$\tilde{\rho} = R \cdot \rho = \left(\sum_{i=1}^{N_m} \alpha_i M_i + \sum_{i=1}^{N_g} \beta_i G_i \right) \cdot \rho$$

The resolving operator R acts like a filter.

Bertero, M. et al. 1985

Tarantola, 2005

Sabatier, P. C and Sebu, C., 2007

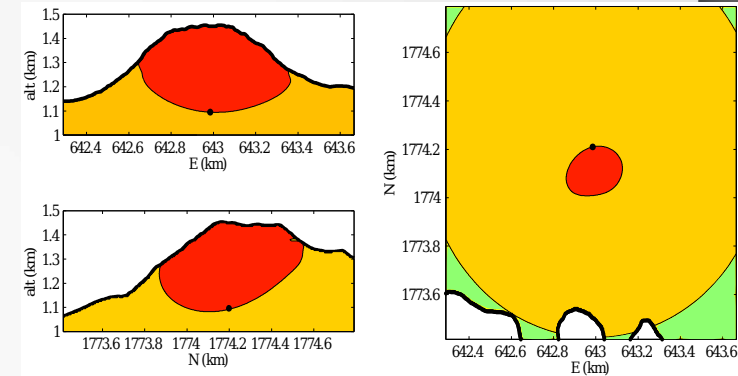
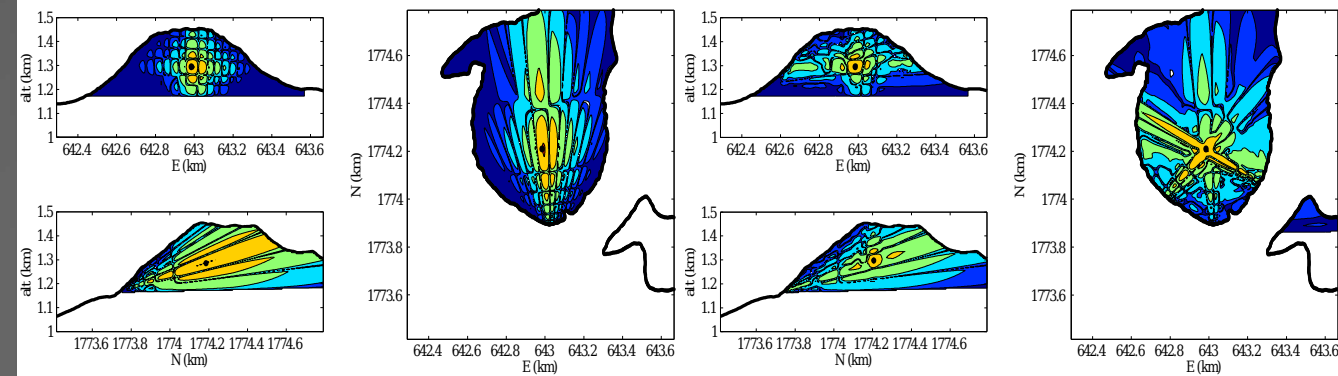


Coupling with gravimetry : results

Ravine Sud tomography data

All sites tomography data

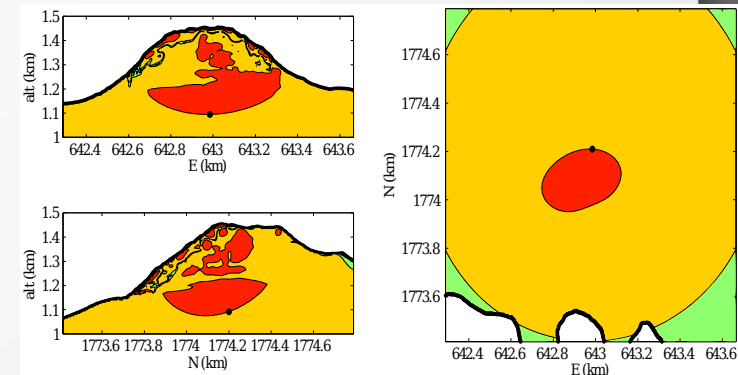
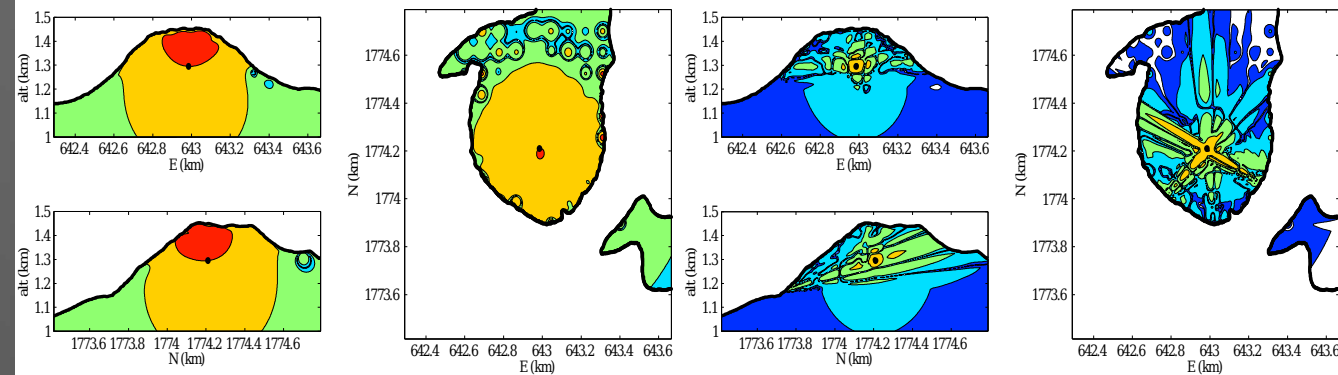
Gravimetry data



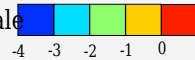
Gravimetry data

Gravimetry and tomography data

Gravimetry and tomography data



Resolving kernel value normalized at point 1 in logarithmic scale



Resolving kernel value normalized at point 2 in logarithmic scale



Conclusions

- ✓ A lot of activities, from the theoretical to the technical fields, oscillating around neutrino physics
- ✓ Neutrino oscillations entered in the precision physics era by accelerated steps
- ✓ Neutrino-nucleus cross-sections are a (now) well-recognized key ingredient of the recipe
- ✓ The precision era requires gigantic detectors, efficient detection methods and readout systems
- ✓ Transverse applications may benefit from fundamental physics with an extra societal dimension